Microstructure Evolution in Irradiated Metals and Alloys: Fundamental Aspects

Steven J. Zinkle

Metals and Ceramics Division, Oak Ridge National Laboratory

NATO Advanced Study Institute
Course on Radiation Effects in Solids

Erice, Sicily, Italy,

July 17-29, 2004

Brief History of Radiation Effects

Ettore Majorana Center/Erice connections

- 1946 First paper on potential importance of radiation damage (E.P. Wigner, J. Appl. Phys. 17 (1946) 857)
  - 1st observation of amorphization ("metamict state") of minerals occurred in late 19th century
- Enrico Fermi International School on Radiation Damage in Solids held in Rome (Academic Press, 1962)
- International School on Radiation Effects in Materials, University of Illinois, Champaigne-Urbana, USA [J. Nucl. Mater. 216 (1994)]

What is "dpa"?

- 1 displacement per atom (dpa) corresponds to stable displacement from their lattice site of all atoms in the material during irradiation near absolute zero (no thermally-activated point defect diffusion)
  - Initial number of atoms knocked off their lattice site during neutron irradiation is ~100 times the dpa value
    - Most of these originally displaced atoms hop onto another lattice site during "thermal spike" phase of the displacement cascade (~1 ps)

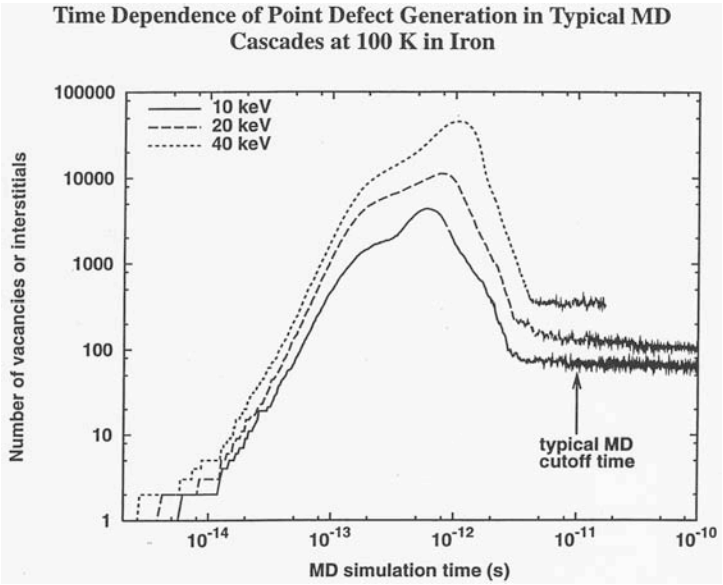

R.E. Stoller

- At non-zero temperatures, many of the created defects recombine so that the net surviving defect fraction is low (<10% NRT dpa)
- Requirement for advanced structural materials in fusion and Gen IV fission reactors (~100 dpa exposure):
  - ~99.9% of "stable" displacement damage must recombine
  - "off-the-shelf" materials typically exhibit 90-99% recombination of "stable" damage

The Equivalency of Displacement Damage Produced by Fission and Fusion Neutrons on dpa basis has been clearly demonstrated

Similar defect clusters produced by fission and fusion neutrons as observed by TEM

Fission
(0.1 - 3 MeV)

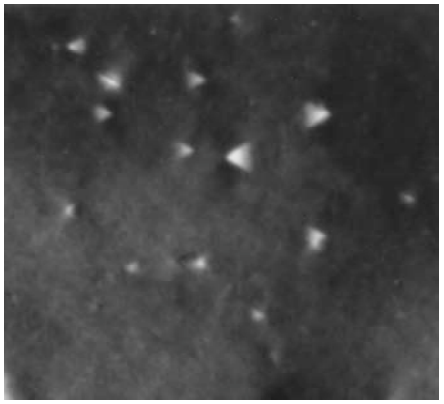

Fusion
(14 MeV)

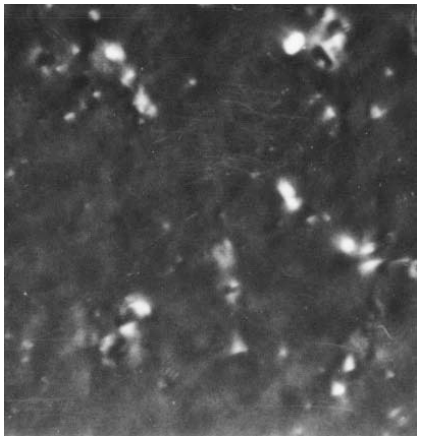

MD computer simulations show that subcascades and defect production are comparable for fission and fusion

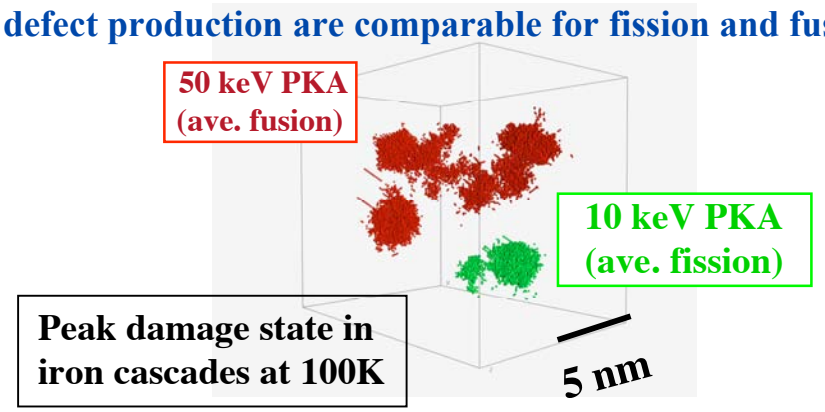

Similar hardening behavior confirms the equivalency

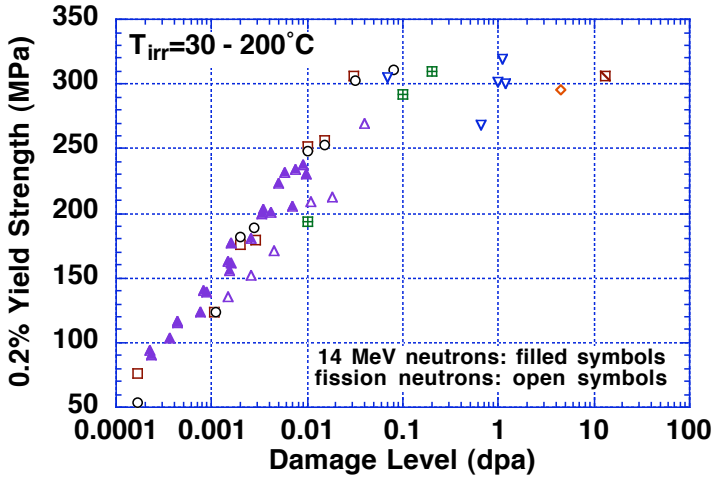

A critical unanswered question is the effect of higher transmutant H and He production in the fusion spectrum

Experimental evidence for nanoscale melting during atomic collisions has been obtained

ZrO_2-SiO_2 Phase Diagram

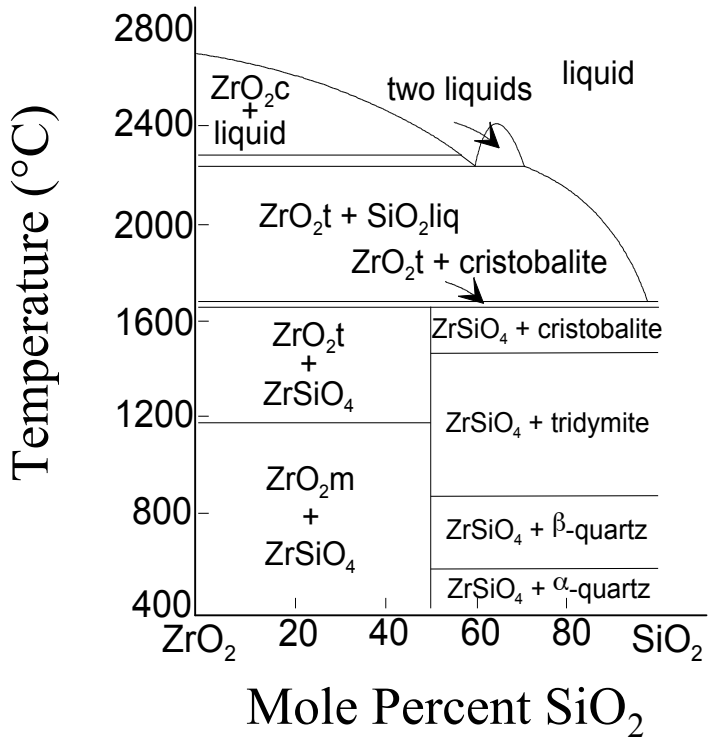

Microstructure of Zircon Irradiated at 800 °C

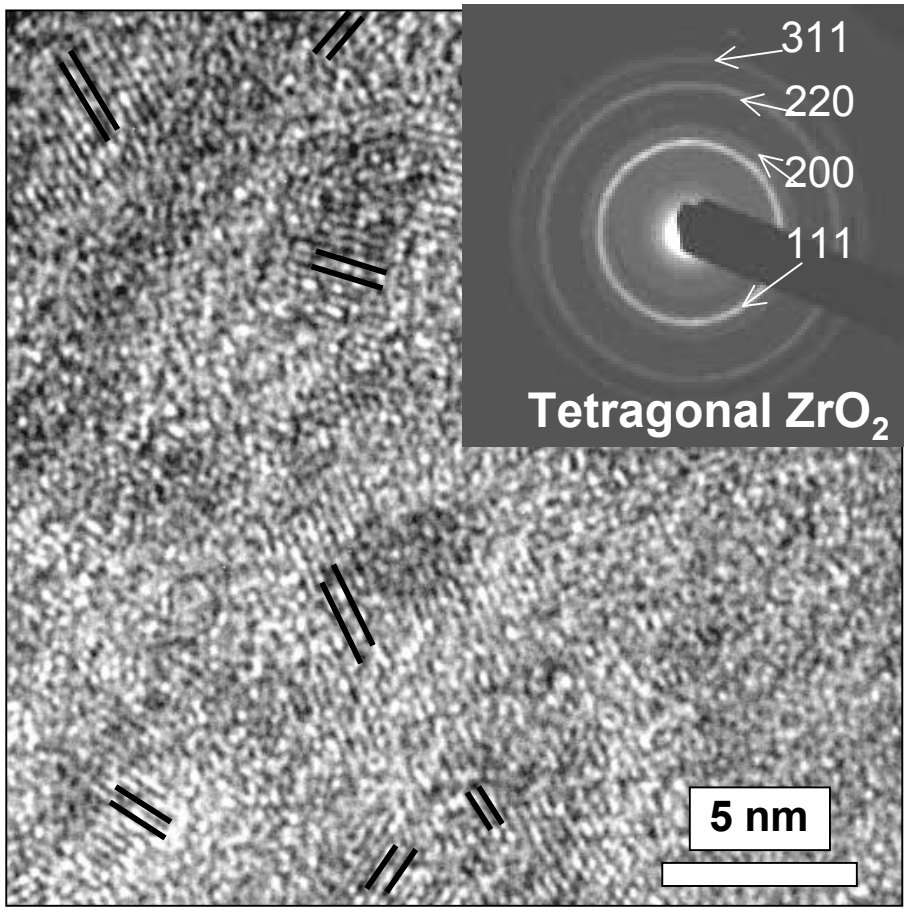

Nature, vol. 395, Sept 5. 1998, p. 56

Outline

- Overview of major microstructural temperature regimes and impact on properties
- Low temperature damage production (below recovery Stage V)
  - Comments on electron microscope imaging techniques for small defect clusters
  - Copper as a representative FCC metal
  - BCC vs. FCC differences
- Effect of irradiation temperature on radiation effects

Radiation Damage can Produce Large Changes in Structural Materials

- Radiation hardening and embrittlement (<0.4 T_M, >0.1 dpa)
- Irradiation creep (<0.45 T_M, >10 dpa)
- Volumetric swelling from void formation (0.3-0.6 T_M, >10 dpa)
- High temperature He embrittlement (>0.5 T_M, >10 dpa)

- All of these property changes are determined by microstructural evolution during irradiation

Some radiation effects nomenclature

- Electrical resistivity recovery stages
  - Stage I: initiation self-interstitial atom migration (correlated and uncorrelated)
  - Stage II: long-range migration of SIA clusters and SIA-impurity complexes
  - Stage III: longstanding controversy; near universal agreement that it is associated with vacancy migration
  - Stage IV: migration of vacancy clusters and vacancy-solute complexes
  - Stage V: thermal dissociation of (displacement cascade-produced) vacancy clusters
- Note: recovery stage temperatures are not unique; they depend on annealing time (e.g., displacement damage rate)

- SFT=stacking fault tetrahedron
- Loop =faulted or perfect dislocation loop (collapsed layer of vacancies or interstitials)
- Void= 3-dimensional vacancy cluster
- Cavity=3D vacancy cluster that may contain impurities (typically He)

Comparison of Stage I recovery behavior in Cu

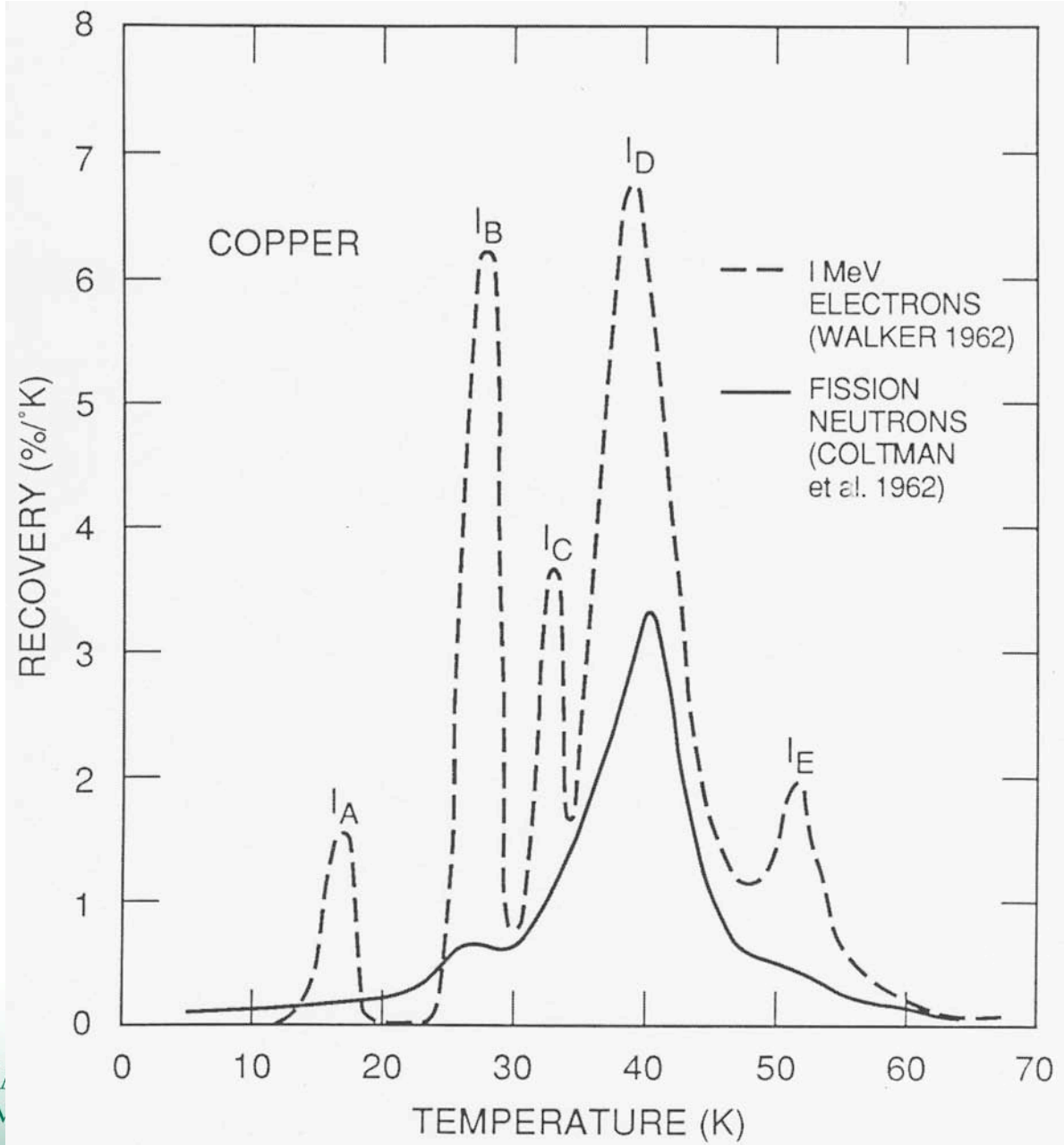

Correlated in-cascade recombination reduces surviving defect fraction due to freely migrating interstitials

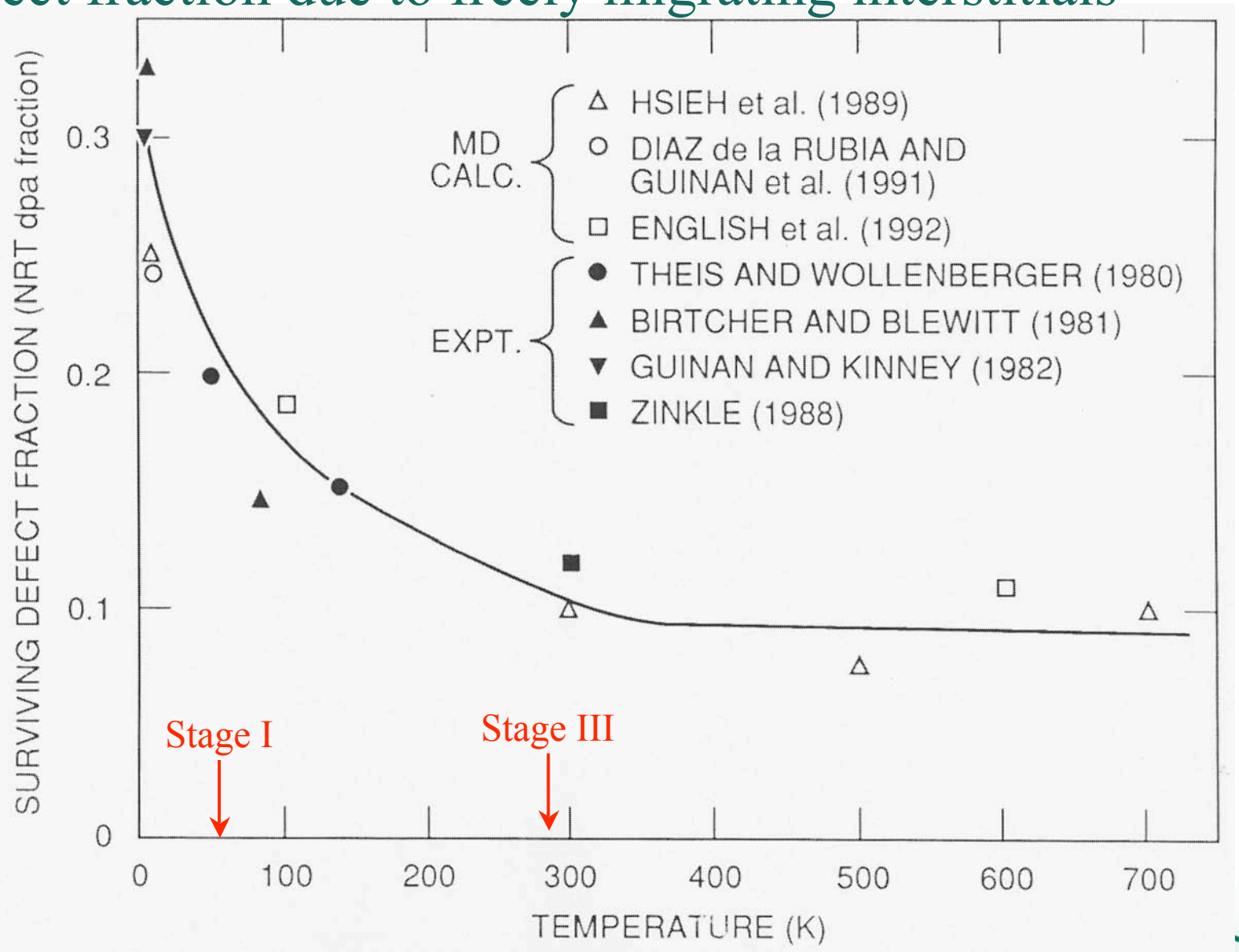

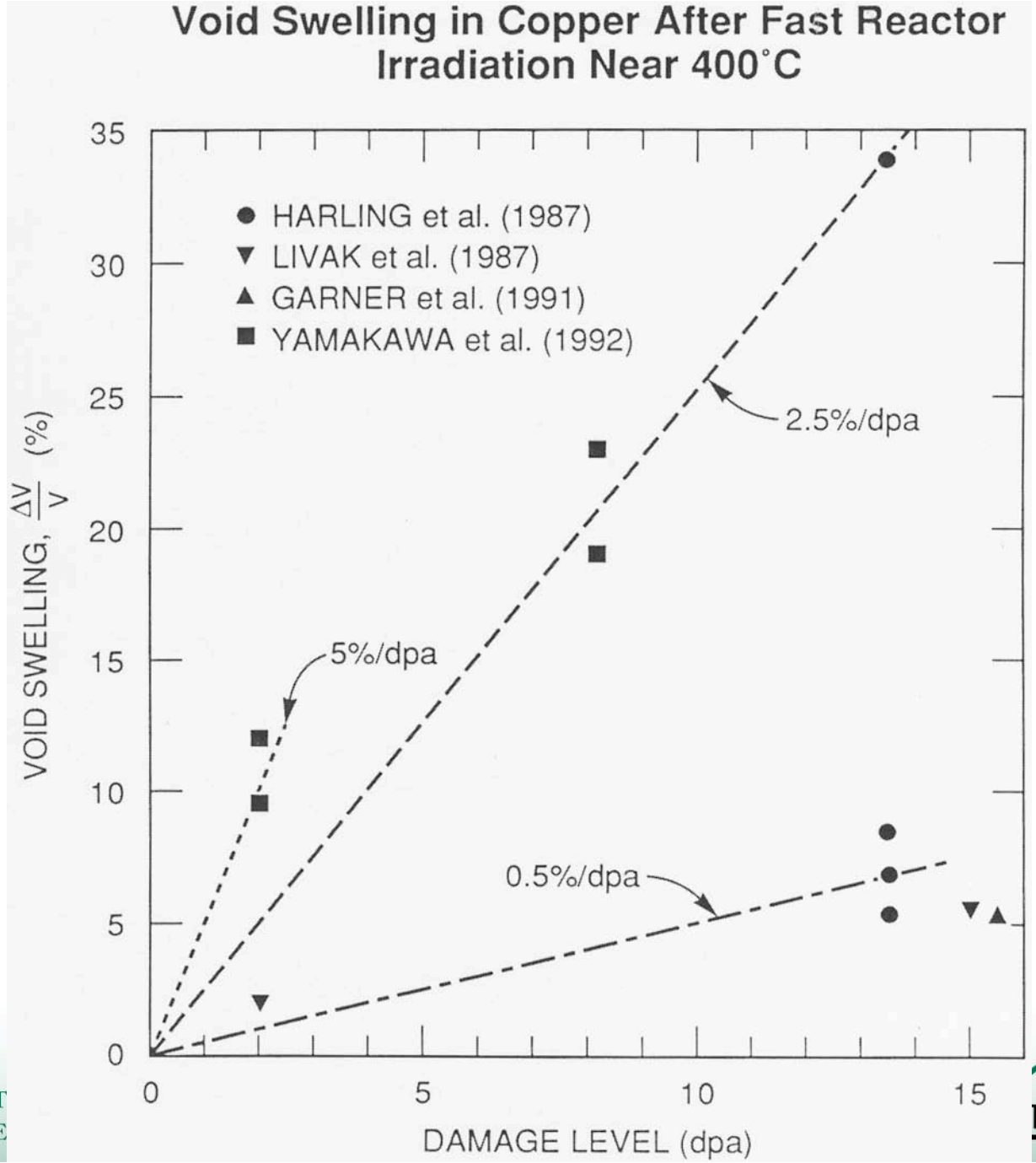
Void Swelling in Copper After Fast Reactor Irradiation Near 400˚C
HARLING et al. (1987)
LIVAK et al. (1987)
GARNER et al. (1991)
YAMAKAWA et al. (1992)
2.5%/dpa
5%/dpa
0.5%/dpa
VOID SWELLING, ΔV/V (%)
DAMAGE LEVEL (dpa)
0
5
10
15
20
25
30
35

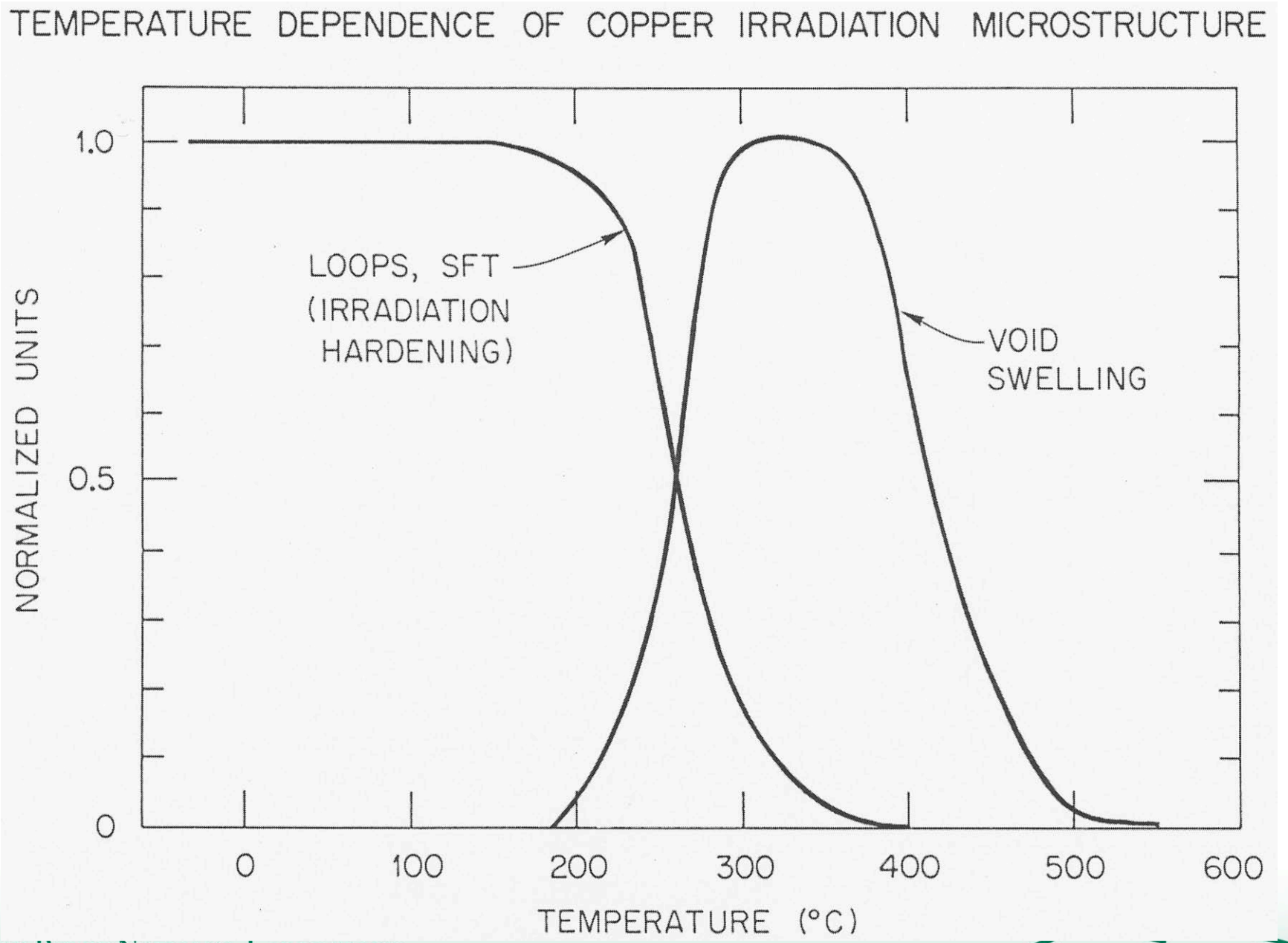
TEMPERATURE DEPENDENCE OF COPPER IRRADIATION MICROSTRUCTURE
NORMALIZED UNITS
1.0
0.5
0
LOOPS, SFT
(IRRADIATION
HARDENING)
VOID
SWELLING
0
100
200
300
400
500
600
TEMPERATURE (°C)

Quantification of small defect clusters is best performed using weak beam microscopy

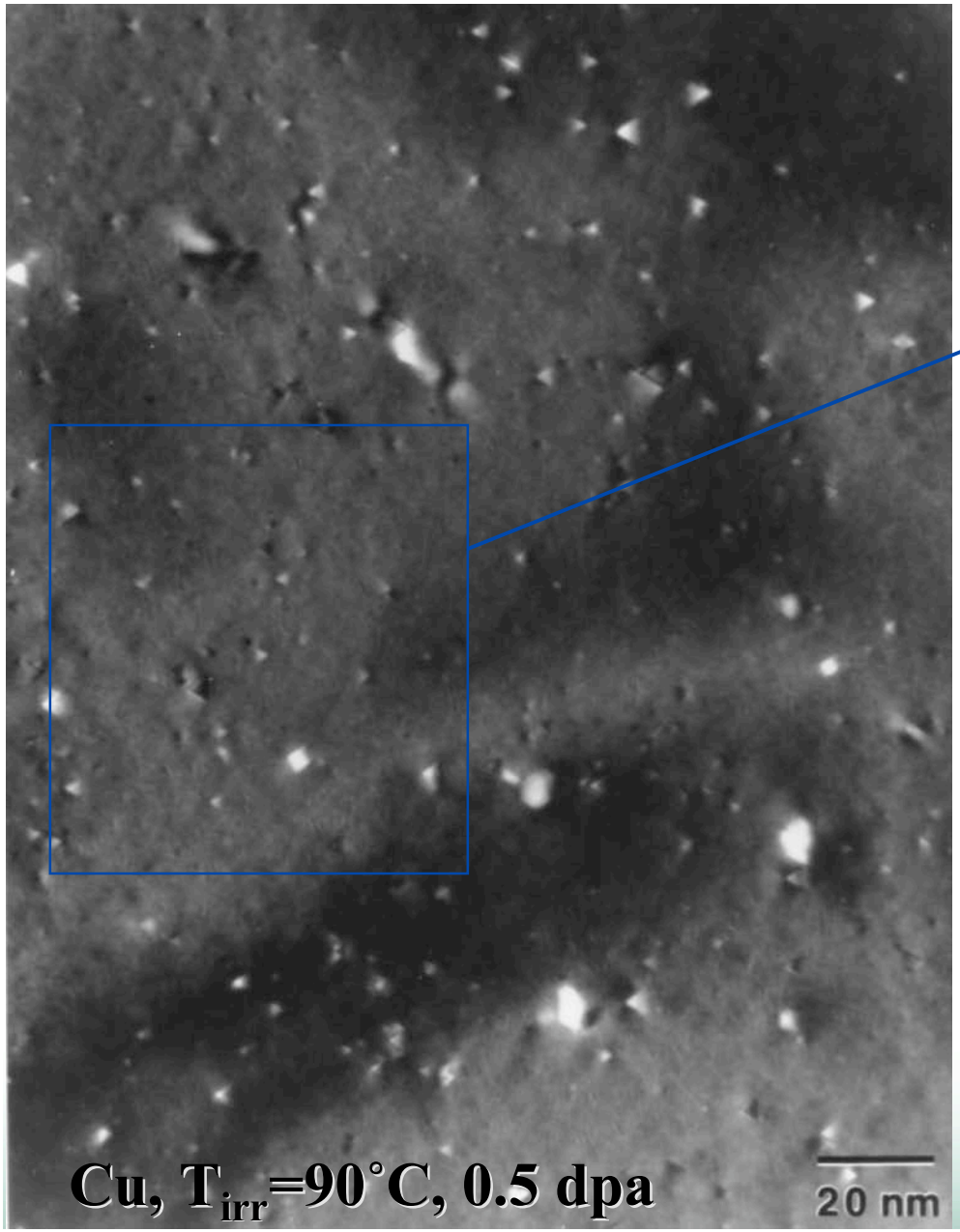

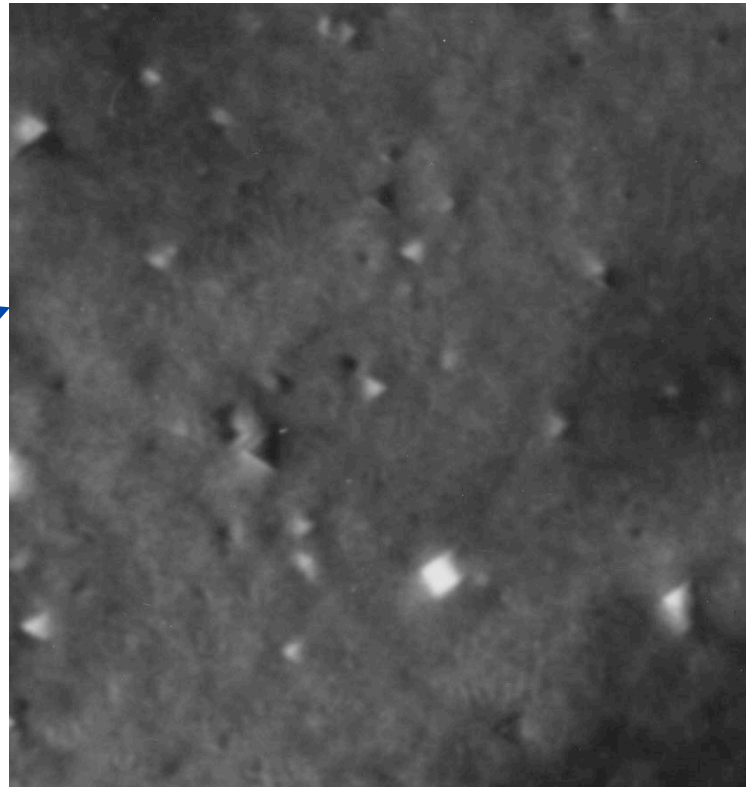

- Dark-diffracting defects are visible in suitably-thin foil regions
- Differentiation between SFTs and partially dissociated loops requires observation at B=001 and B=110

UT-BATTELLE

Small defect clusters are not visible in foils with thickness above ~40 nm

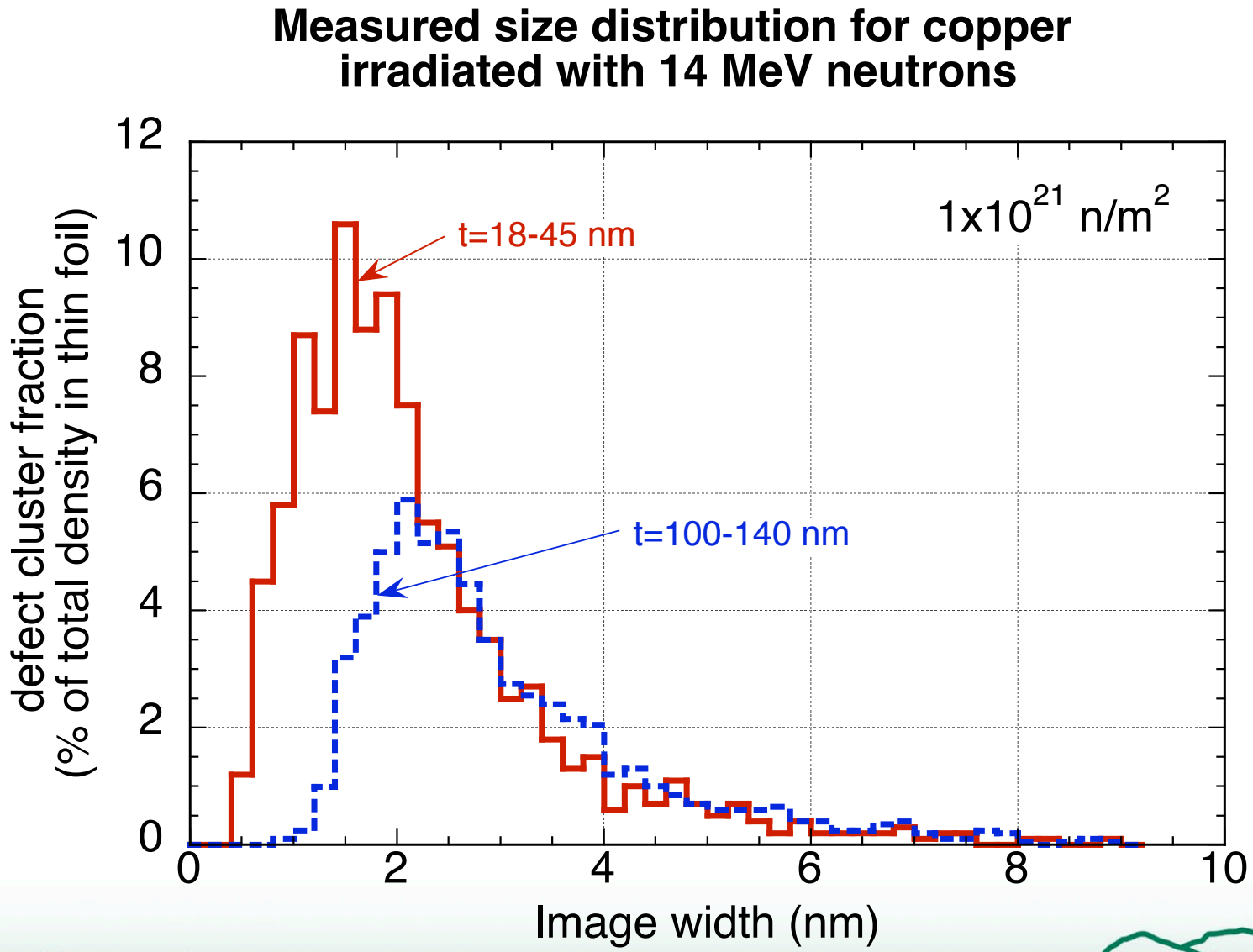

Defect cluster microstructure in Cu irradiated to 1 dpa at low temperature (~90˚C)

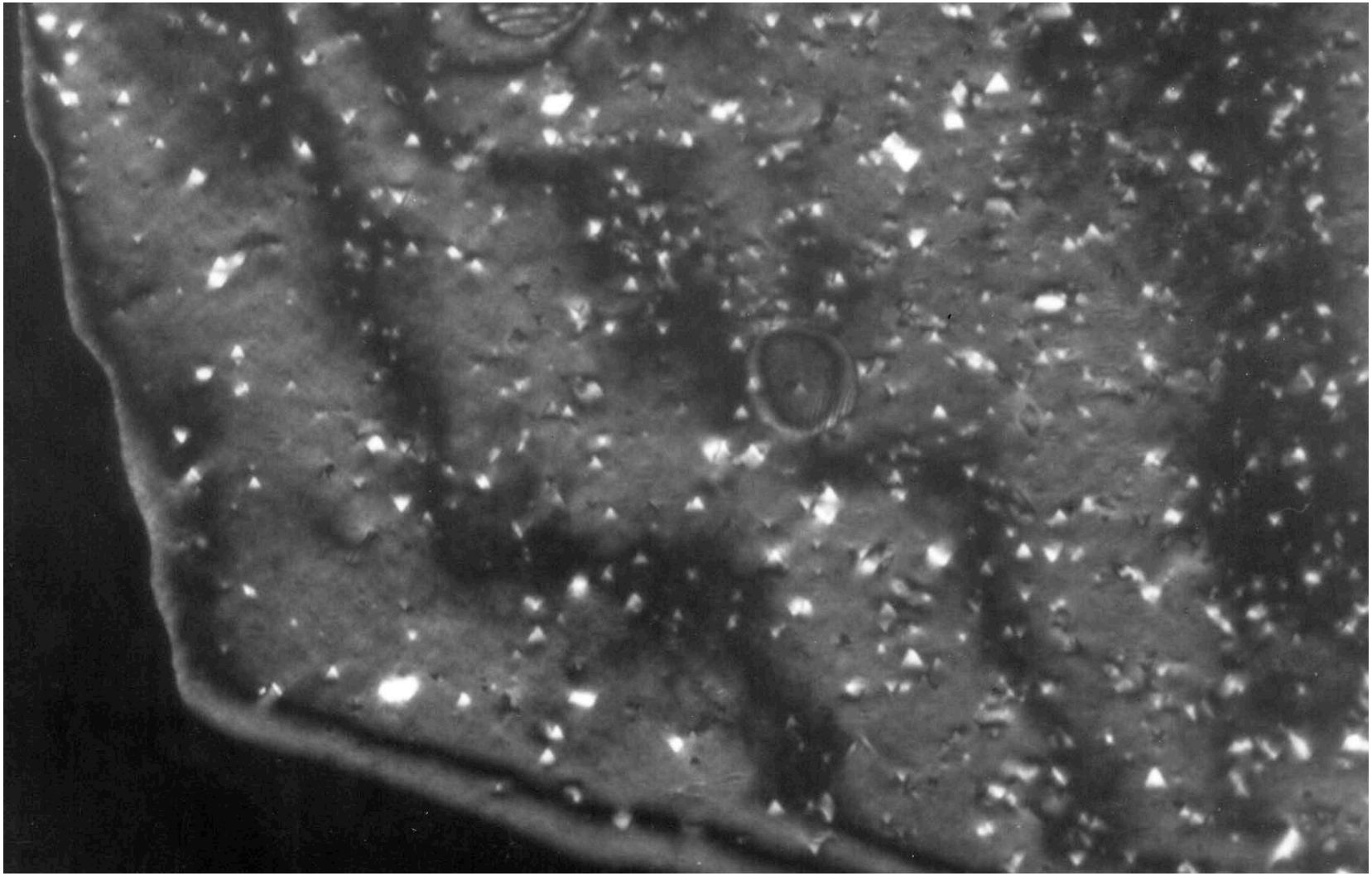

Visible microstructure depends on observation conditions

Medium-high magnification, thin region

Medium magnification, thicker region

Low magnification, thickest region

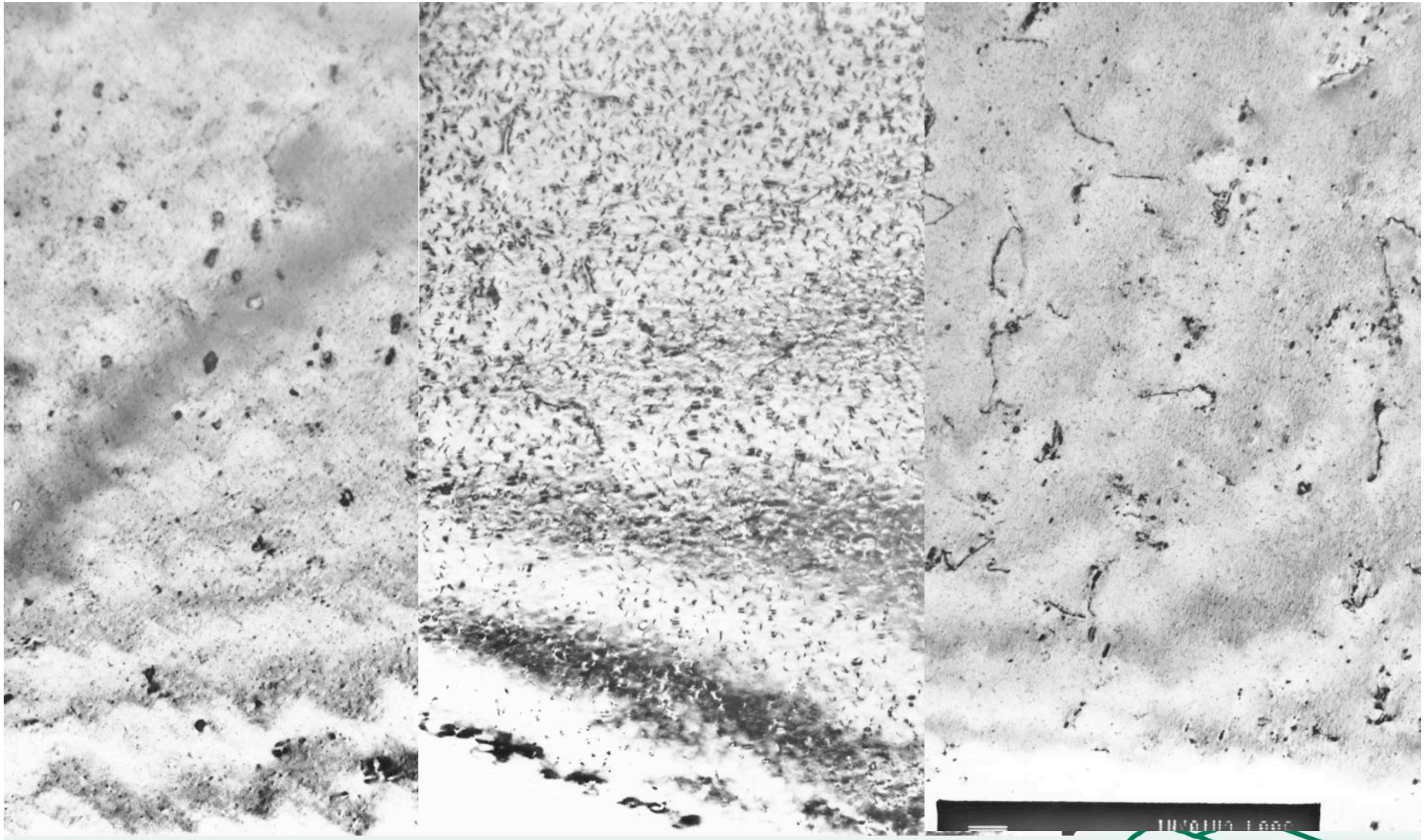

Neutron irradiated Cu, 14 dpa, 210˚C

Essential steps for accurate measurement of defect cluster densities

- Use very thin regions (t<40 nm) to count SFTs and small defect clusters (d<3 nm), using total magnifications >500 kx
- Count larger (d>3 nm) defect clusters vs. foil thickness in "thicker" foil regions (50-200 nm)
- Check for possible defect cluster invisibility and/or loss of glissile clusters to foil surface by analyzing areal cluster density vs. foil thickness
  - Plot should linearly extrapolate to the origin

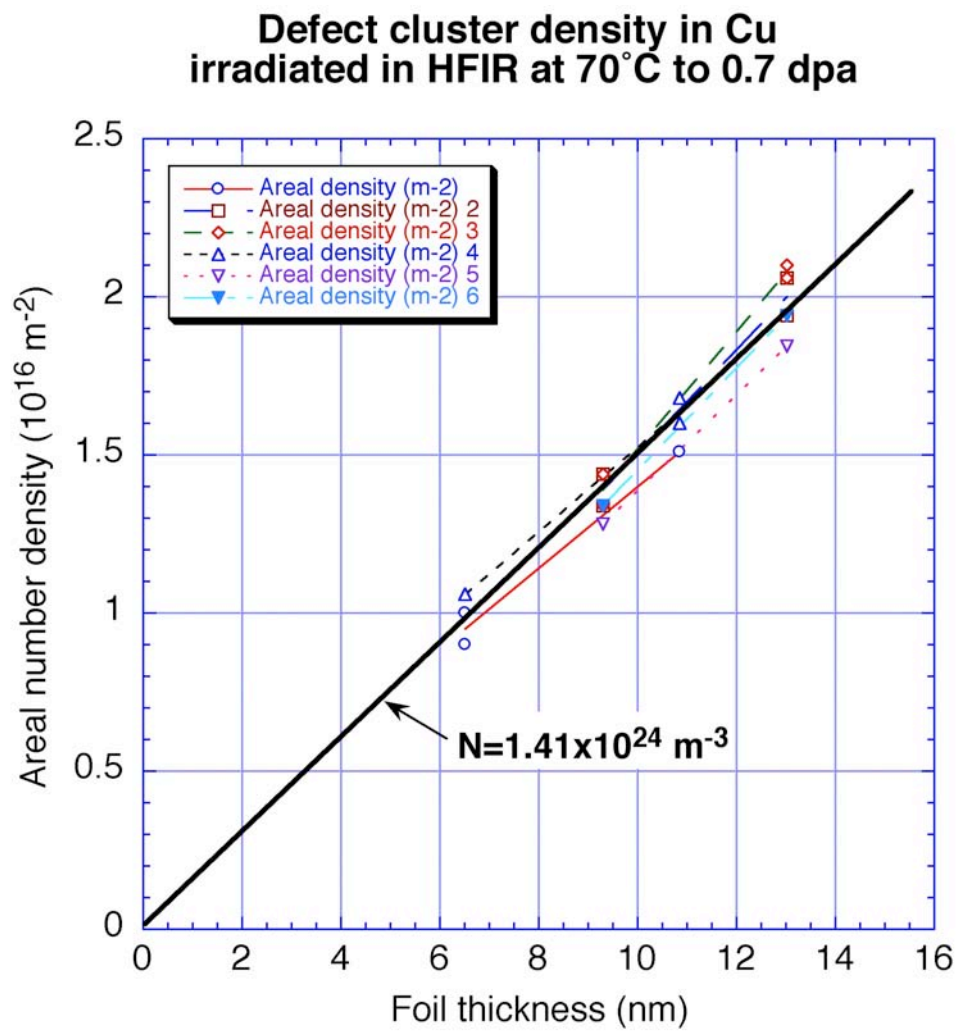

Dose Dependence of Defect Cluster Accumulation

(T_{irr}>Stage I)

- Early studies reported "nearly linear" dose dependence despite significant deviation from linearity
- Dose dependence even for early TEM studies of irradiated pure metals is better described by square root accumulation behavior

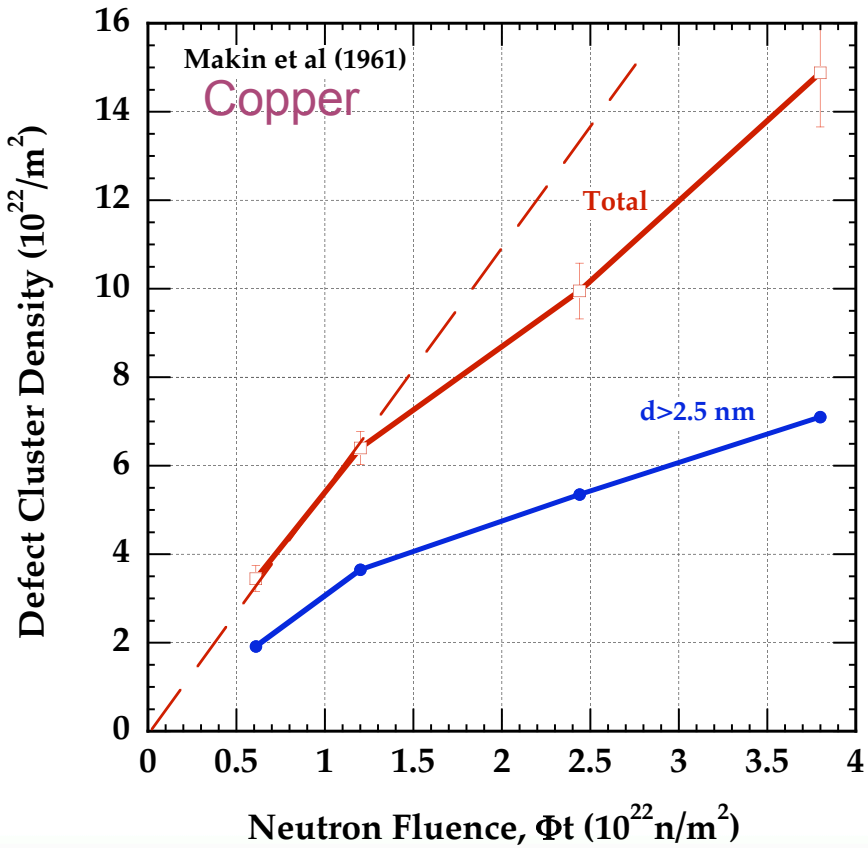

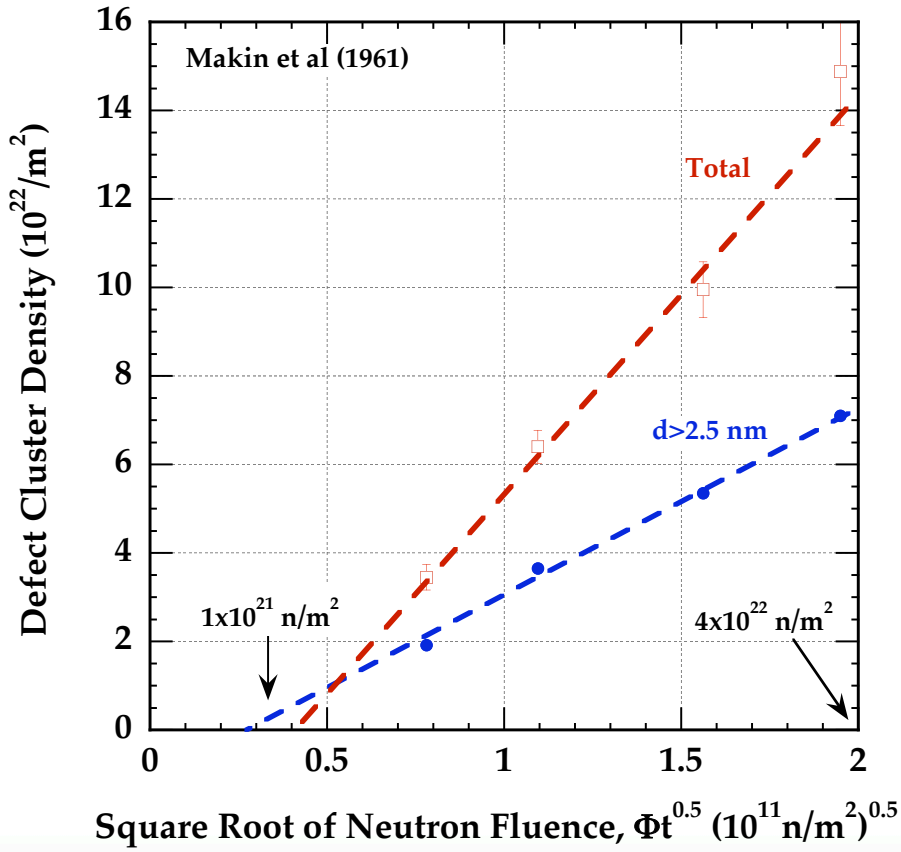

Dose Dependence of Defect Cluster Accumulation

Comparison of Dose Dependence of Electrical Resistivity and Defect Cluster Density in 14 MeV Neutron Irradiated Copper

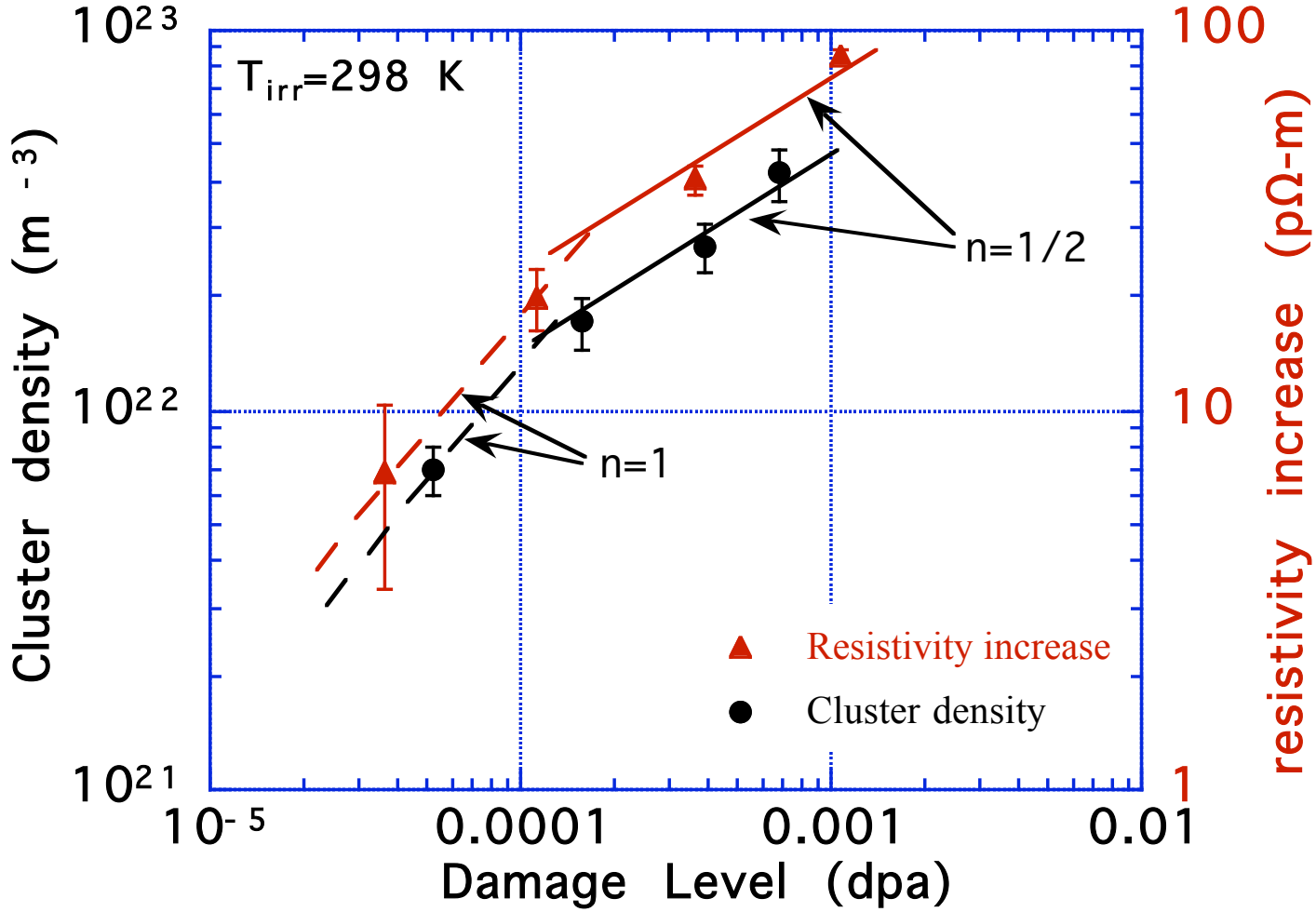

- Data analysis based on unsaturable trap model indicates freely migrating interstitial fraction is f_i~11%

Electrical resistivity is very sensitive to solute clustering events (overwhelms radiation defect resistivity increase)

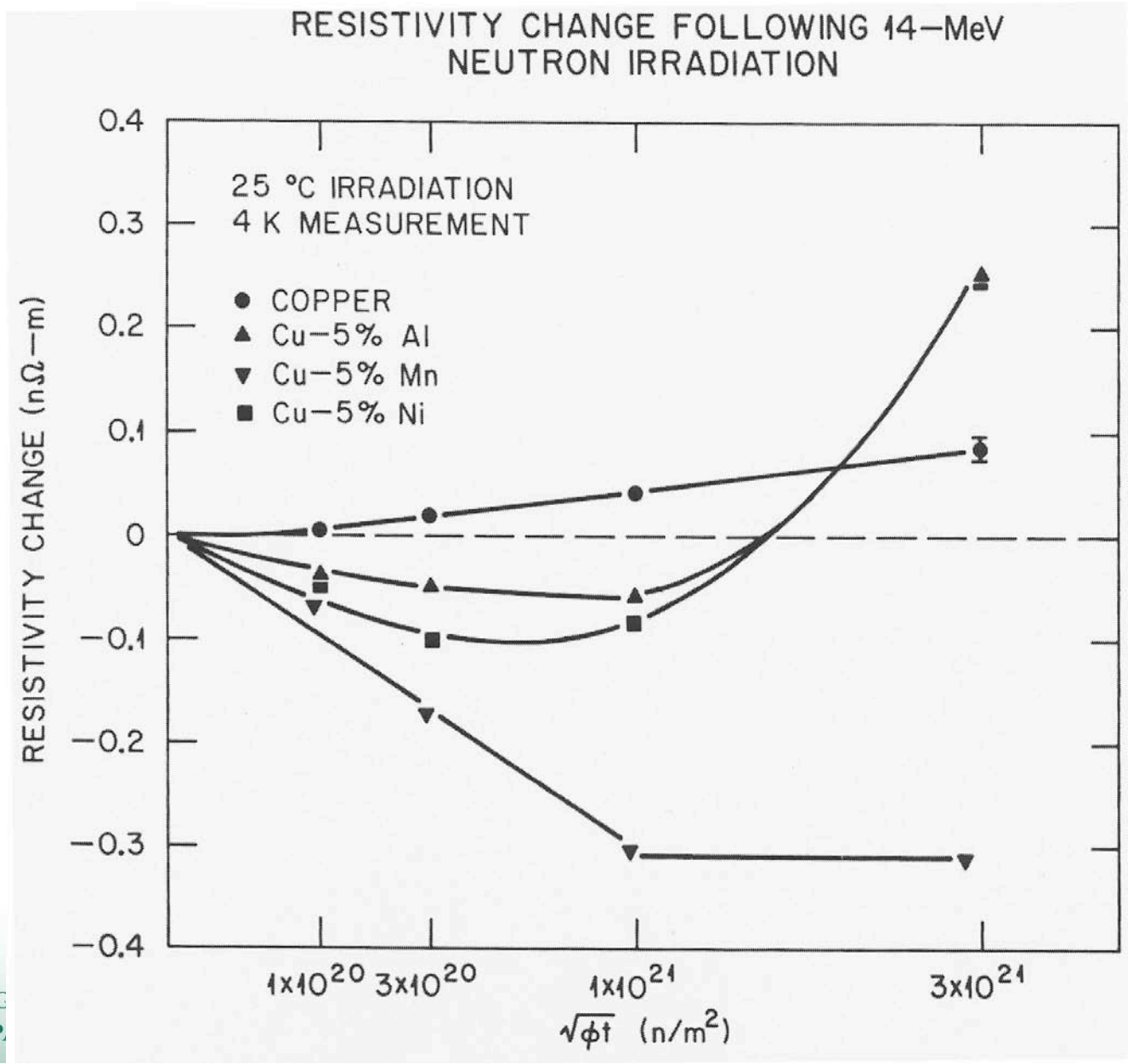

Defect clusters in neutron irradiated copper (low T)

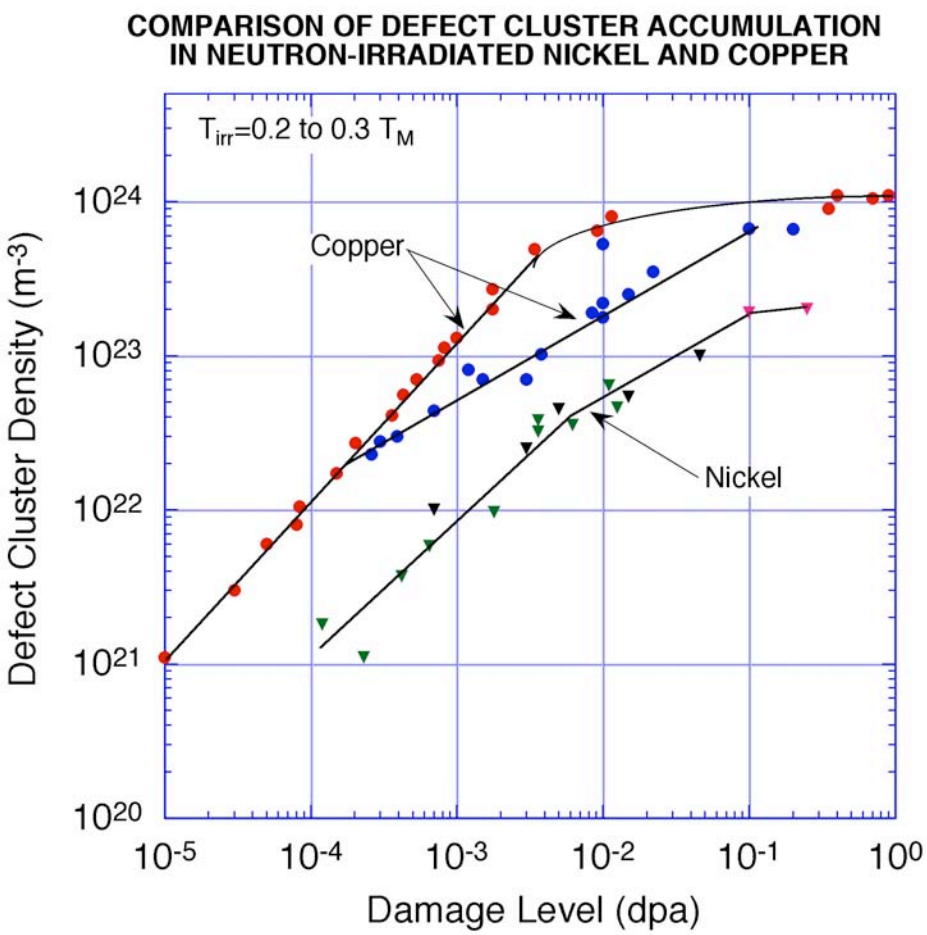

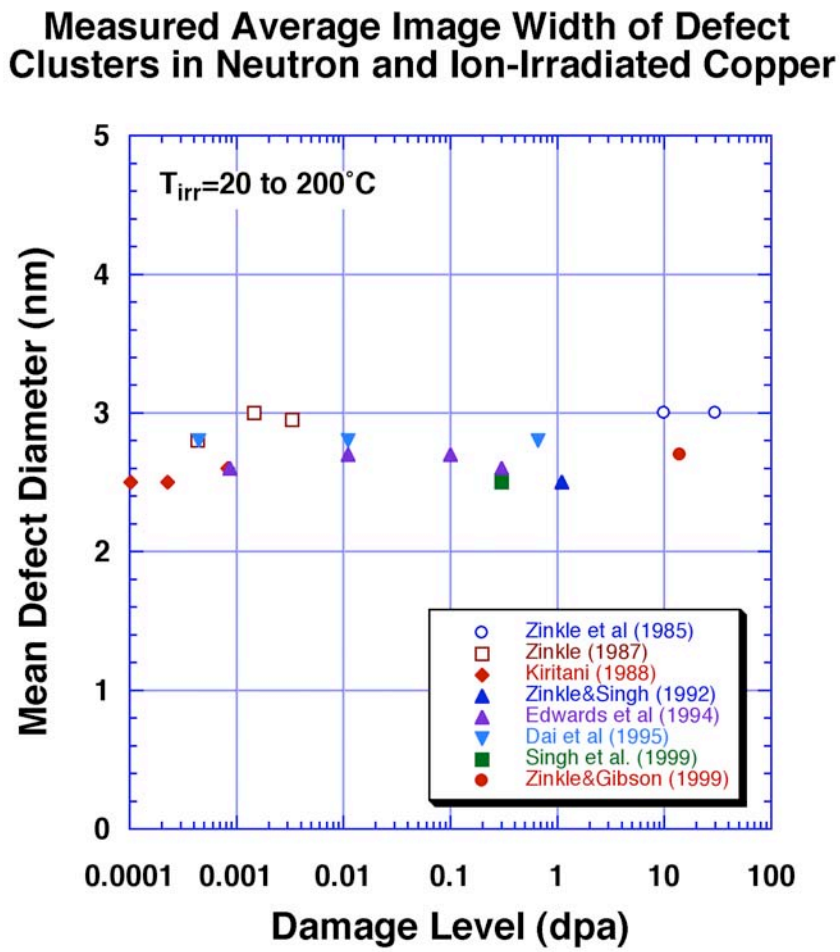

Evidence for direct formation of SFTs in displacement cascades in irradiated copper

- SFTs are observed at doses as low as ~10^{-5} dpa (lowest dose investigated)
  - Observed in both bulk and thin-foil neutron irradiated specimens, with comparable densities at low doses
- SFT density is proportional to dose up to cluster densities where significant annihilation due to mobile interstitials or cascade overlap processes occur
- SFT density is similar in irradiated pure Cu and Cu-100 ppm B alloy containing a high cavity density (cavity sink strength ~$10^{15}/m^2$)
- SFT mean size is approximately constant for doses ranging over ~6 orders of magnitude (10^{-5} to 10 dpa)

Copper and nickel neutron-irradiated to ~0.1 dpa at 230˚C

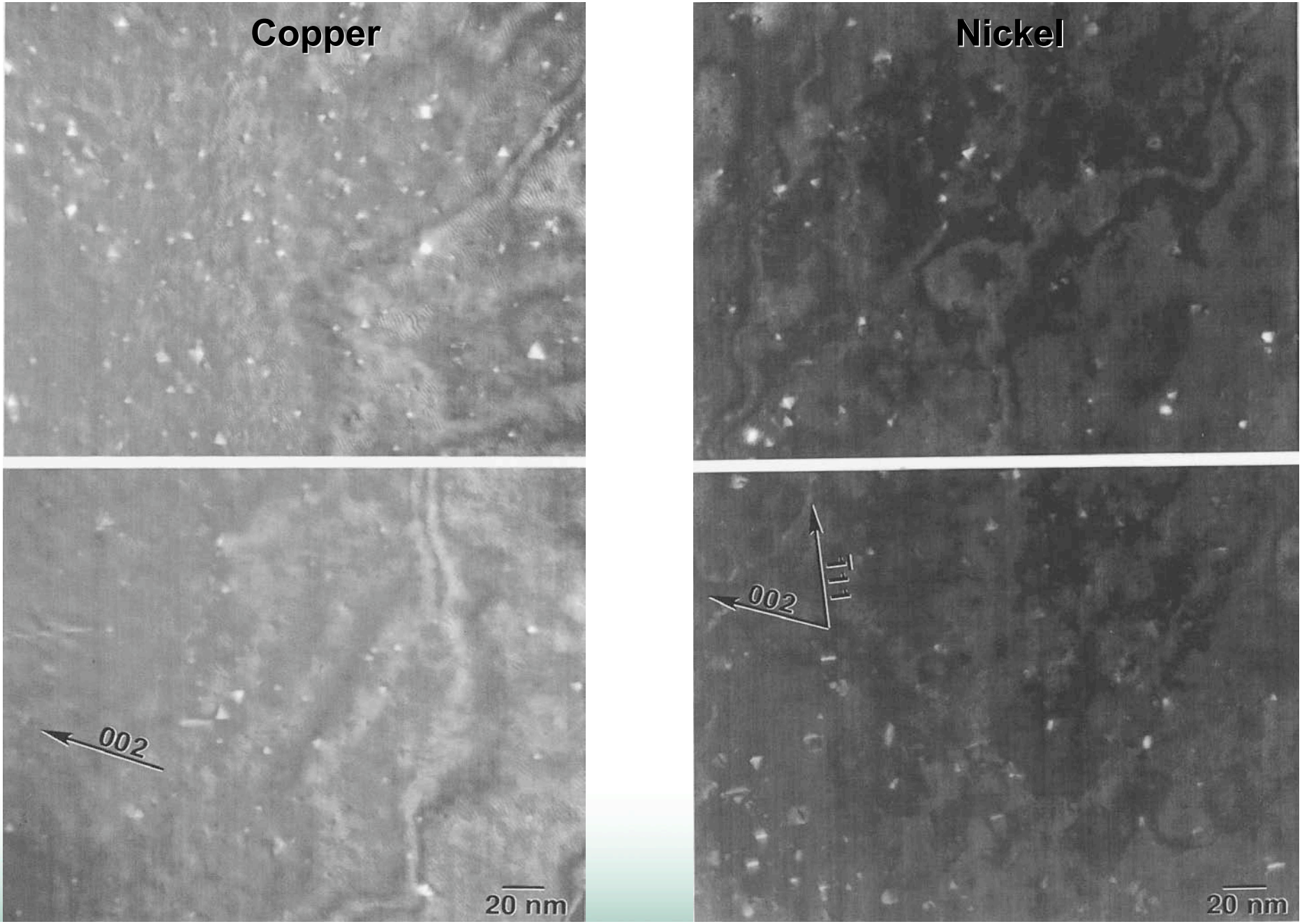

Comparison of defect cluster evolution in neutron irradiated Cu and Ni (low T)

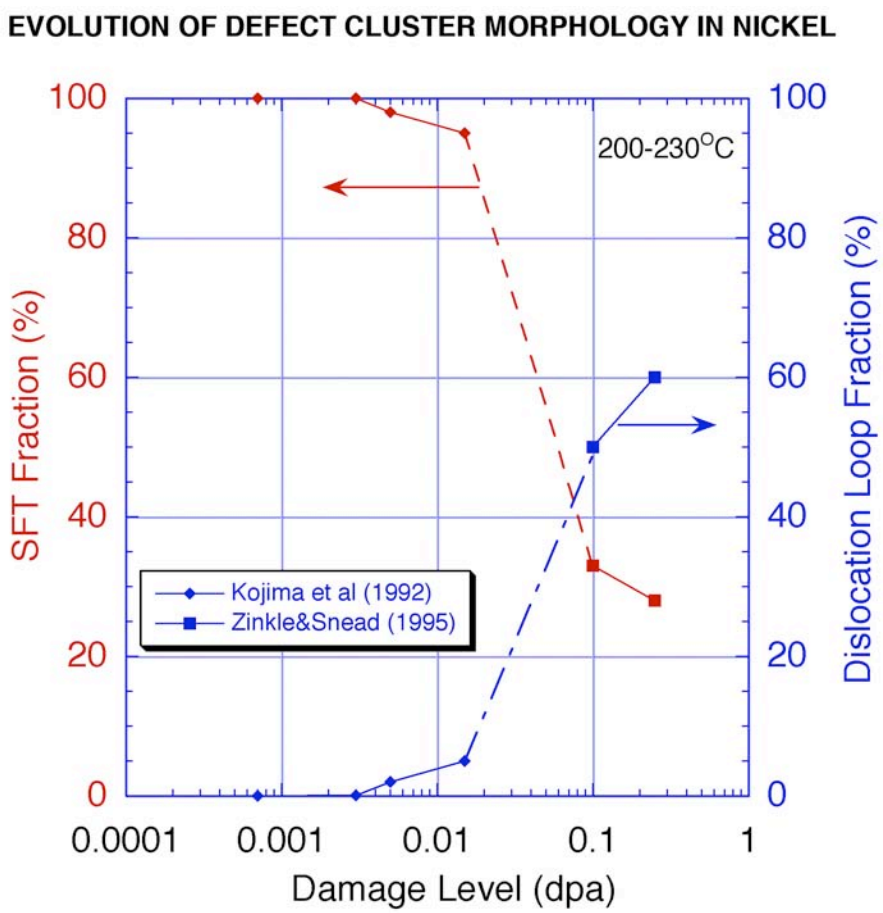

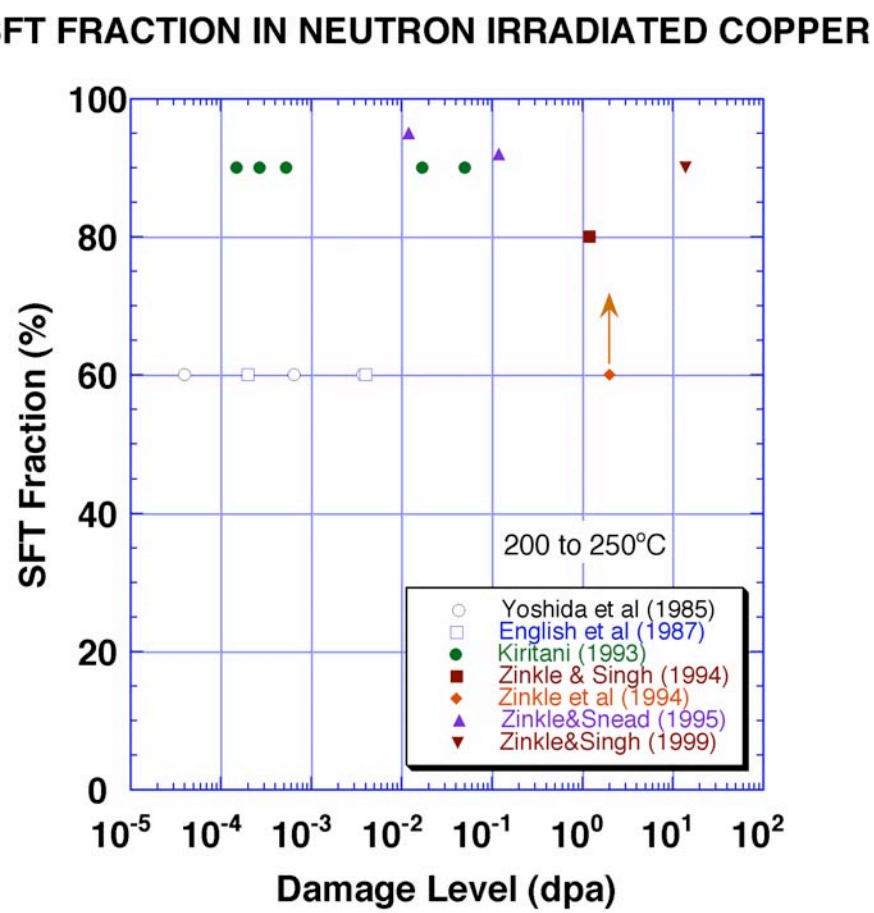

Defect cluster density in neutron-irradiated stainless steel coarsens slightly between 0.06 and 0.5 dpa

T_{irr}=120˚C

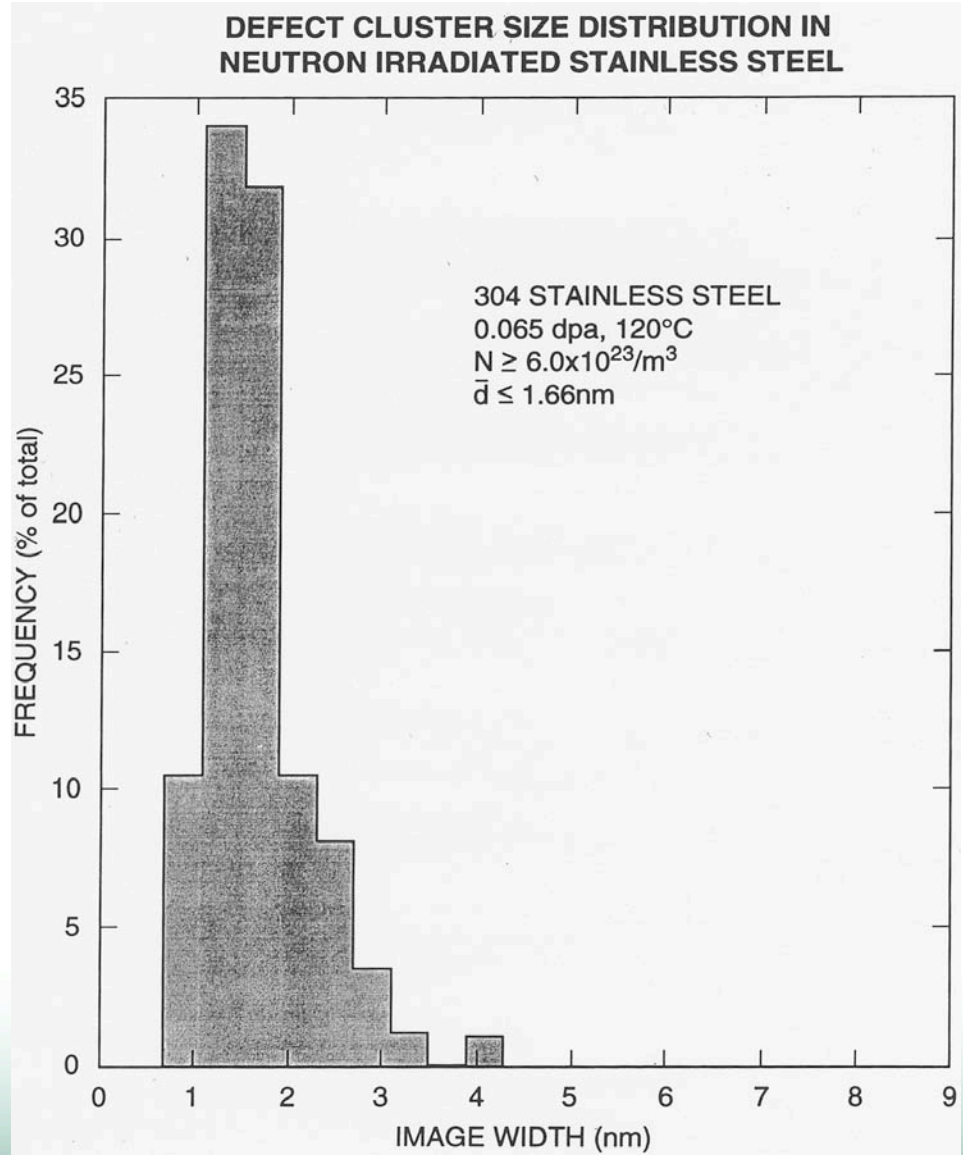

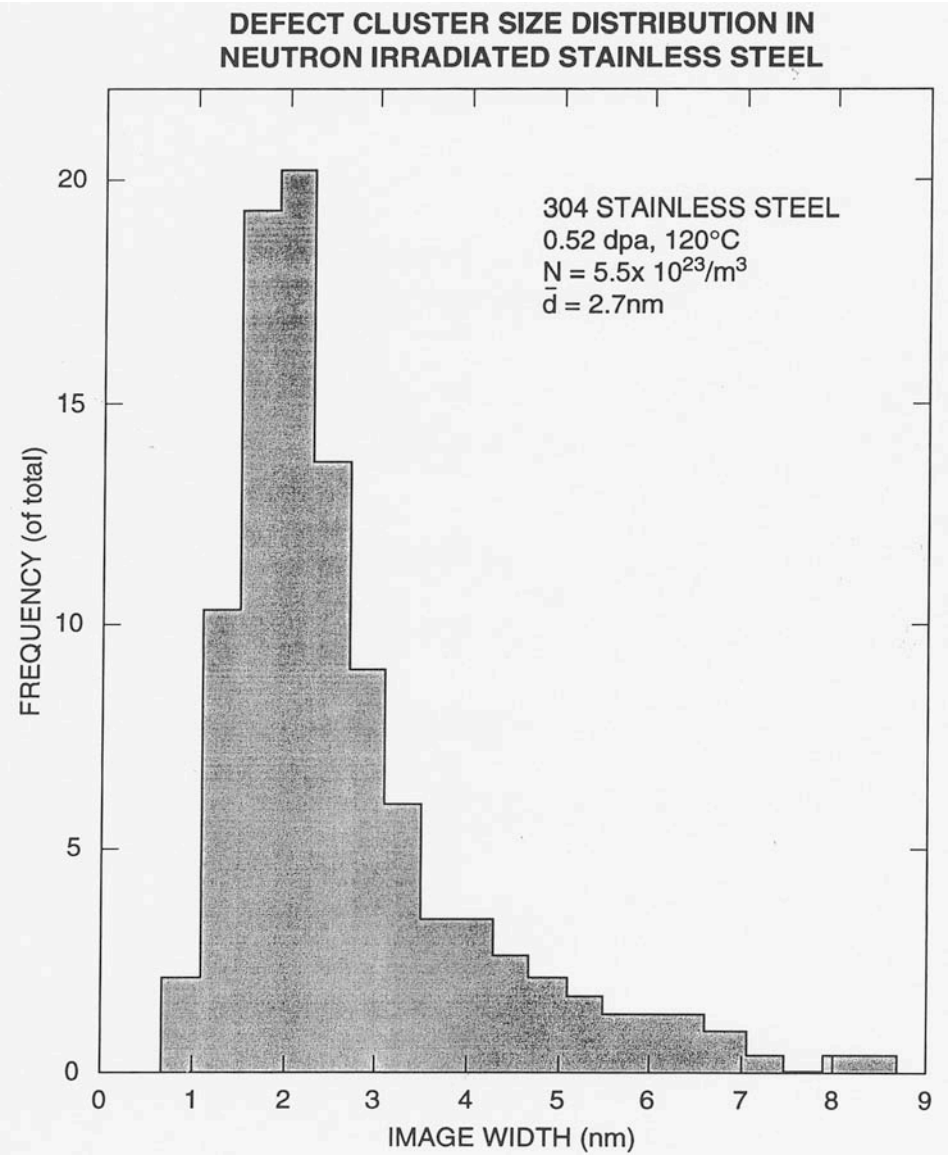

Black Spot Defect Cluster evolution in neutron-irradiated Cu at 70˚C

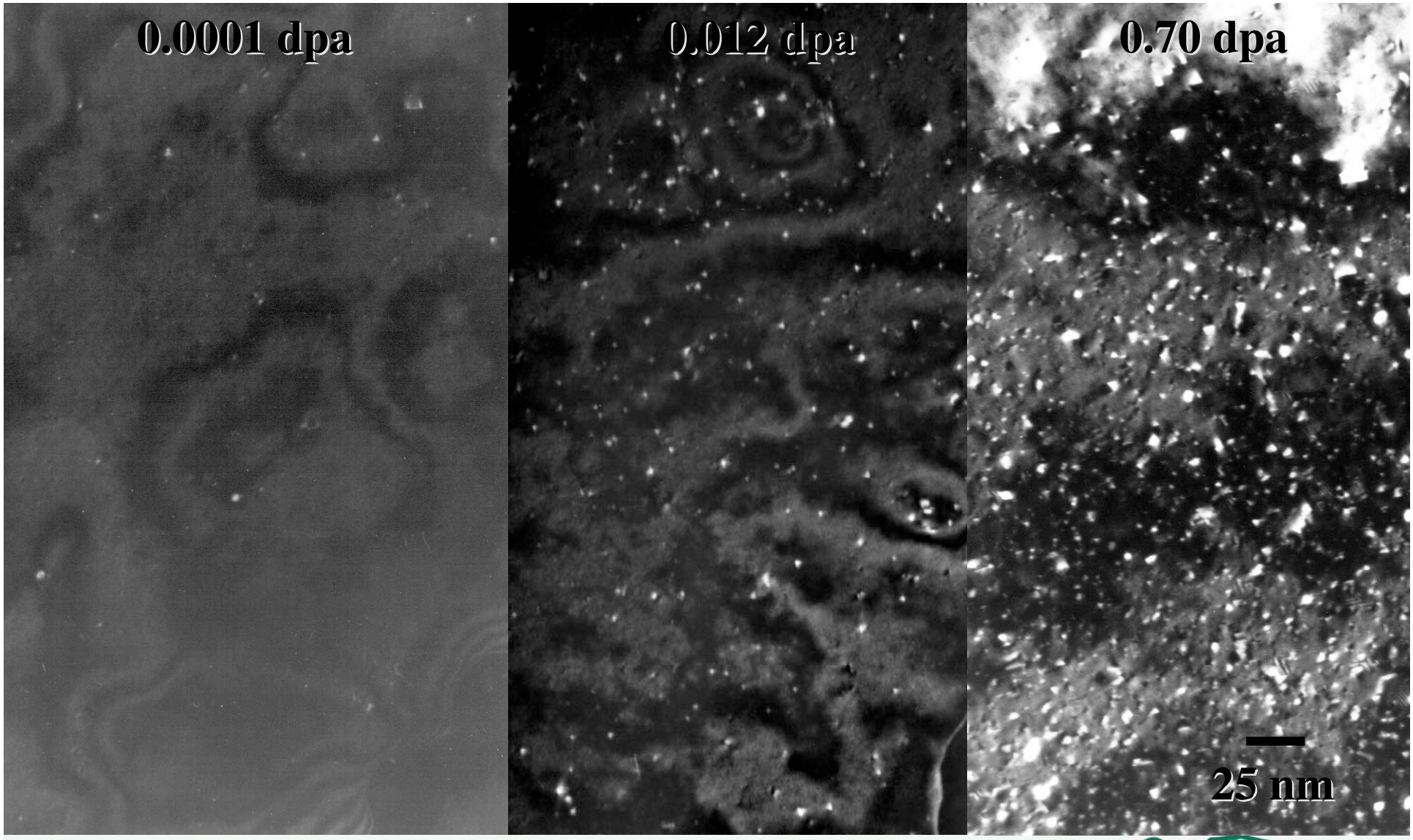

Dislocation loop evolution in neutron-irradiated Cu at 70°C

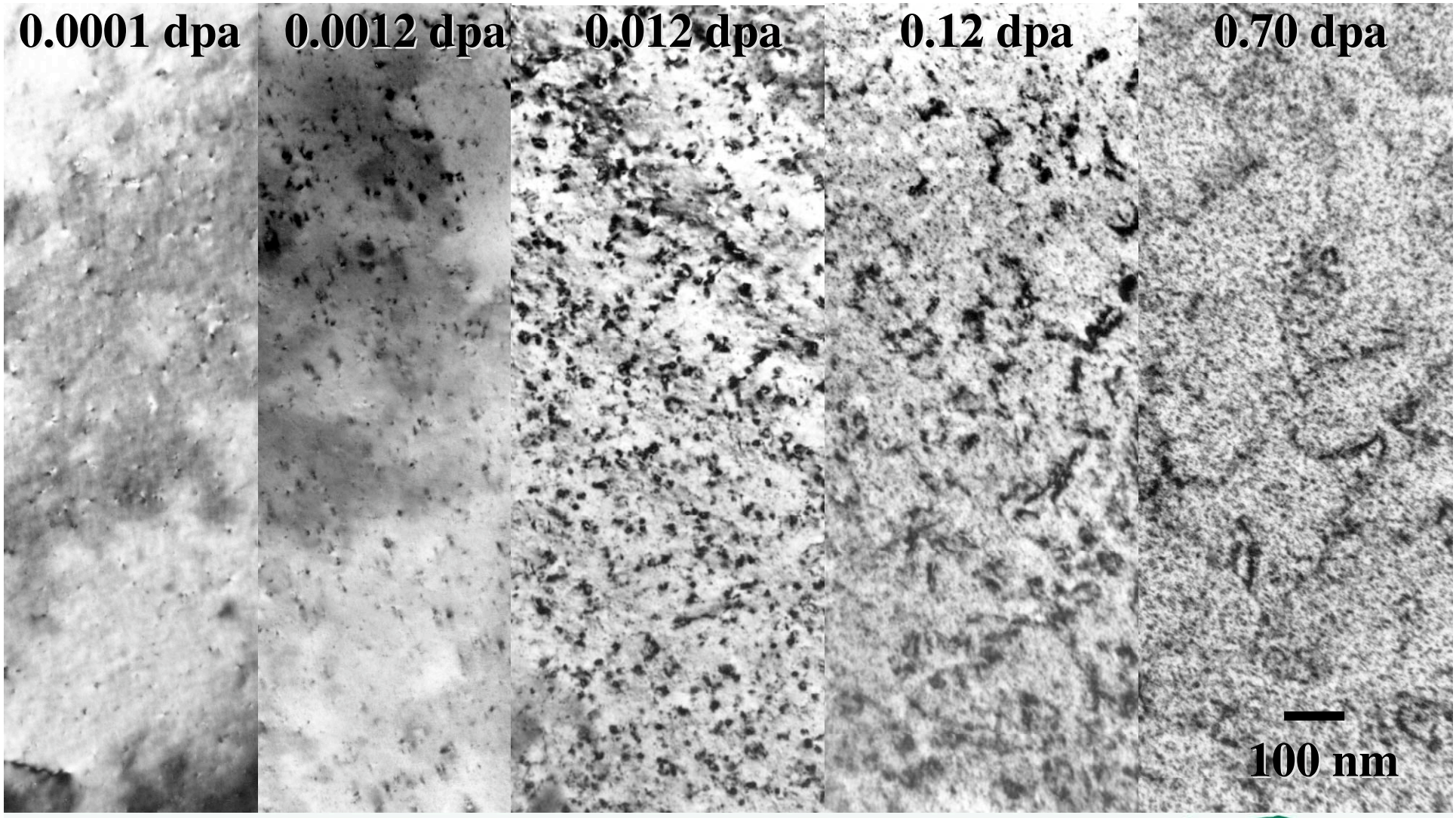

Peak loop density occurs at ~0.01 dpa

Dislocation loop formation is enhanced in Cu alloys irradiated below Stage V

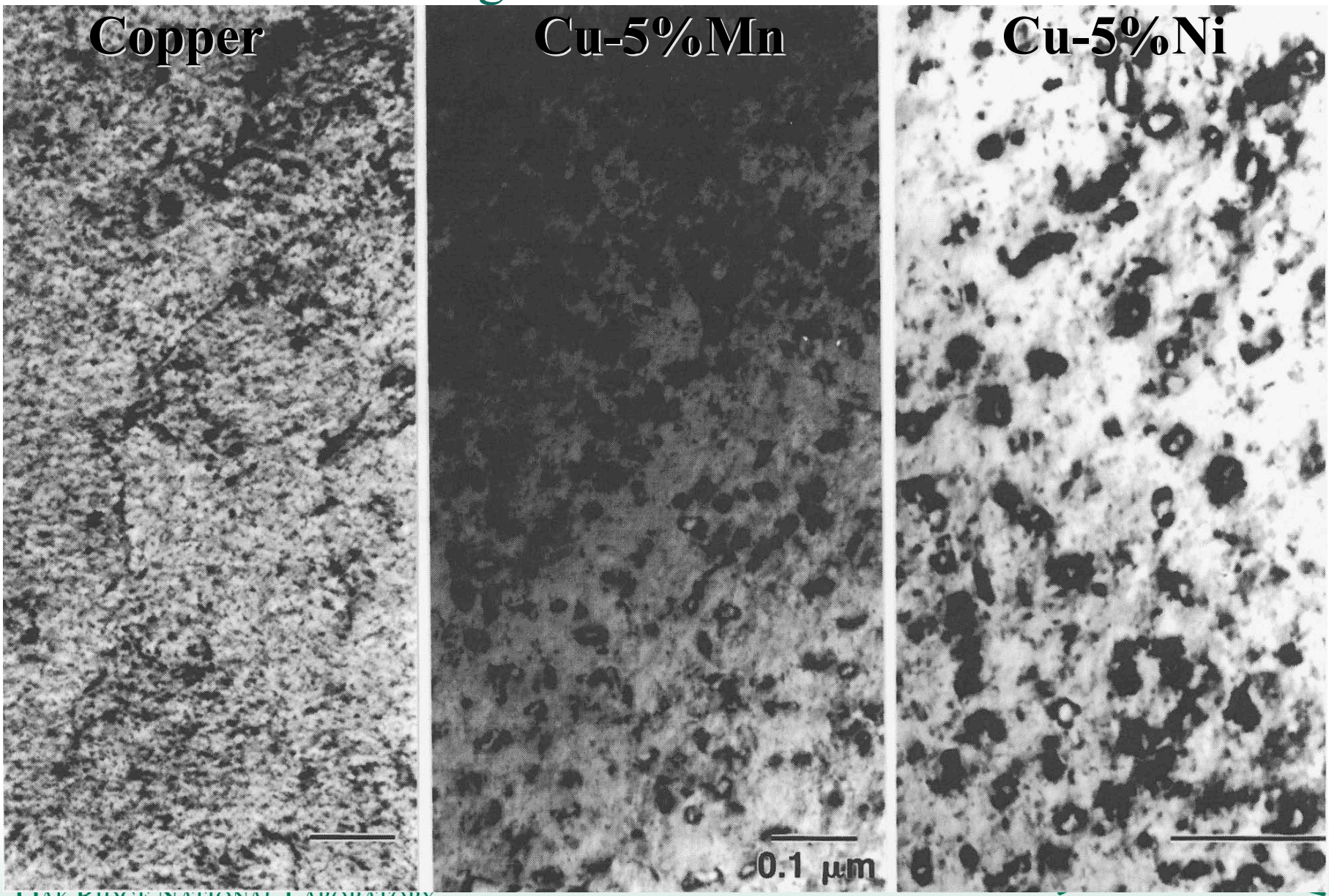

~1 dpa, 100˚C, LAMPF

Dislocation loop formation is enhanced in Cu alloys irradiated below Stage V

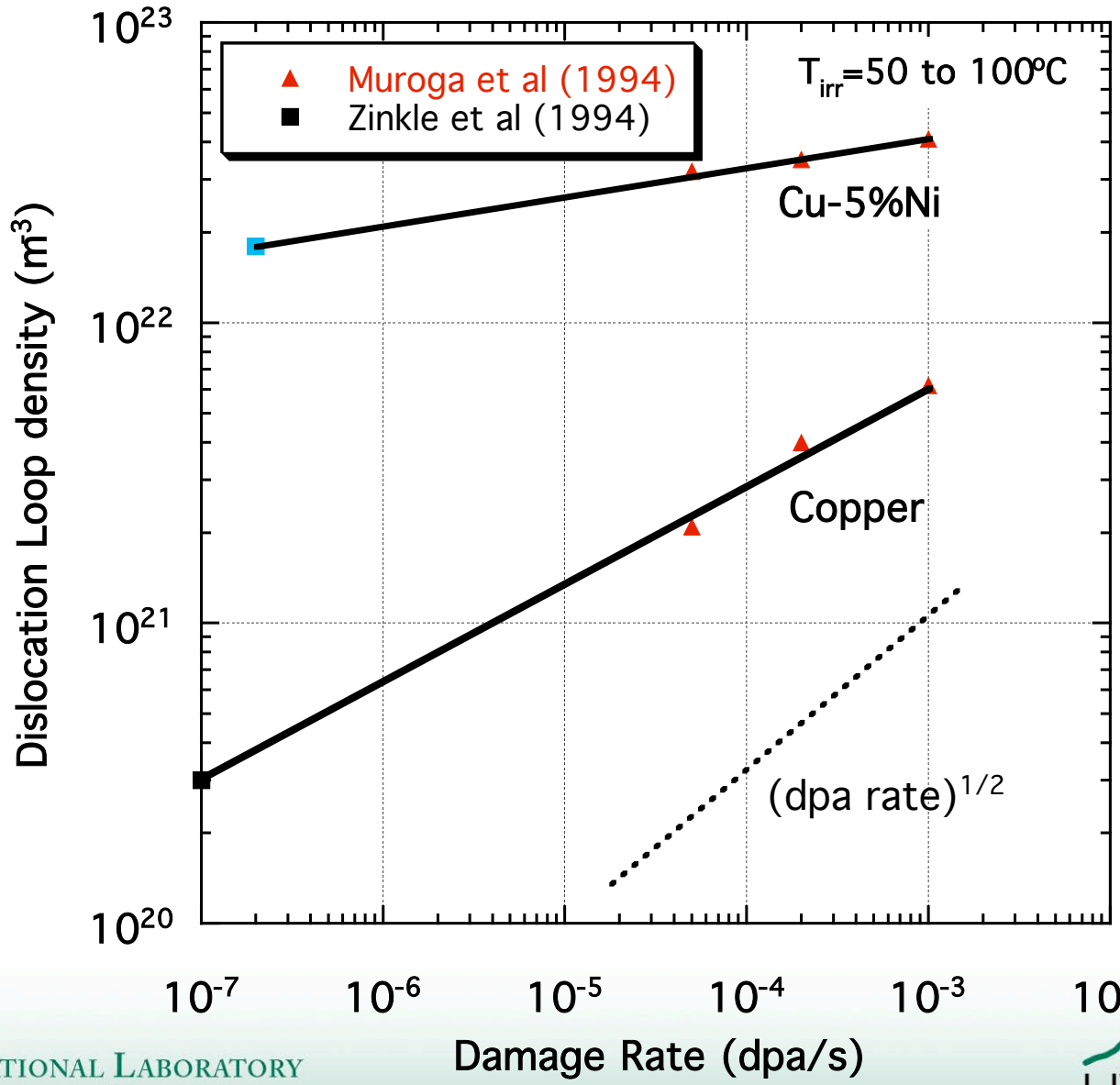

Alloying effect on Cu dislocation loop formation appears to be minor above Stage V

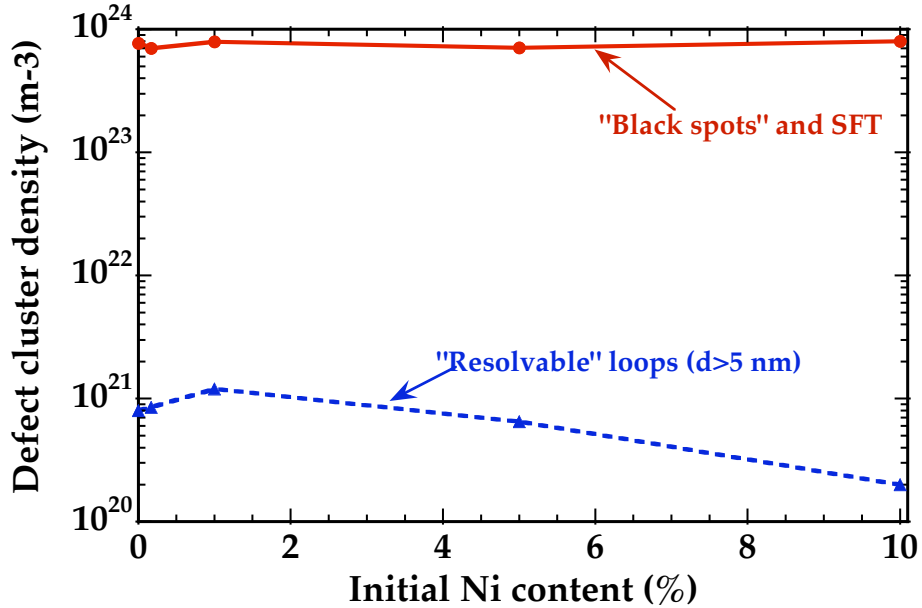

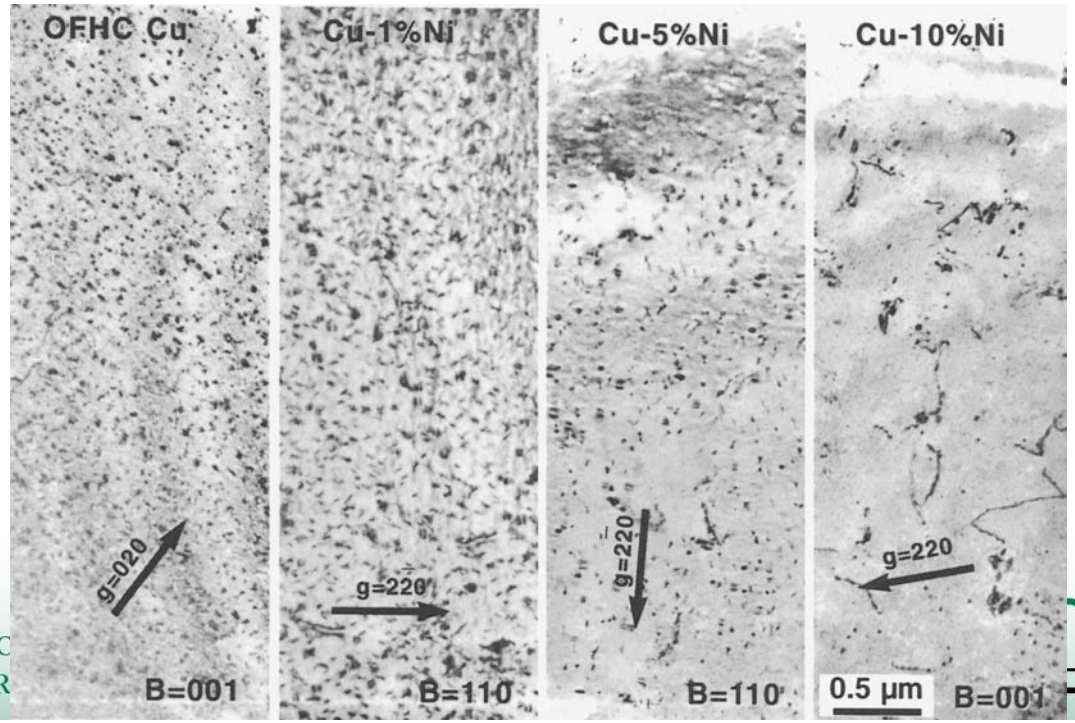

Comparison of 20 keV cascades in iron and copper based on molecular dynamics simulations

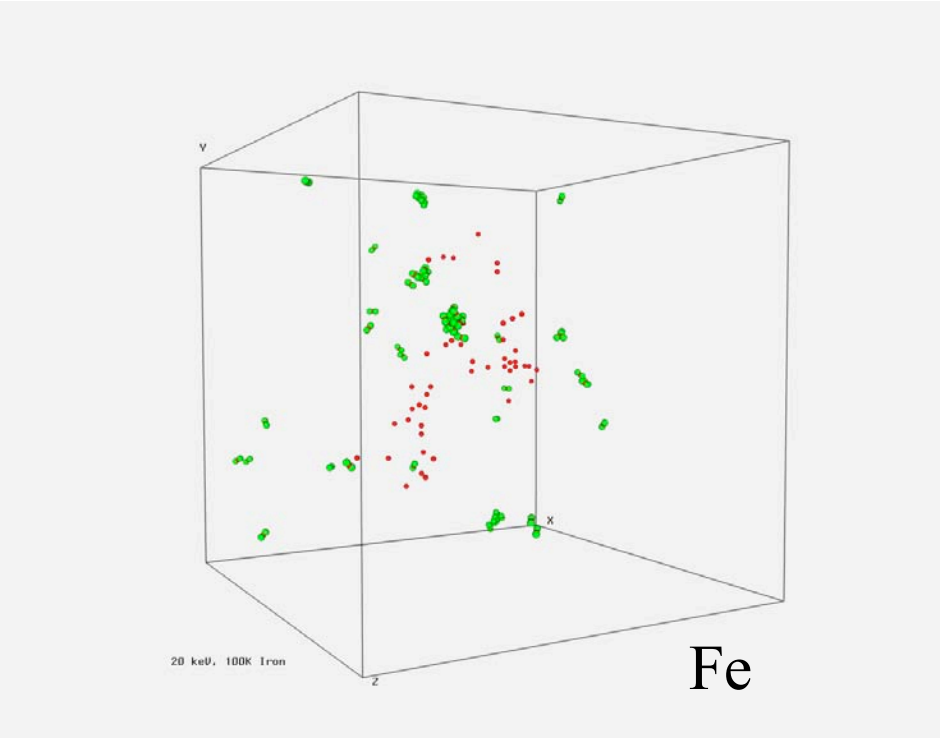

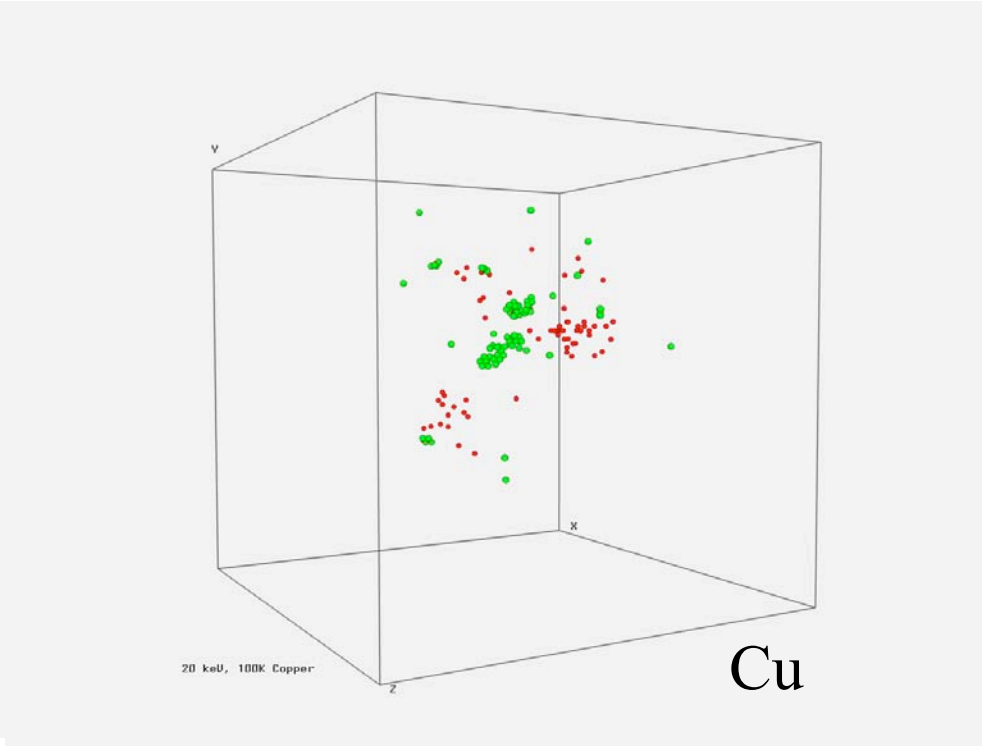

- Similar embedded atom type interatomic potentials, edge length of simulation cells are $50a_o$.
- Note higher level of in-cascade clustering in more-compact copper cascade.
- Defect survival (relative to NRT) is lower in copper than in iron.

Comparison of the defect cluster accumulation behavior of irradiated Cu and Fe

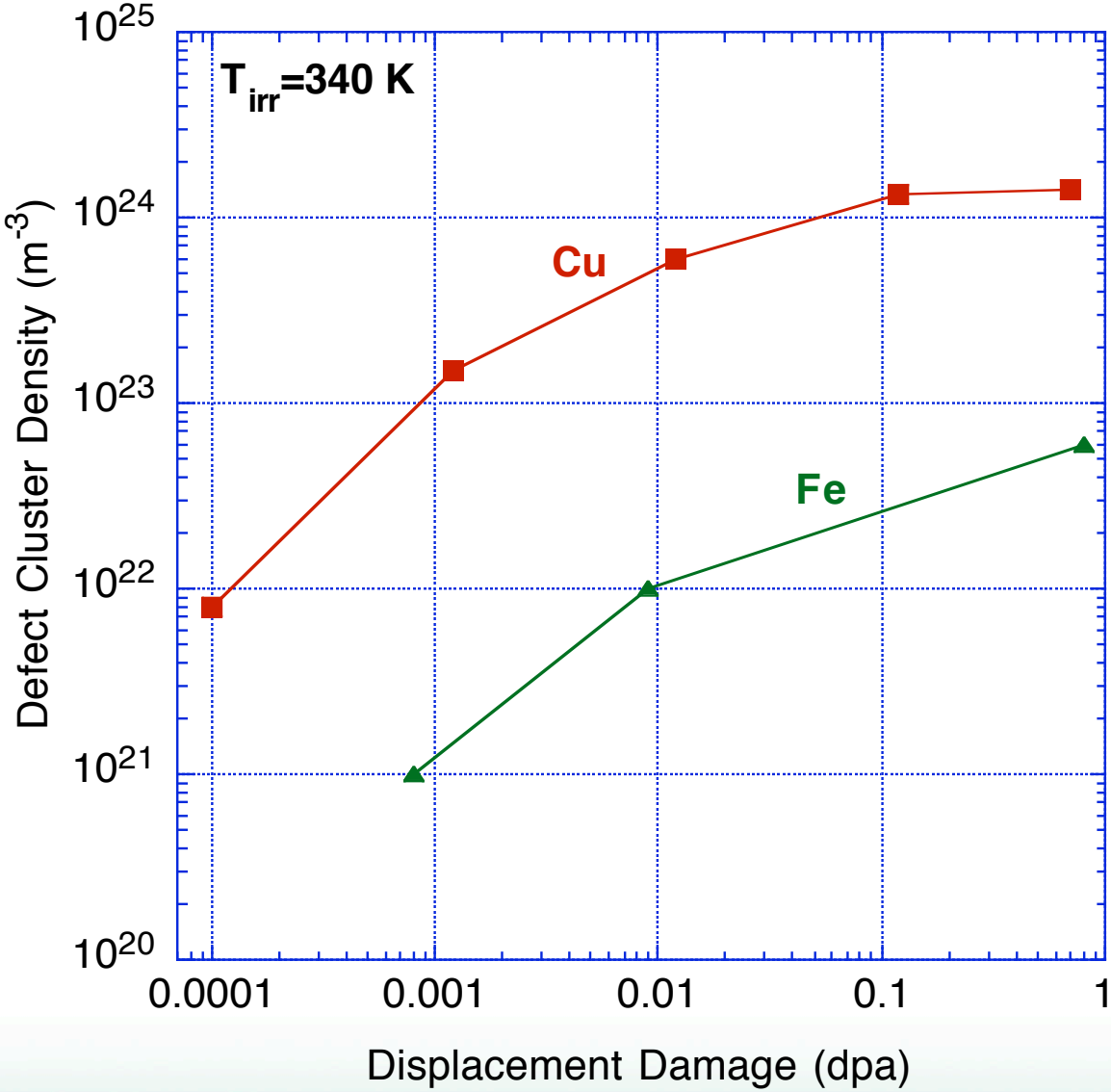

- Visible defect cluster densities are >10x lower for Fe than Cu
- Cu clusters are vacancy-type; Fe clusters are interstitial-type
- Dominant vacancy-type clusters in Fe (nanovoids) is not visible via TEM
  - Can be detected by positron annihilation spectroscopy
- Since vacancies are not tied up in planar defect clusters below Stage V in BCC metals, void swelling can occur at low temperature

Dislocation loop evolution in neutron-irradiated Fe at 70˚C

Visible defect clusters in Fe are not produced directly in displacement cascades

0.0001 dpa **0.0008 dpa** **0.009 dpa** **0.80 dpa**

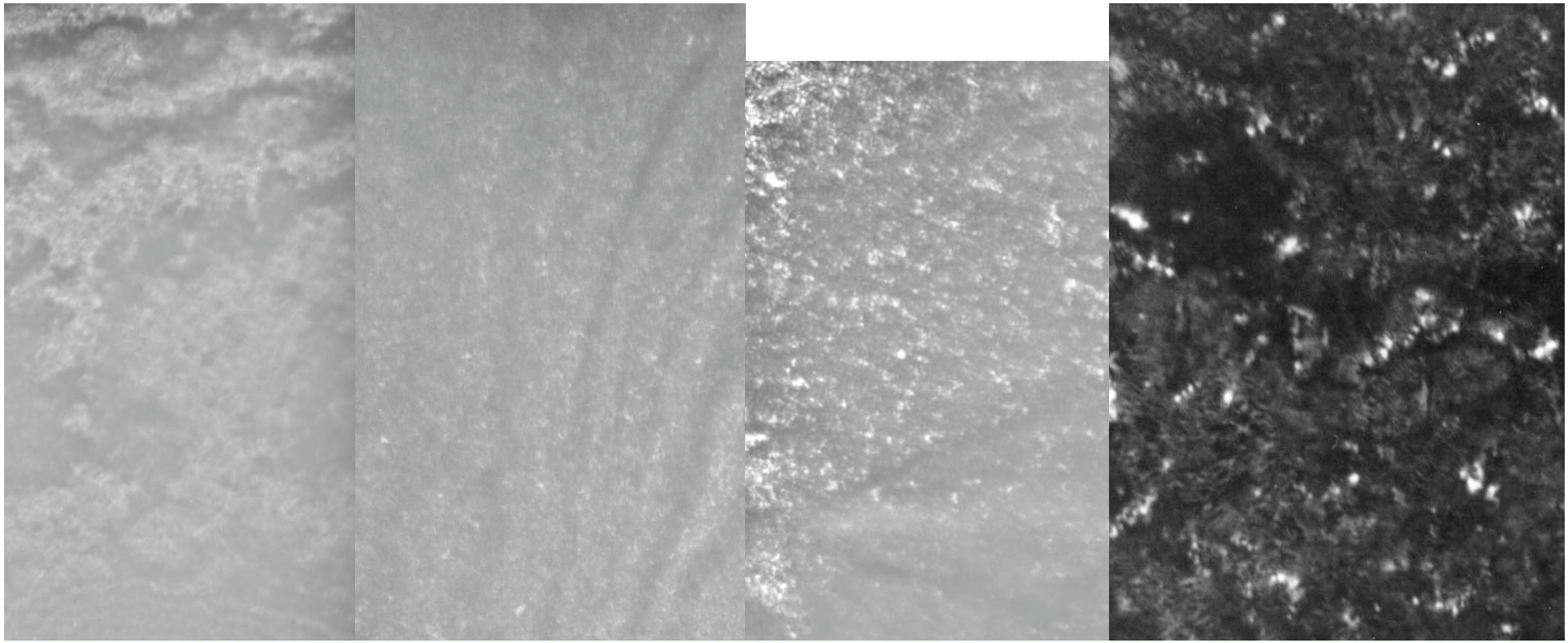

Loop density increases with dose up to ~0.8 dpa

Formation of dislocation loop rafts in Fe after neutron irradiation to 0.8 dpa at 70°C

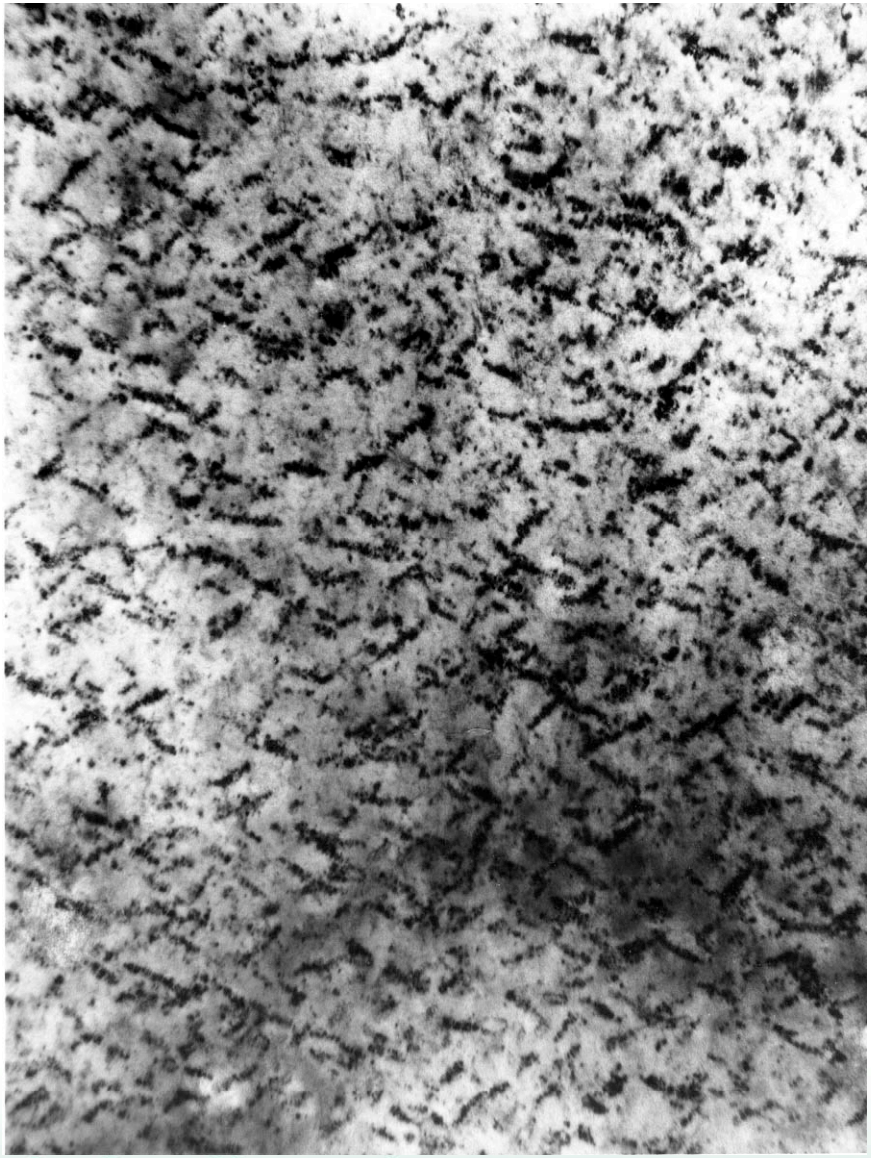

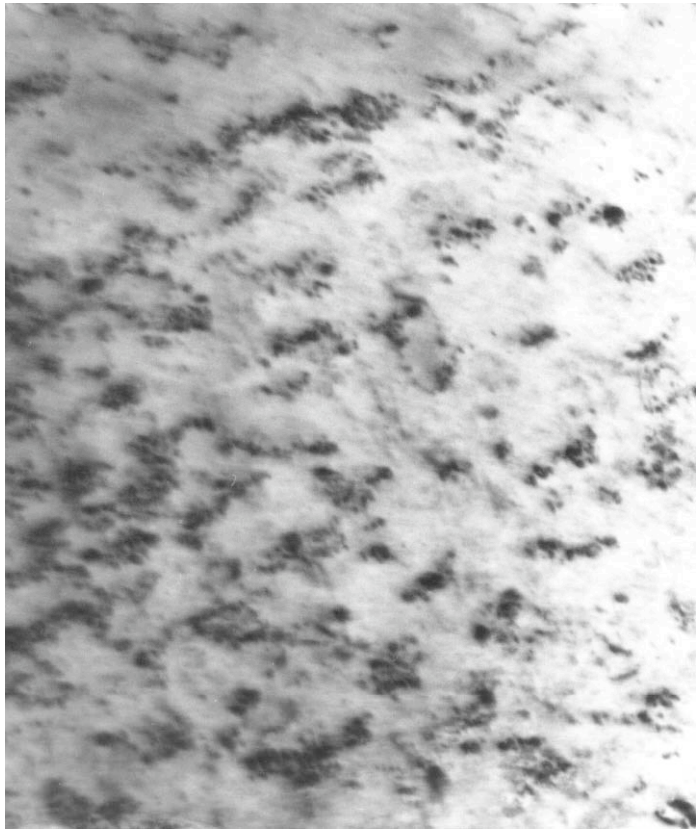

Experimental observation of dislocation loops

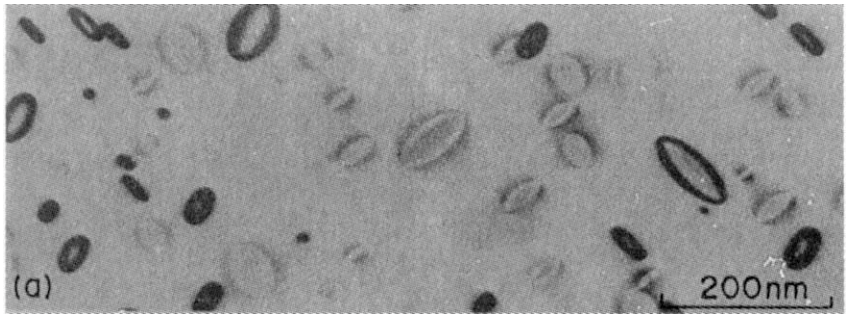

Al

e^- - irradiation
T above recovery stage III
all loops are interstitial in nature

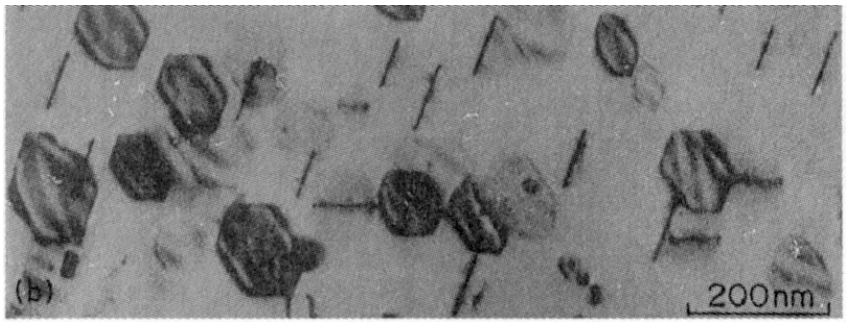

Cu

Ni

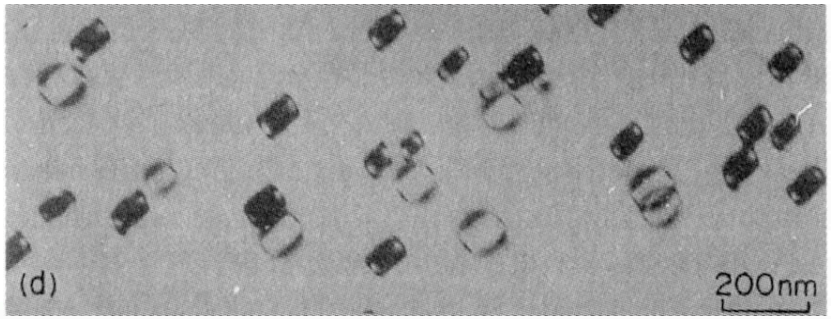

Fe

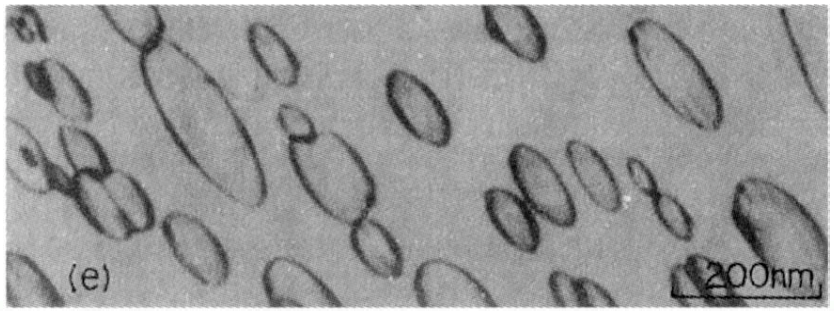

Zn (basal plane)

Defect microstructure in irradiated $MgAl_2O_4$ spinel

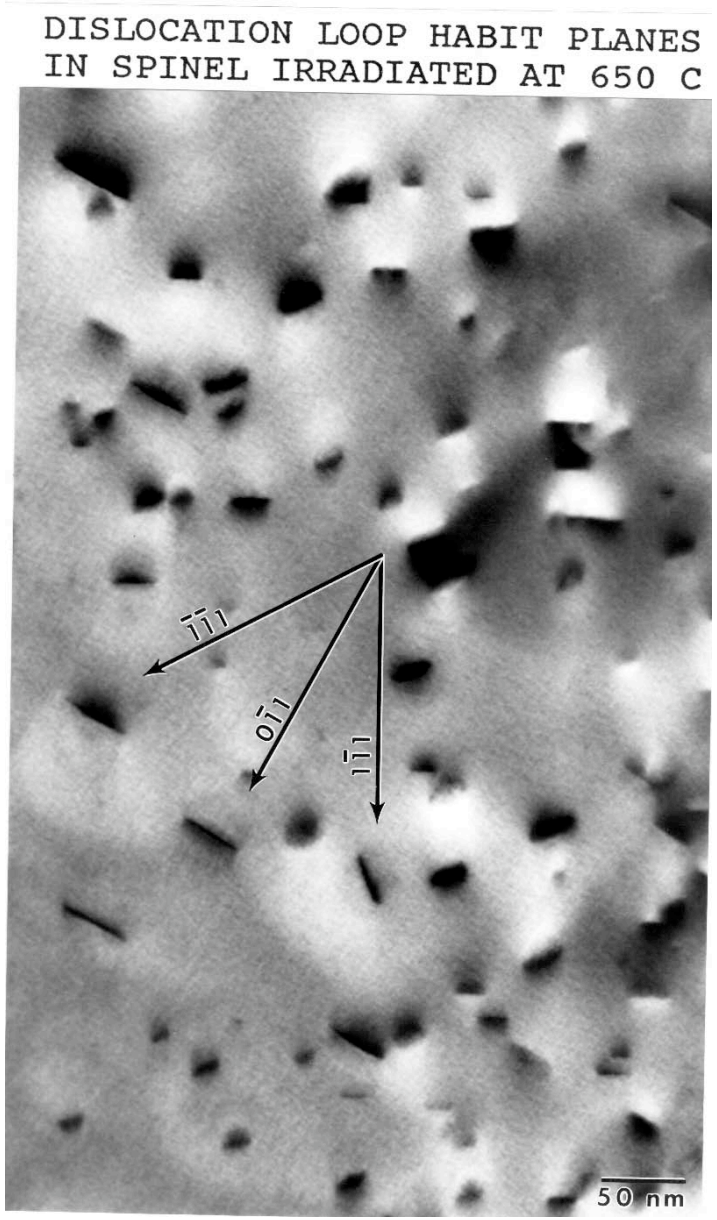

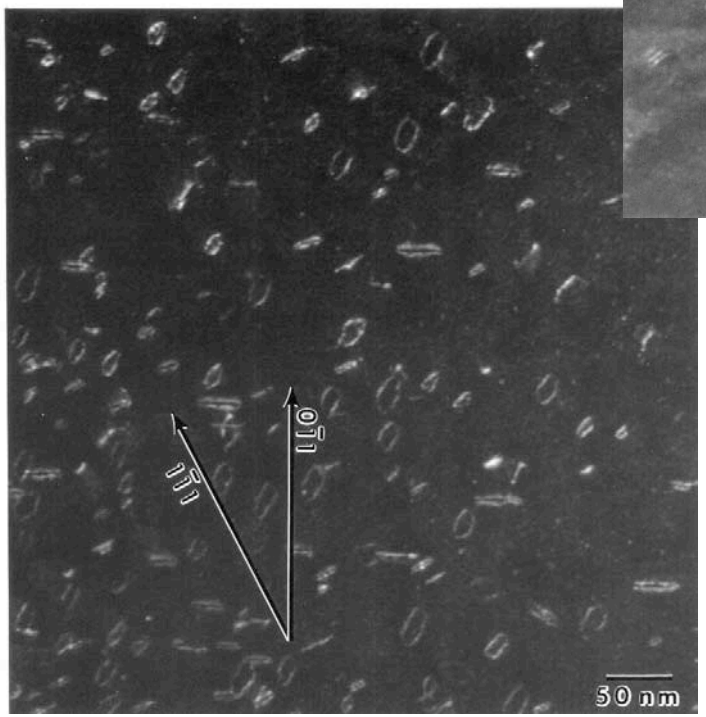

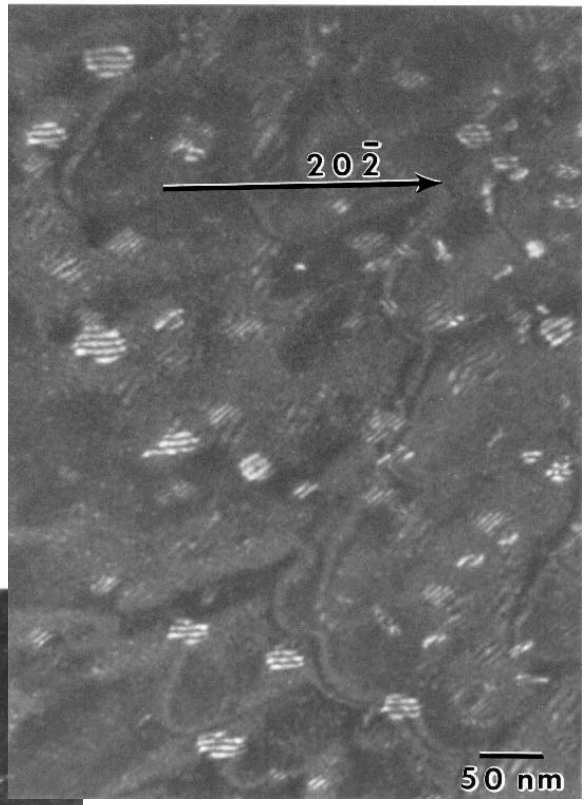

Faulted loops in neutron irradiated stainless steel

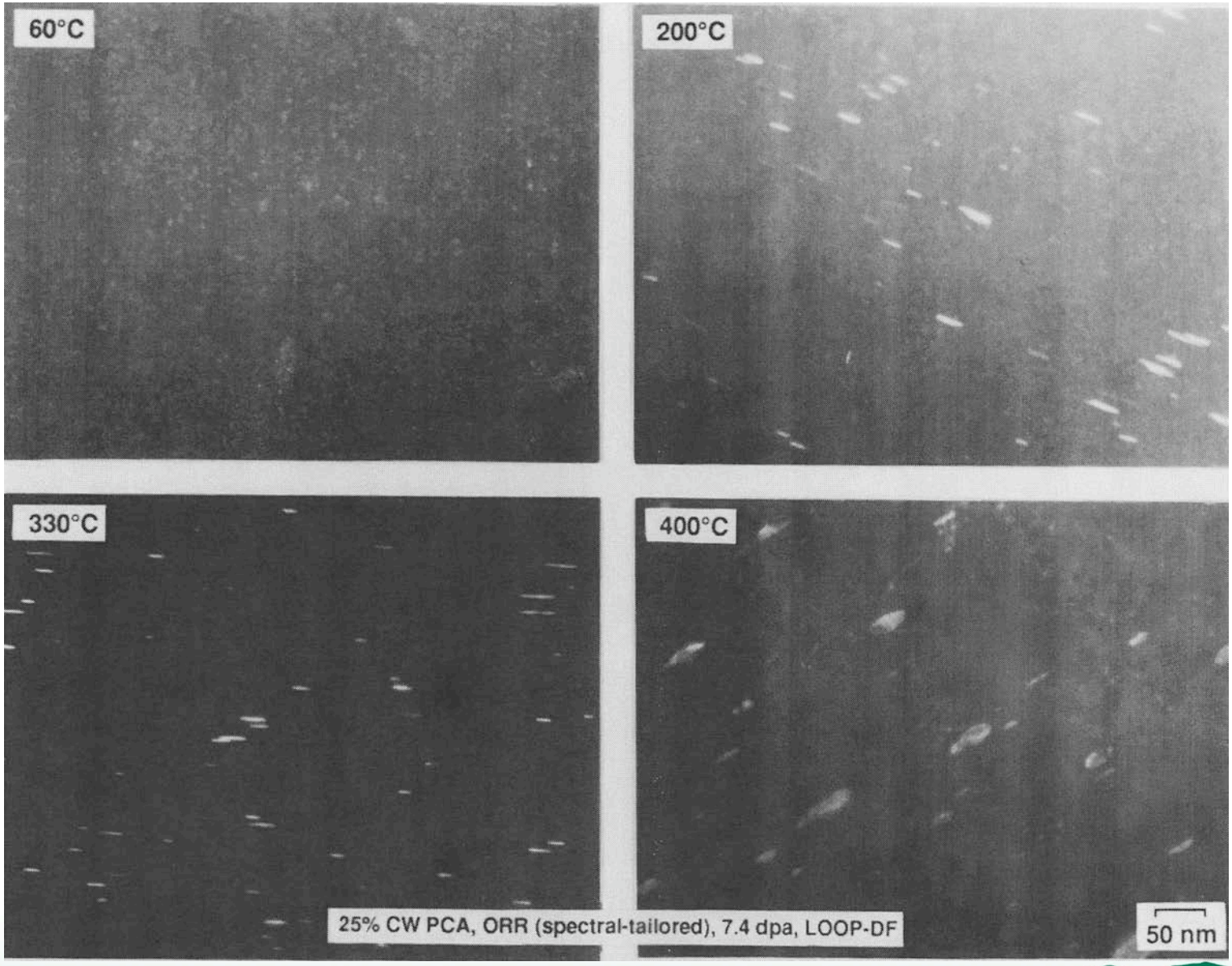

Temperature dependence of defect cluster density in neutron irradiated metals

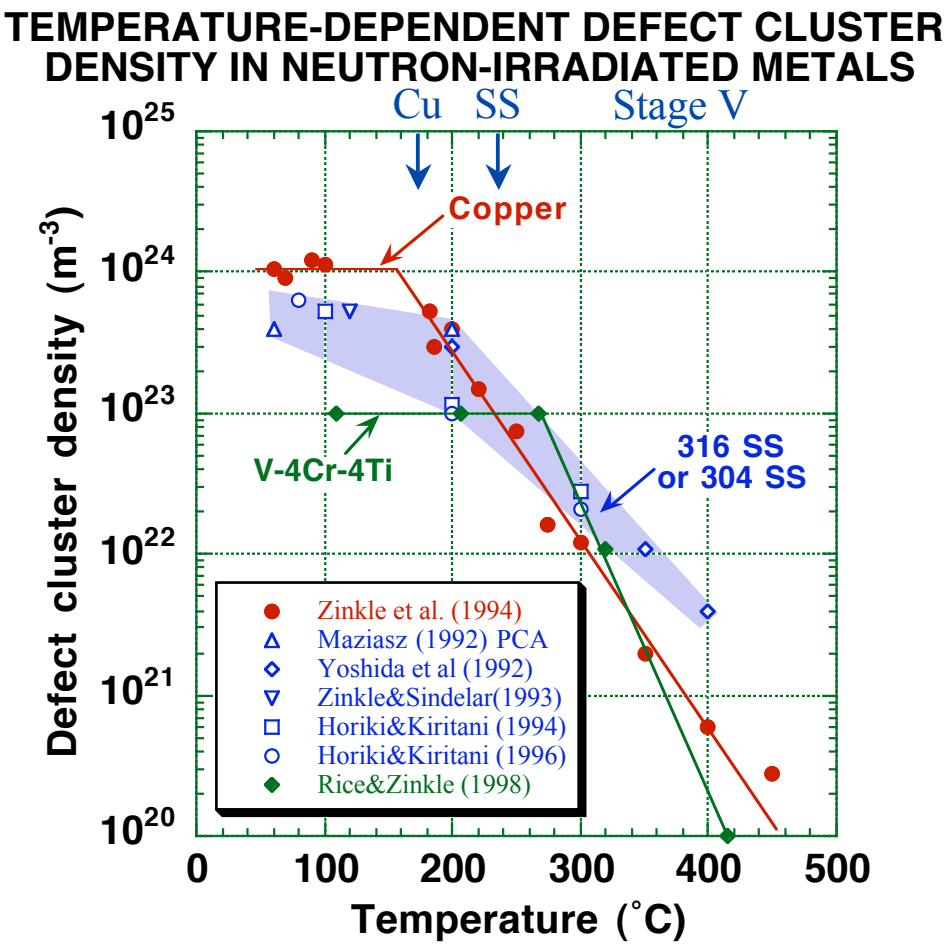

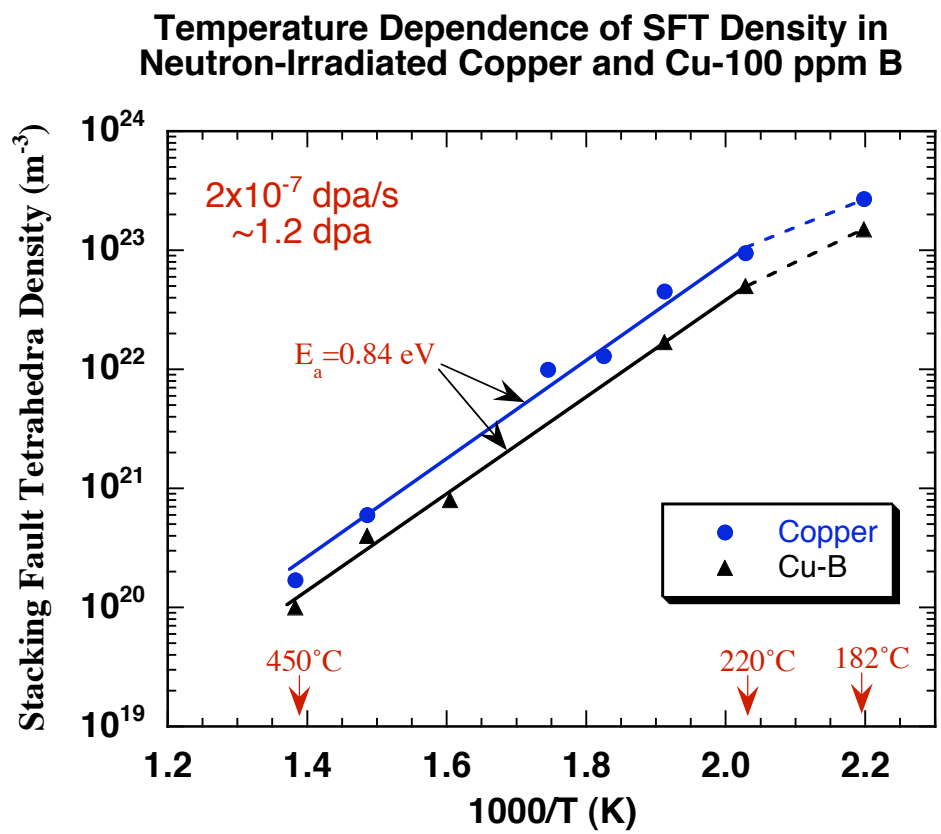

Void swelling in stainless steel would occur for neutron irradiation temperatures as low as 250˚C based on vacancy cluster Stage V, but interstitial loops provide high sink strength to 300-350˚C

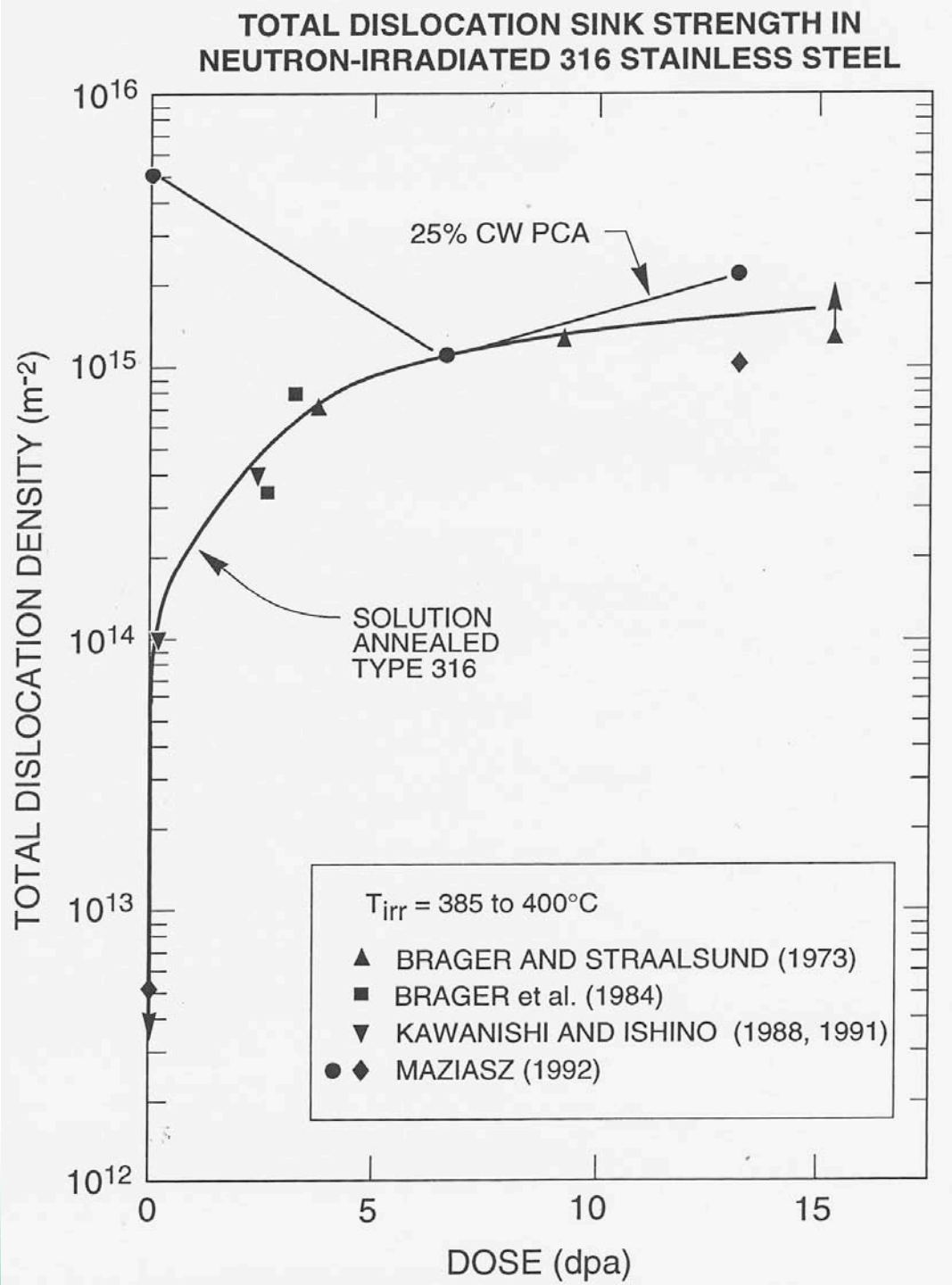
TOTAL DISLOCATION SINK STRENGTH IN
NEUTRON-IRRADIATED 316 STAINLESS STEEL
TOTAL DISLOCATION DENSITY (m-2)
10^16
10^15
10^14
10^13
10^12
0
5
10
15
DOSE (dpa)
25% CW PCA
SOLUTION
ANNEALED
TYPE 316
Tirr = 385 to 400°C
BRAGER AND STRAALSUND (1973)
BRAGER et al. (1984)
KAWANISHI AND ISHINO (1988, 1991)
MAZIASZ (1992)

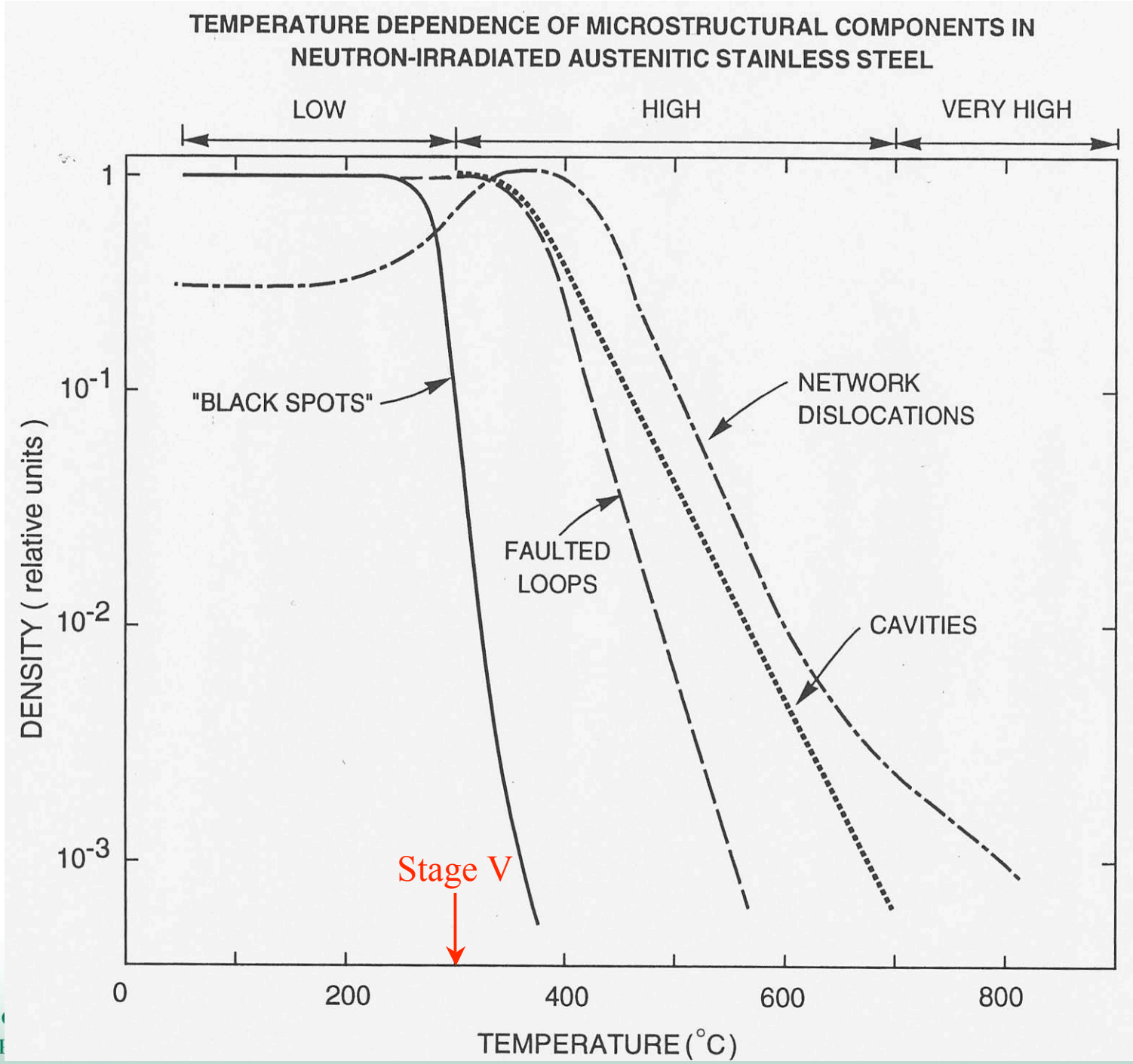
TEMPERATURE DEPENDENCE OF MICROSTRUCTURAL COMPONENTS IN NEUTRON-IRRADIATED AUSTENITIC STAINLESS STEEL
LOW
HIGH
VERY HIGH
1
10-1
10-2
10-3
DENSITY (relative units)
"BLACK SPOTS"
NETWORK DISLOCATIONS
FAULTED LOOPS
CAVITIES
Stage V
0
200
400
600
800
TEMPERATURE (°C)

TEMPERATURE DEPENDENCE OF FAULTED LOOP DENSITY IN NEUTRON-IRRADIATED 316 STAINLESS STEEL

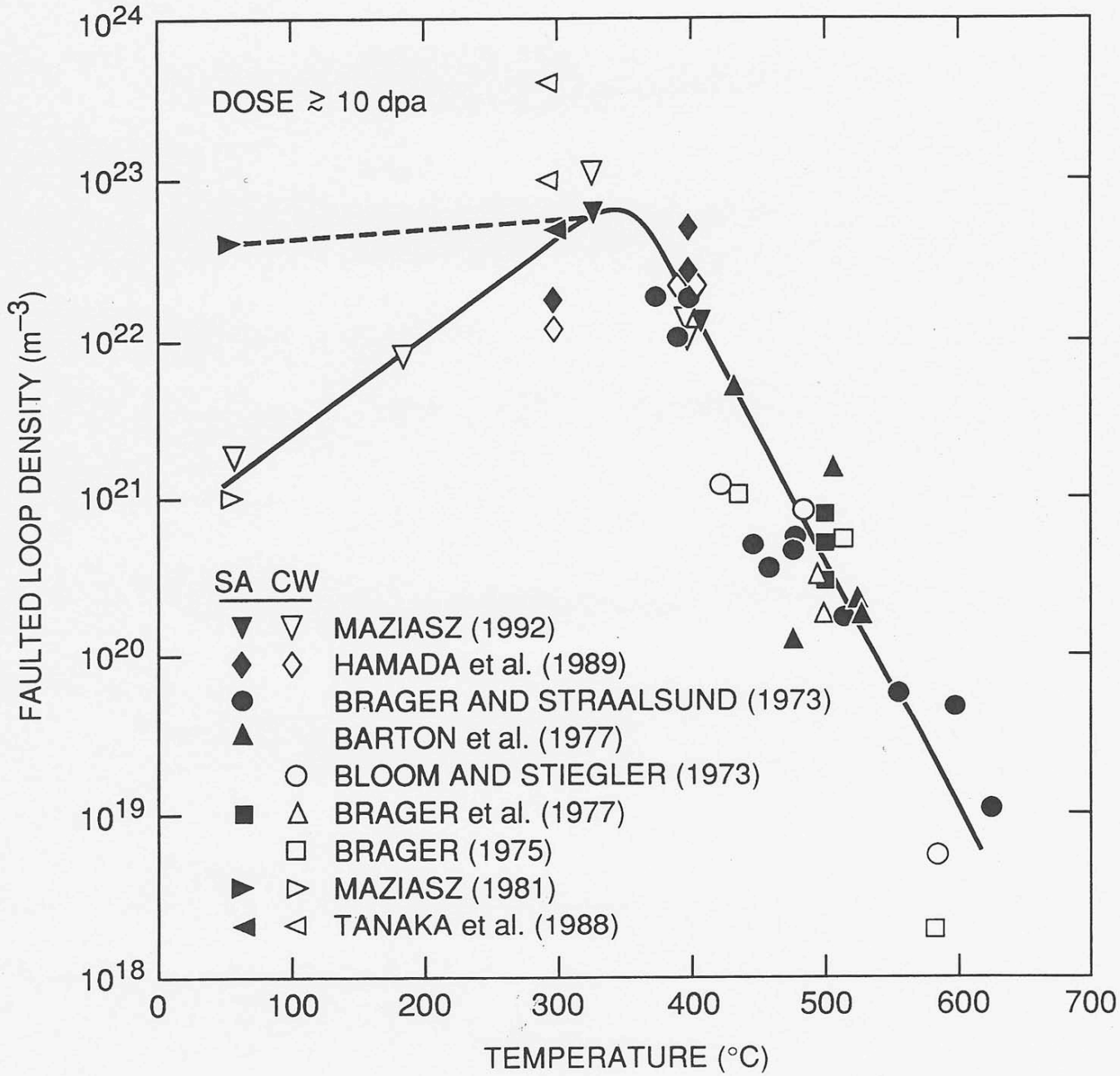

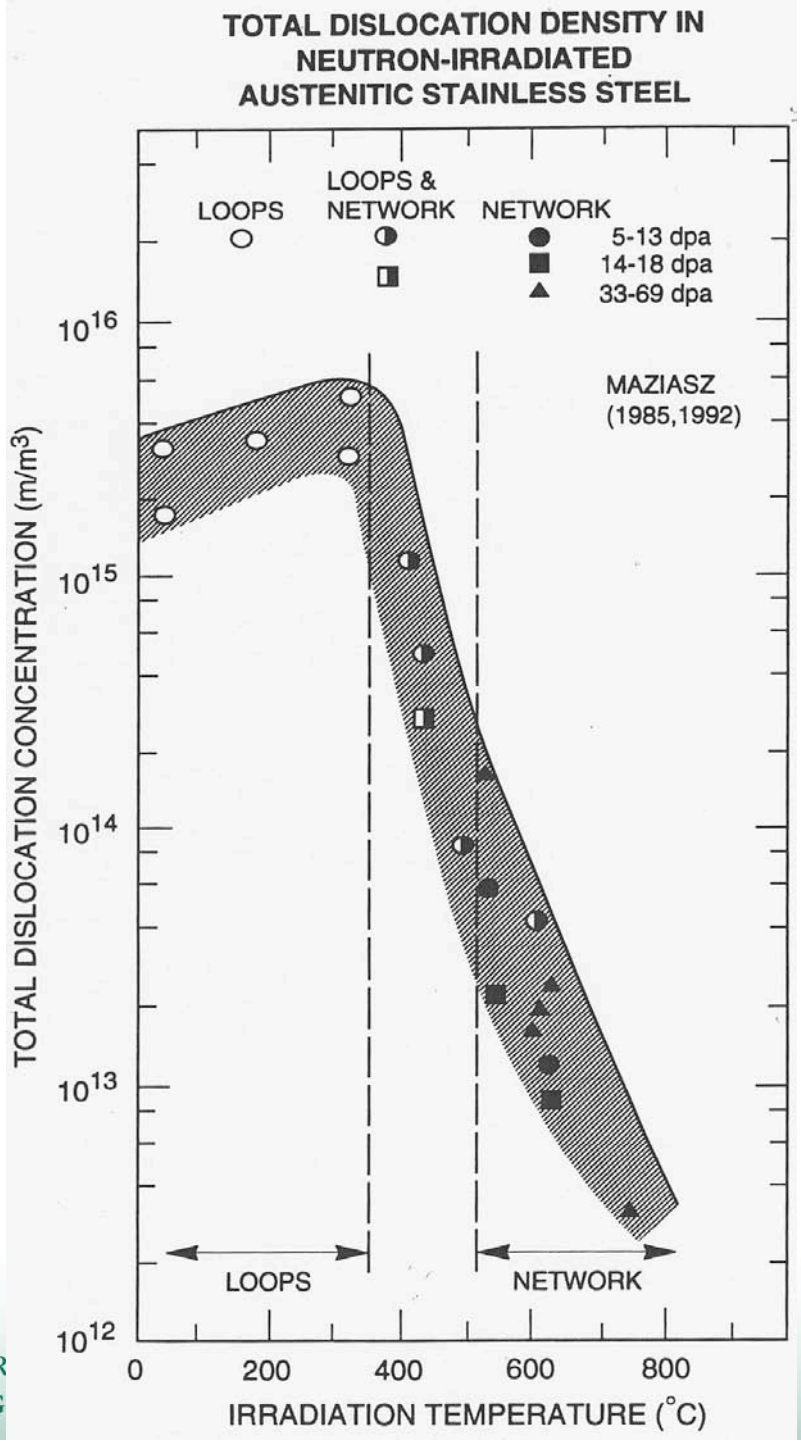
TOTAL DISLOCATION DENSITY IN
NEUTRON-IRRADIATED
AUSTENITIC STAINLESS STEEL
LOOPS
LOOPS &
NETWORK
NETWORK
5-13 dpa
14-18 dpa
33-69 dpa
MAZIASZ
(1985,1992)
TOTAL DISLOCATION CONCENTRATION (m/m3)
10^16
10^15
10^14
10^13
10^12
LOOPS
NETWORK
0
200
400
600
800
IRRADIATION TEMPERATURE (°C)

Volumetric Swelling in Pure Copper and Cu-B Irradiated with Fission Neutrons to ~1.1 dpa

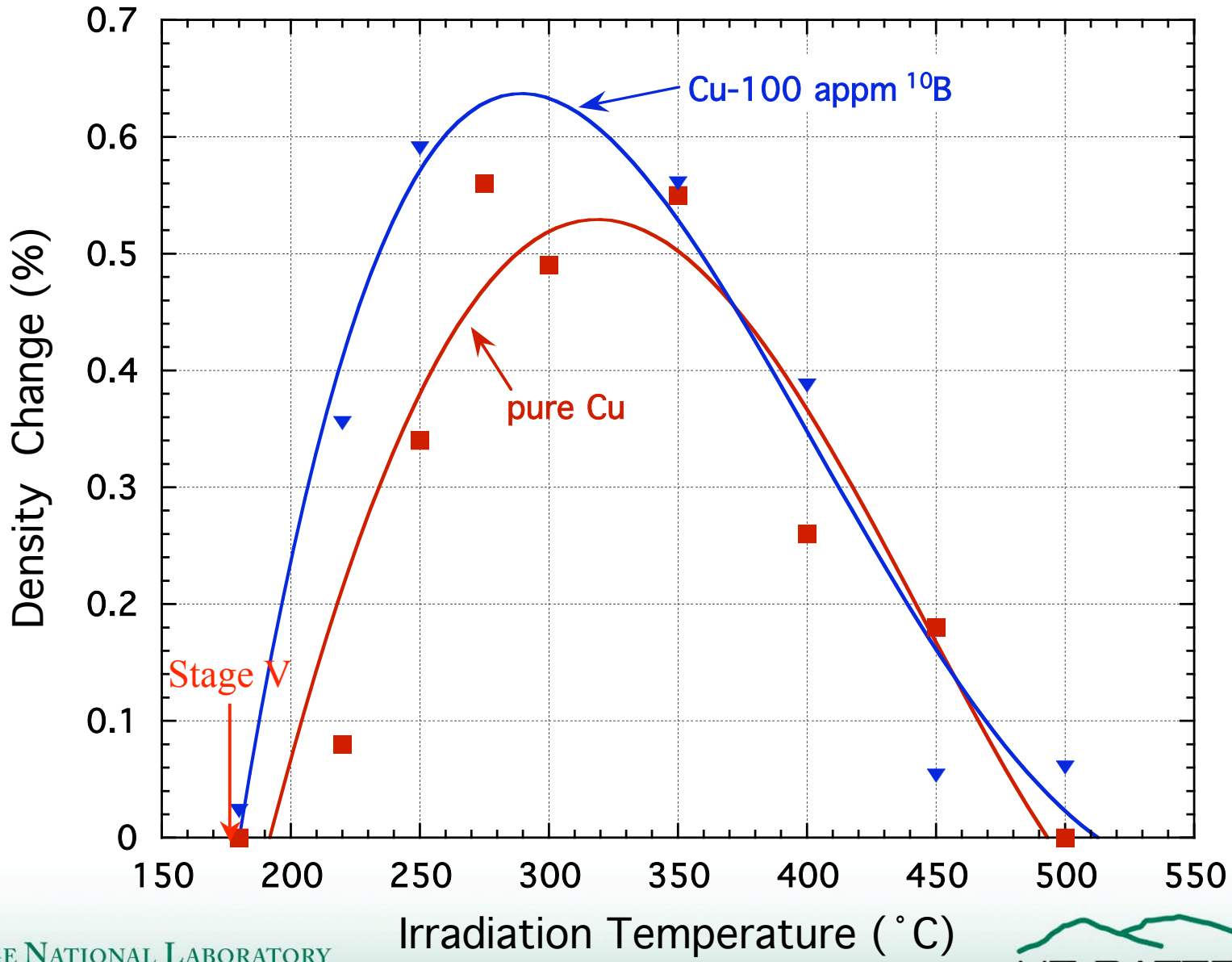

Voids in Cu-100 ppm B irradiated at 182˚C in ORR (1 dpa)

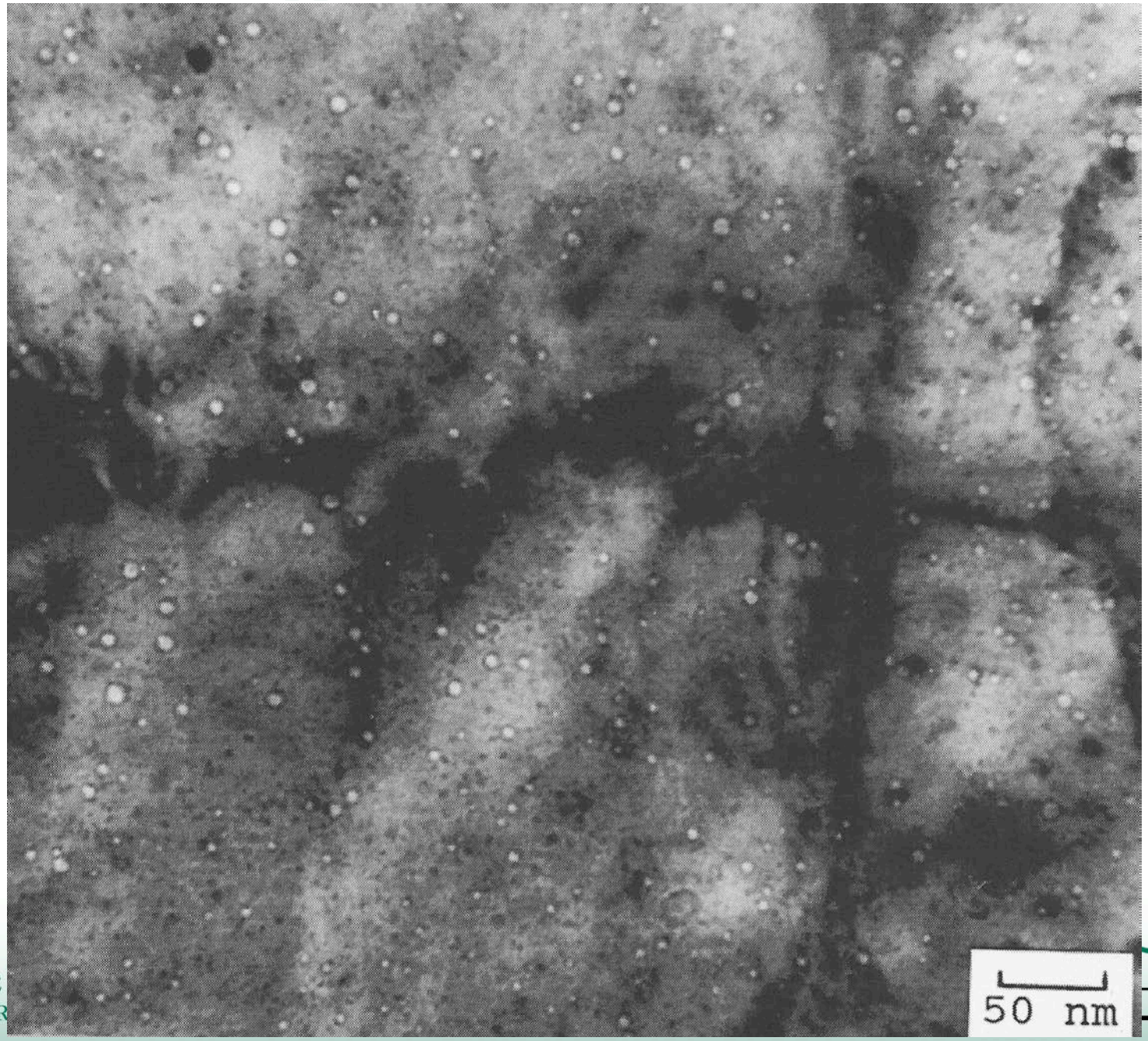

Copper irradiated at 300˚C in ORR fission reactor (1 dpa)

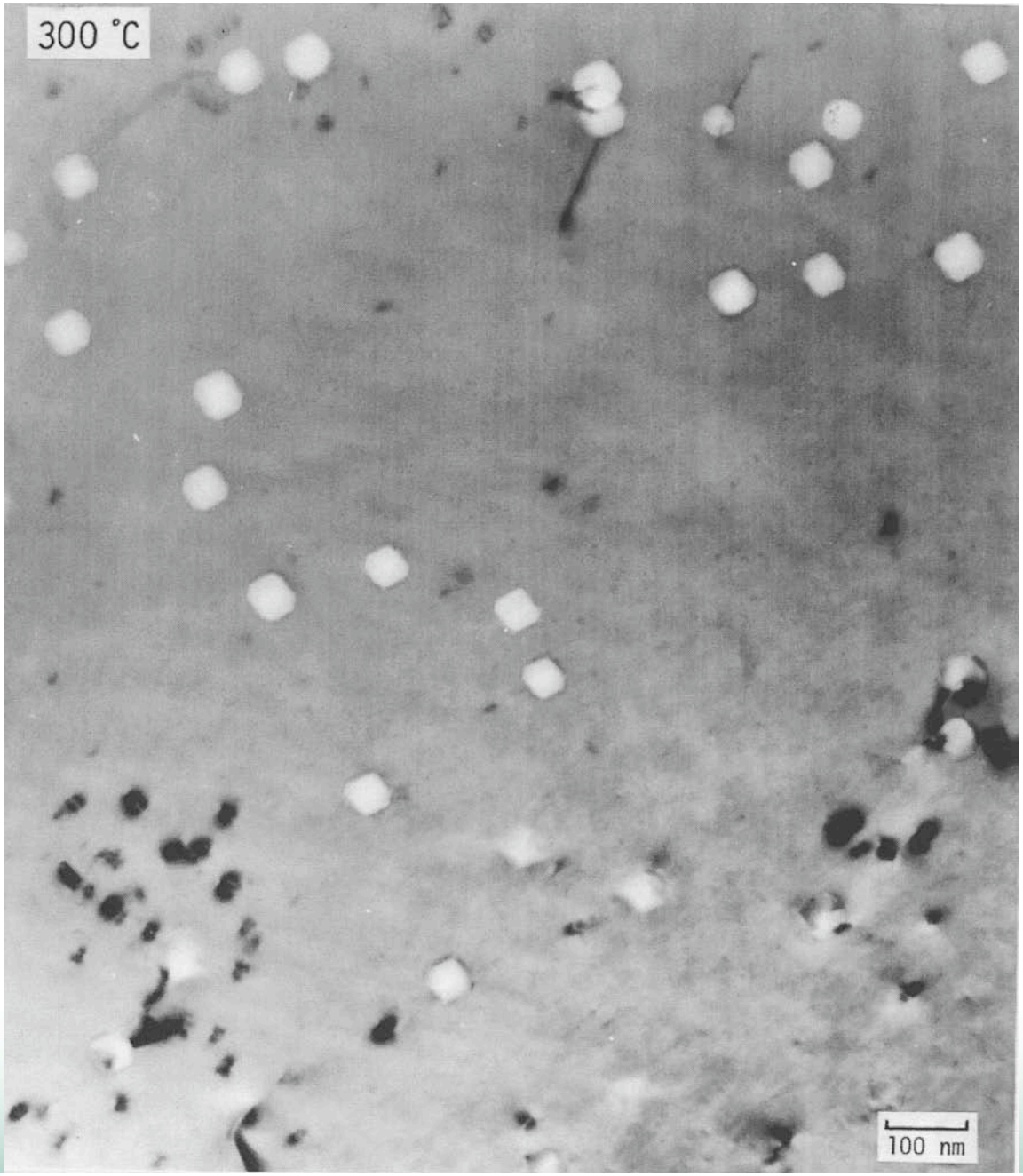

- Voids are not spatially correlated with network dislocations

UT-BATTELLE

Void-free regions surrounding twin boundaries in Cu-100 ppm B irradiated in ORR fission reactor (1 dpa)

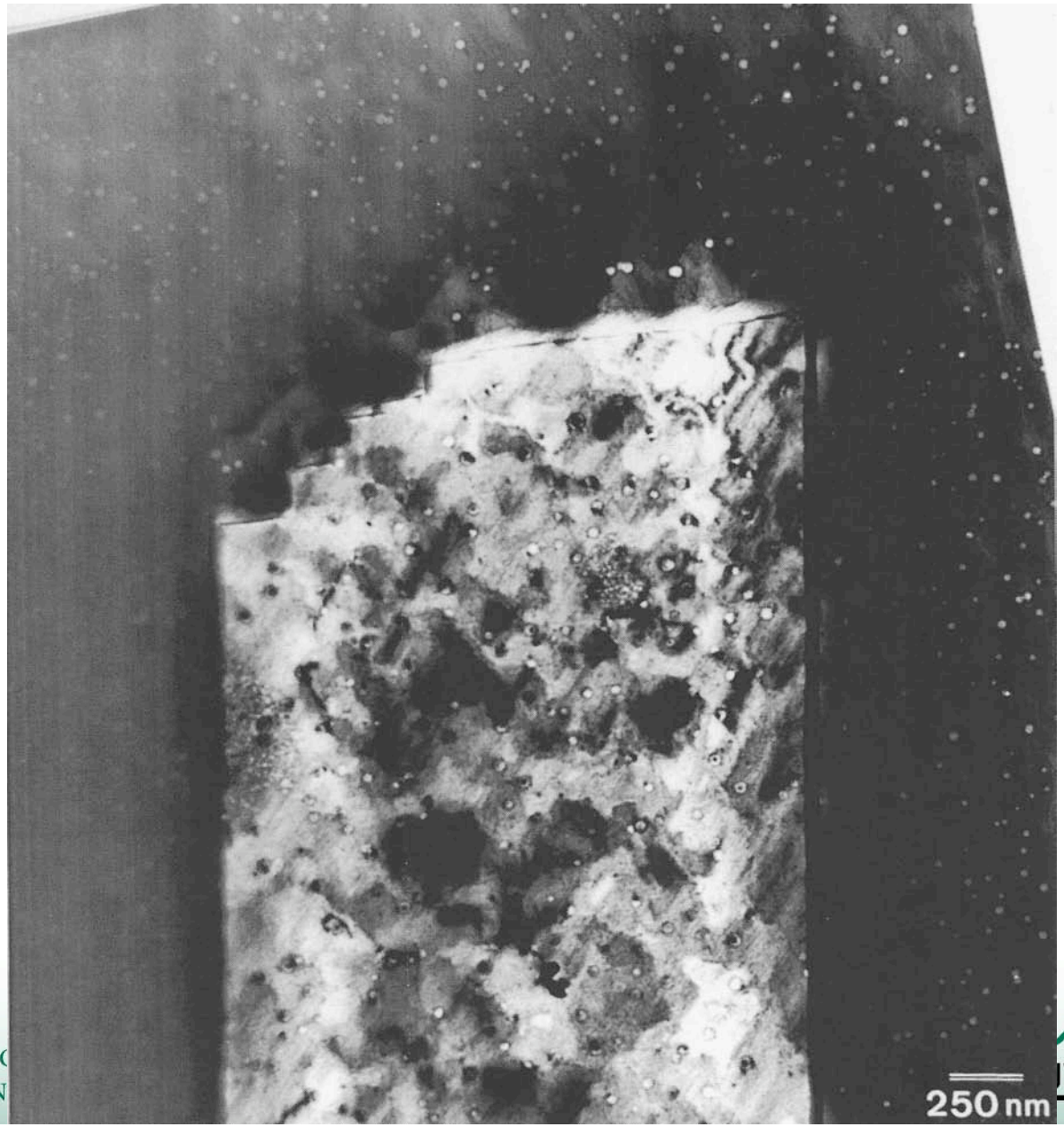

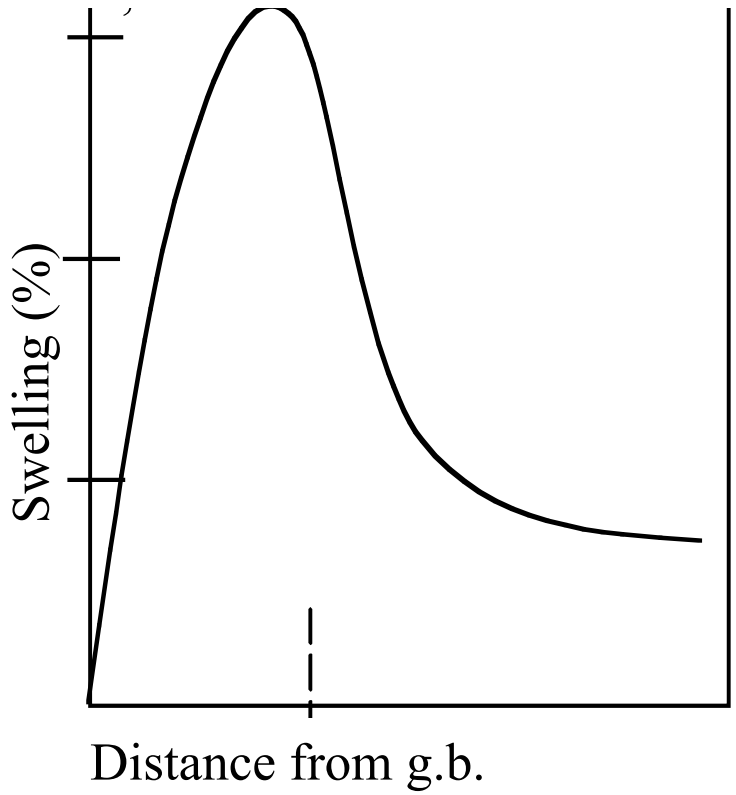

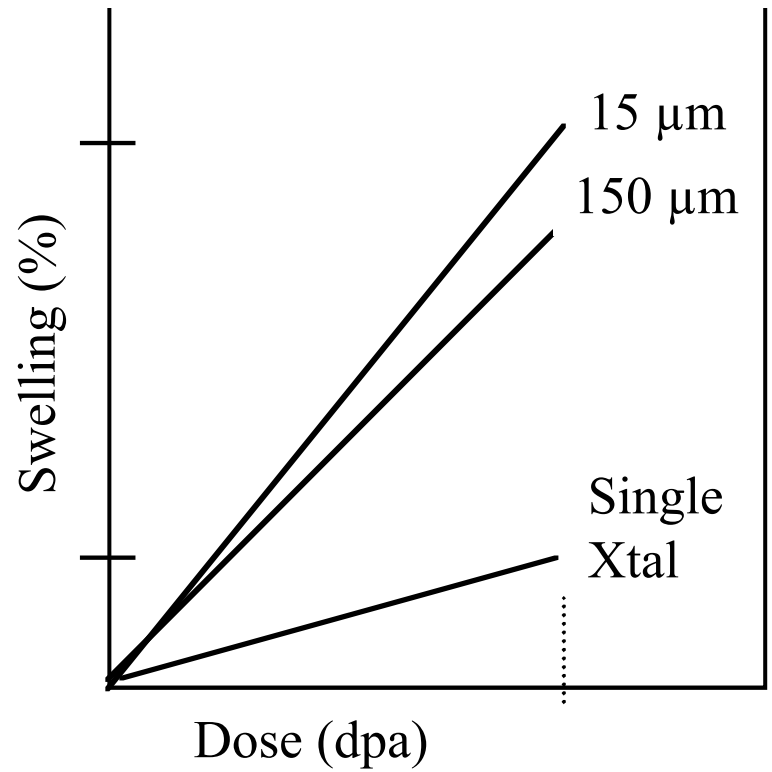

Variation of void swelling vs. distance from grain boundaries in pure well-annealed Al irradiated with fission neutrons at 120°C. Note enhancement in swelling in a relatively wide zone near the grain boundaries (after Singh 1999).

Dose dependence of void swelling for three different grain sizes (Singh 1999). All specimens were irradiated in the same capsule at 350°C to a dose level of ~0.3dpa

Voids and helium bubbles in Cu-100 ppm B irradiated at 350˚C in ORR fission reactor (1 dpa)

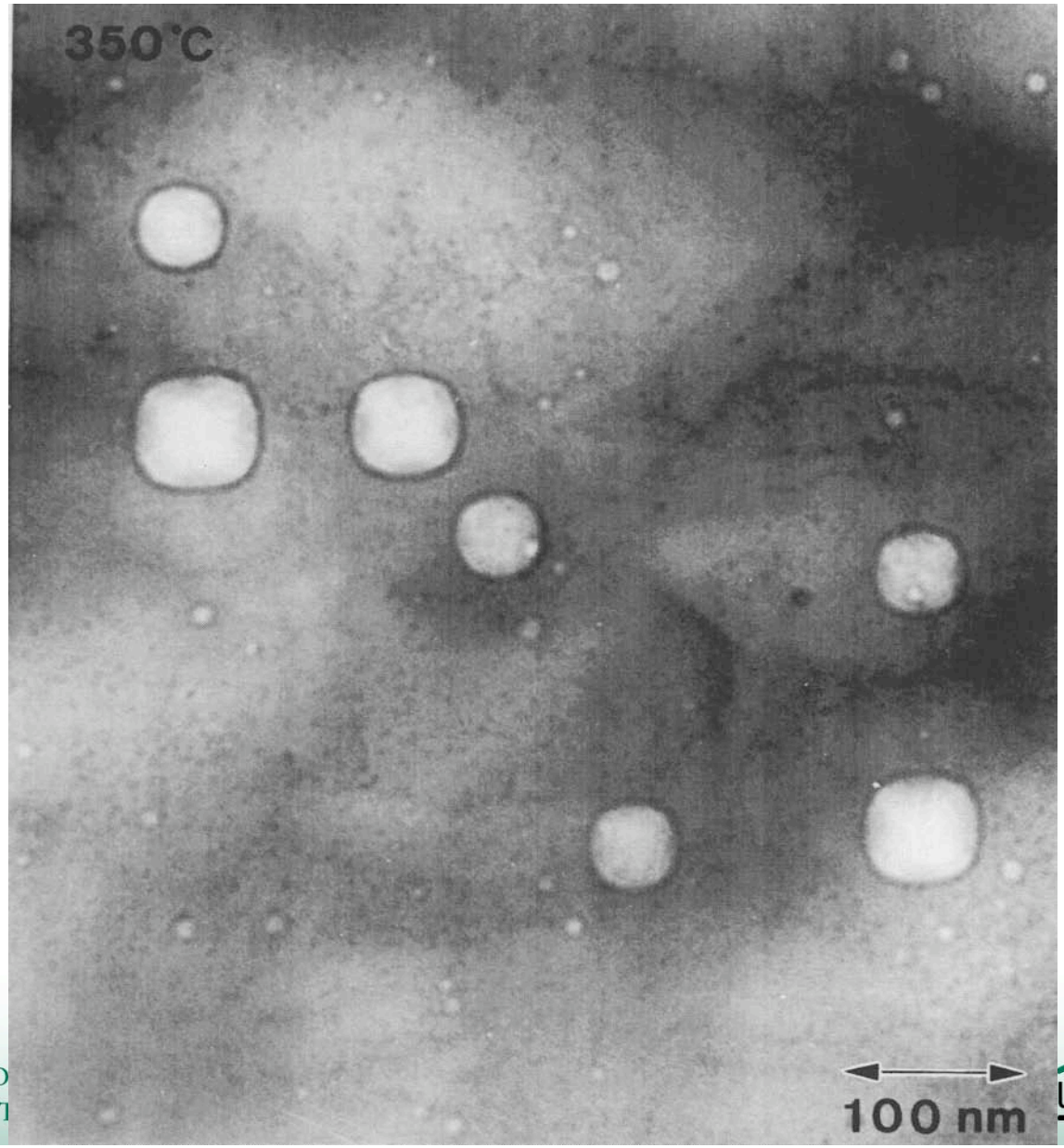

There is a critical size and a critical number of gas atoms beyond which a bubble converts to a void and grows without limit

p-2γ/r

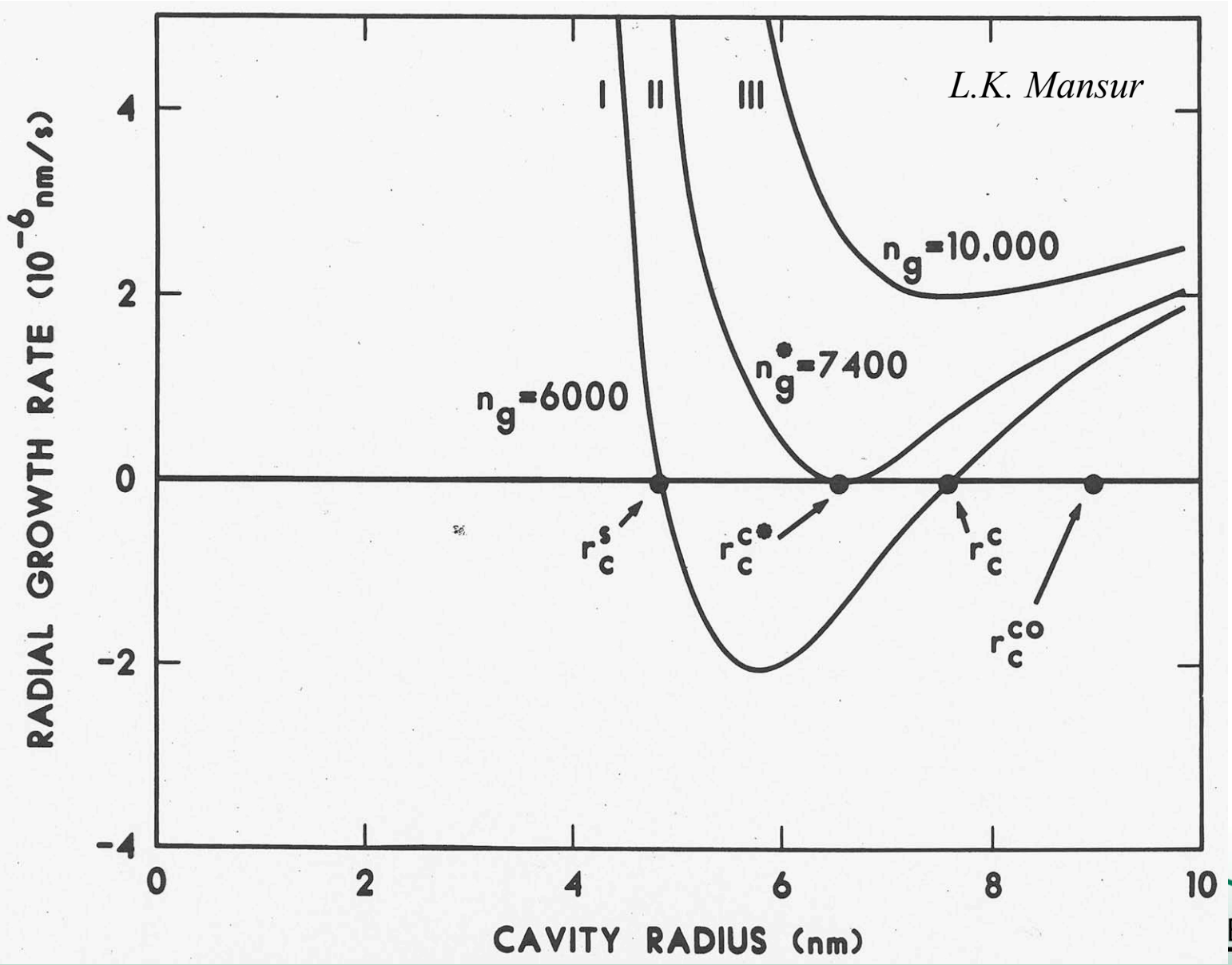

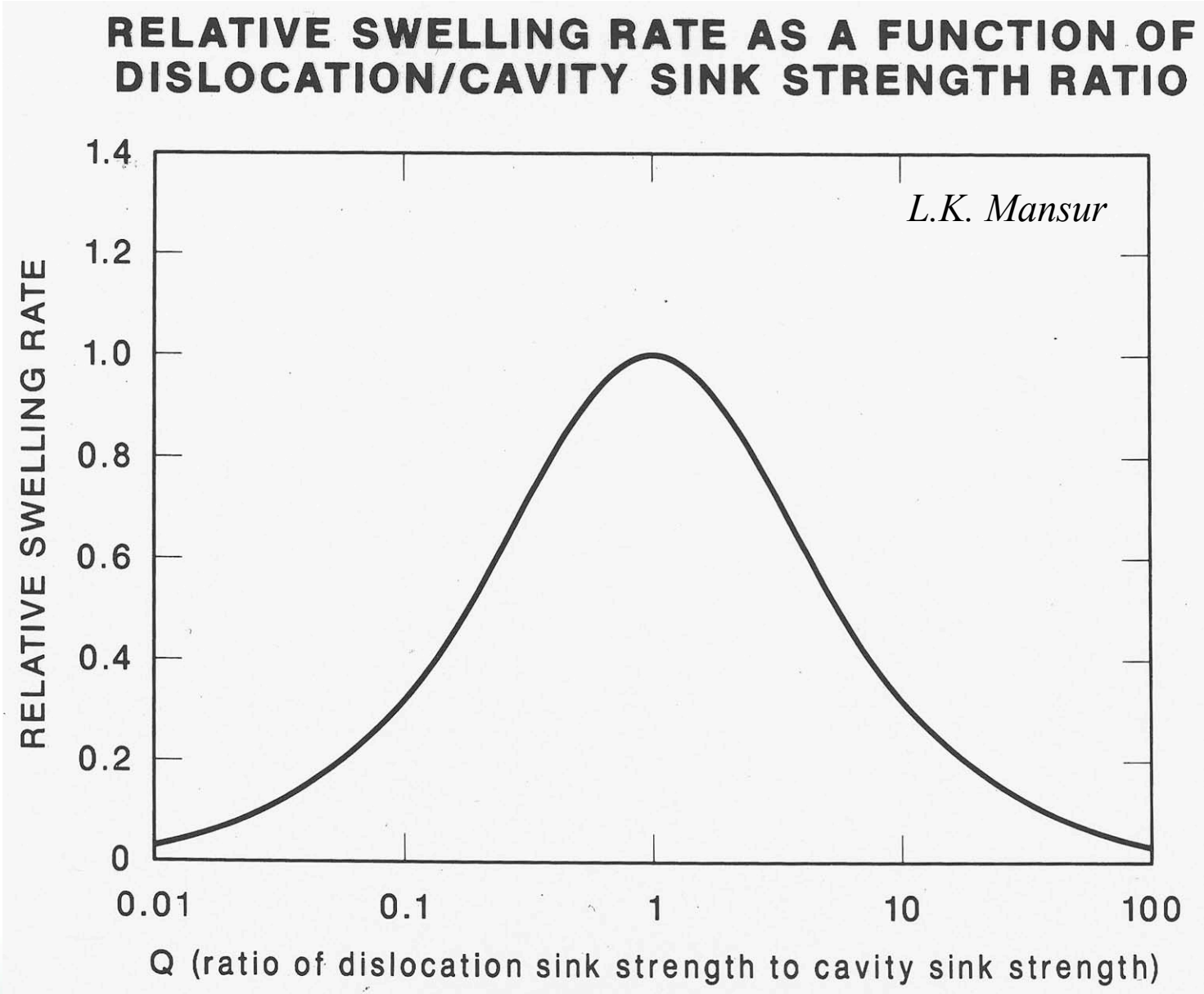
RELATIVE SWELLING RATE AS A FUNCTION OF DISLOCATION/CAVITY SINK STRENGTH RATIO
L.K. Mansur
RELATIVE SWELLING RATE
1.4
1.2
1.0
0.8
0.6
0.4
0.2
0
0.01
0.1
1
10
100
Q (ratio of dislocation sink strength to cavity sink strength)

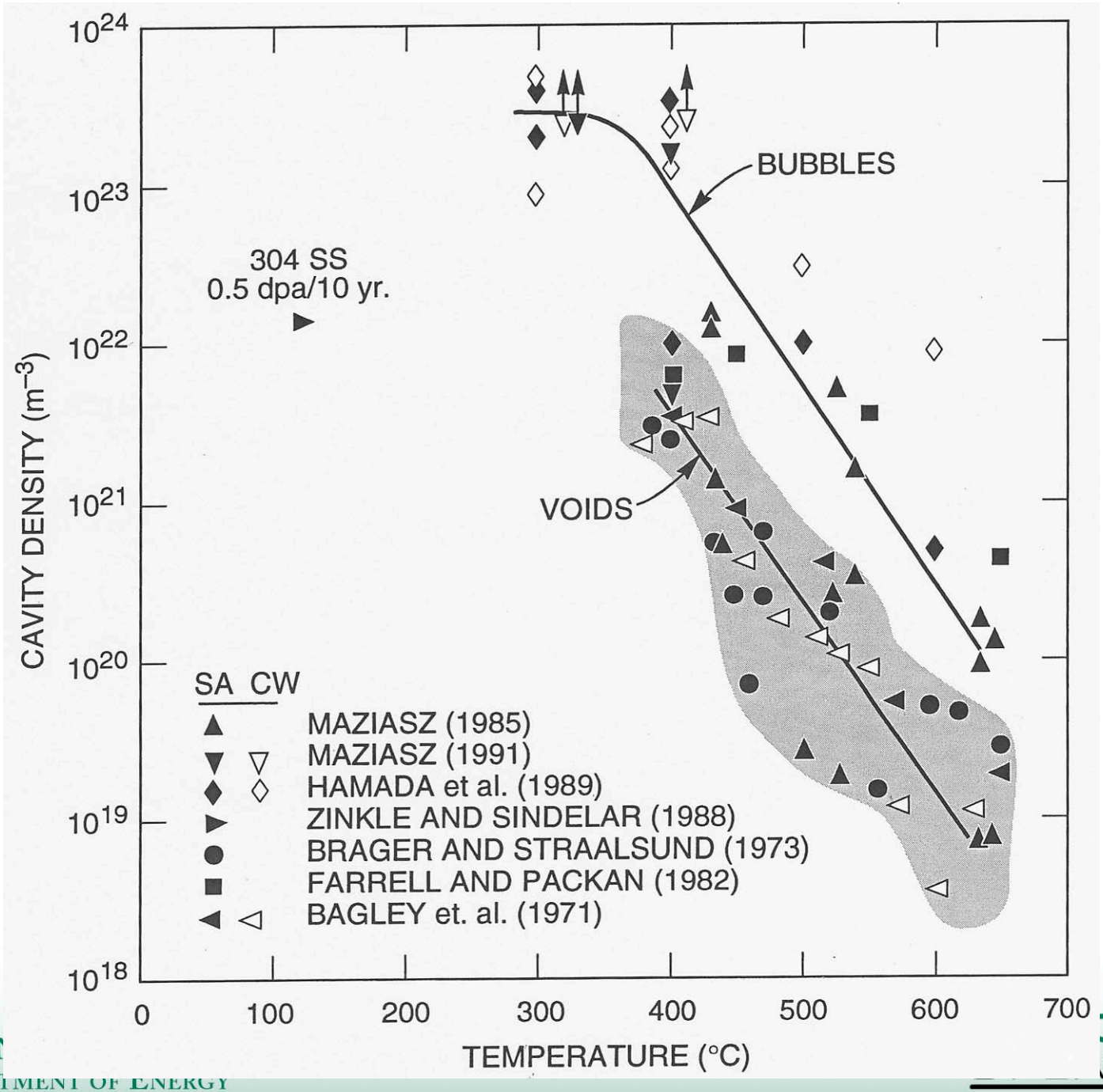
CAVITY DENSITY (m^{-3})
10^{24}
10^{23}
10^{22}
10^{21}
10^{20}
10^{19}
10^{18}
0
100
200
300
400
500
600
700
TEMPERATURE (°C)
BUBBLES
VOIDS
304 SS
0.5 dpa/10 yr.
SA CW
MAZIASZ (1985)
MAZIASZ (1991)
HAMADA et al. (1989)
ZINKLE AND SINDELAR (1988)
BRAGER AND STRAALSUND (1973)
FARRELL AND PACKAN (1982)
BAGLEY et. al. (1971)

Swelling Resistant Alloys For FBRs Were Developed

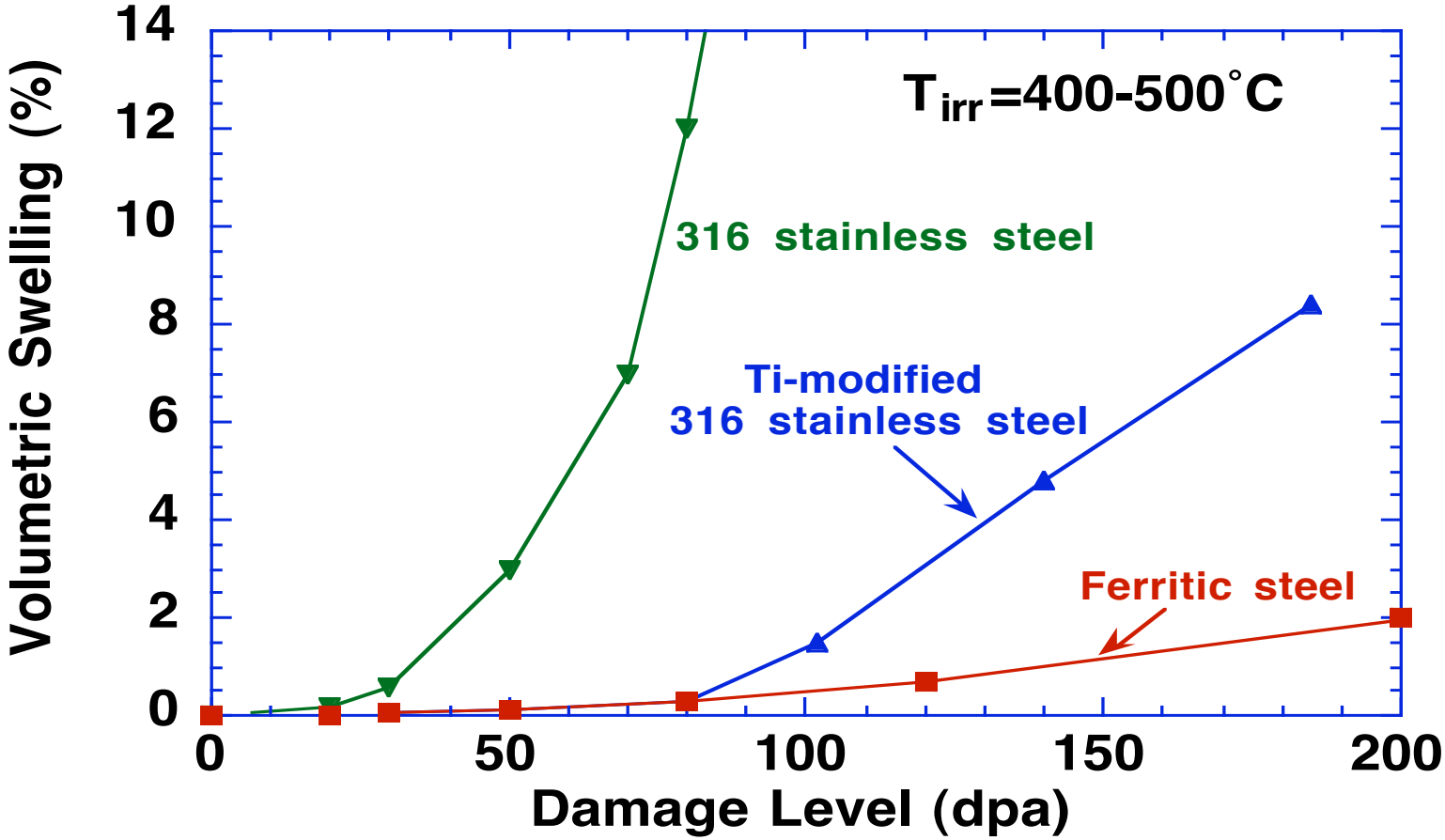

- Lowest swelling is observed in body-centered cubic alloys (V alloys, ferritic steel)
- Materials science strategy used for stainless steel can be applied to new alloys

Packan & Farrell (1982)

REFINEMENT OF CAVITIES BY HELIUM

"Pure" stainless steel bombarded with 4Mev Ni ions to 70 dpa at 900 K.

appm He/dpa=20 (N.H.Packan,K.Farrell)

NO He	COIMPLANTED	PREIMPLANTED	
	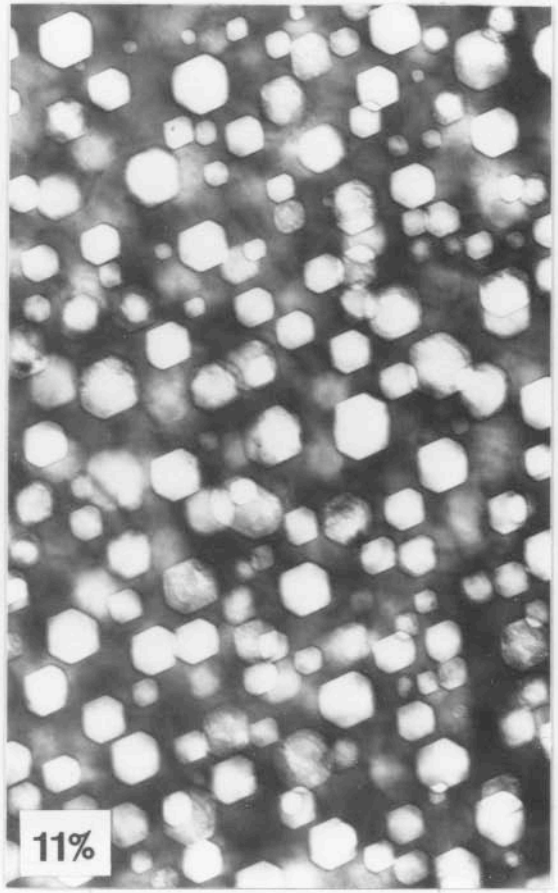	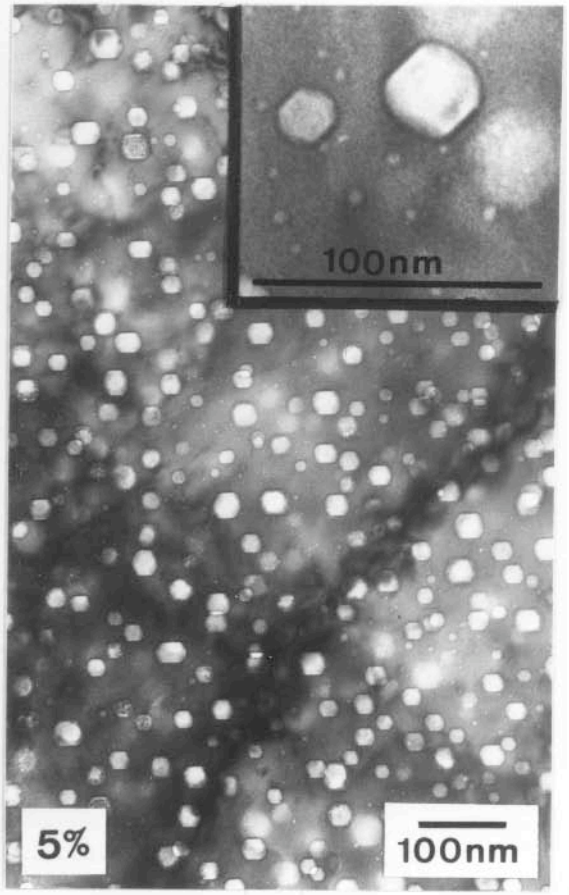	
$N=4.2\times10^{20}/m^3$	1.6×10^{21}	4.4×10^{21}	1.5×10^{22}
d=88nm	49	27	4.4

Effect of He preimplantation method on cavities in ion-irradiated austenitic stainless steel (625˚C, 70 dpa)

No helium

1400 appm He
Hot preinject
at 625˚C

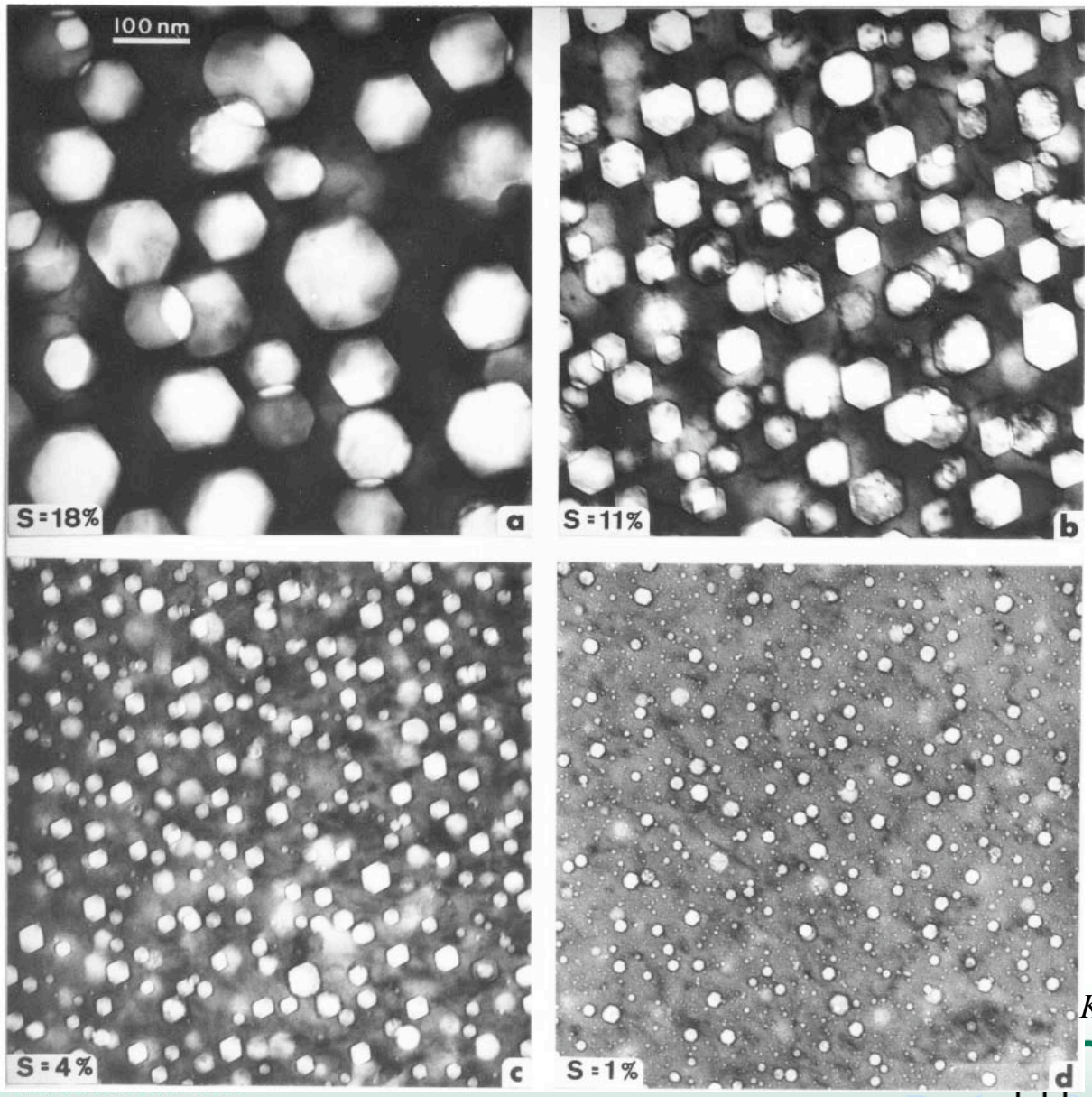

1400 appm He
Coimplant
at 625˚C

1400 appm He
Cold preinject
at 20˚C

K. Farrell & E.H. Lee

HELIUM TRAPPING AT MC PARTICLES IMPROVES SWELLING RESISTANCE OF AUSTENITIC STAINLESS STEELS IRRADIATED TO 45 dpa AND 2500 appm HELIUM

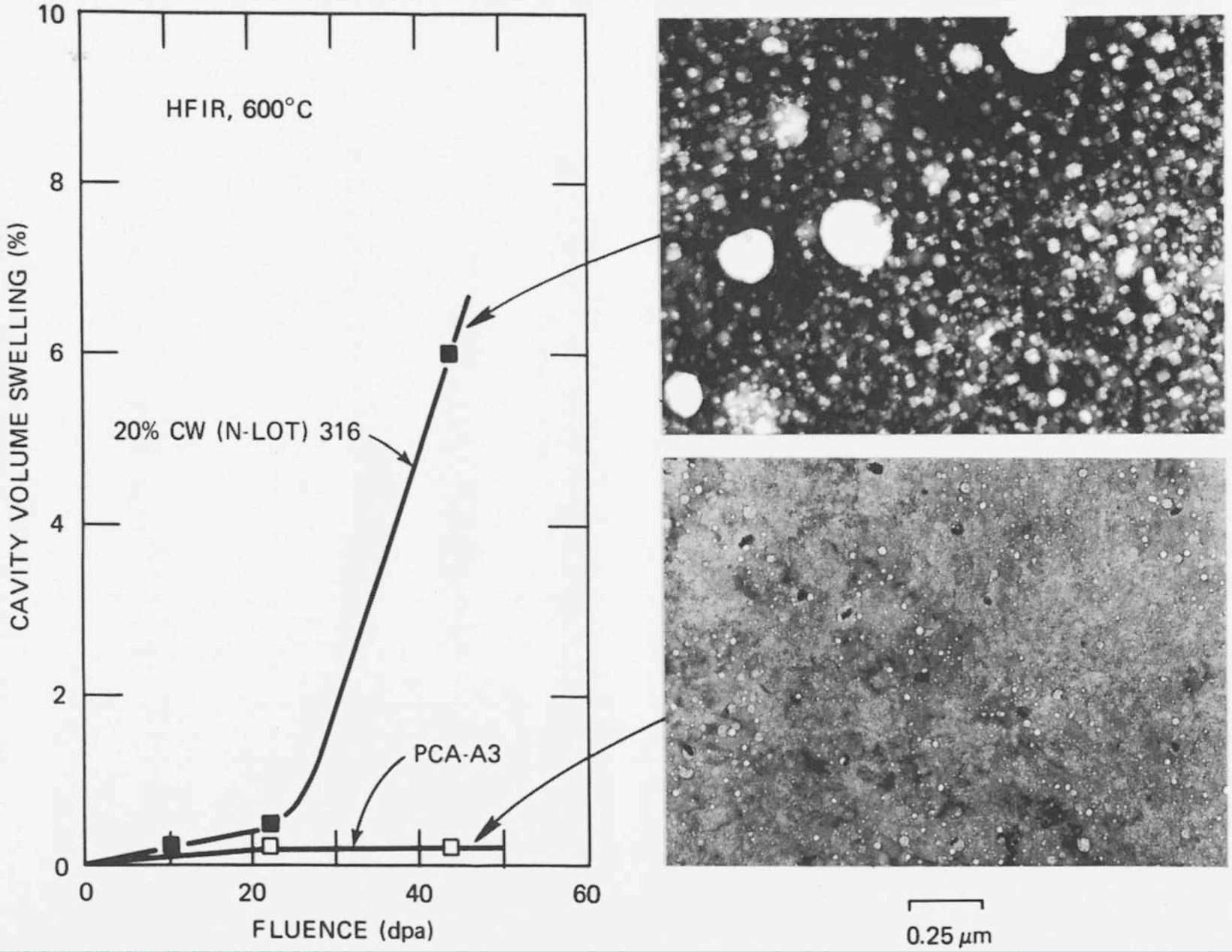

MICROSTRUCTURE OF LOW-SWELLING ALLOY TRAPS HELIUM IN MANY SUB-CRITICAL BUBBLES

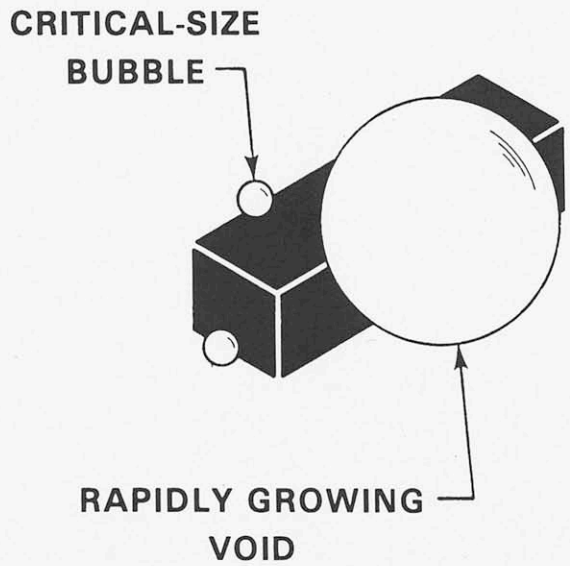

A FEW LARGE PARTICLES
(HIGH-SWELLING)

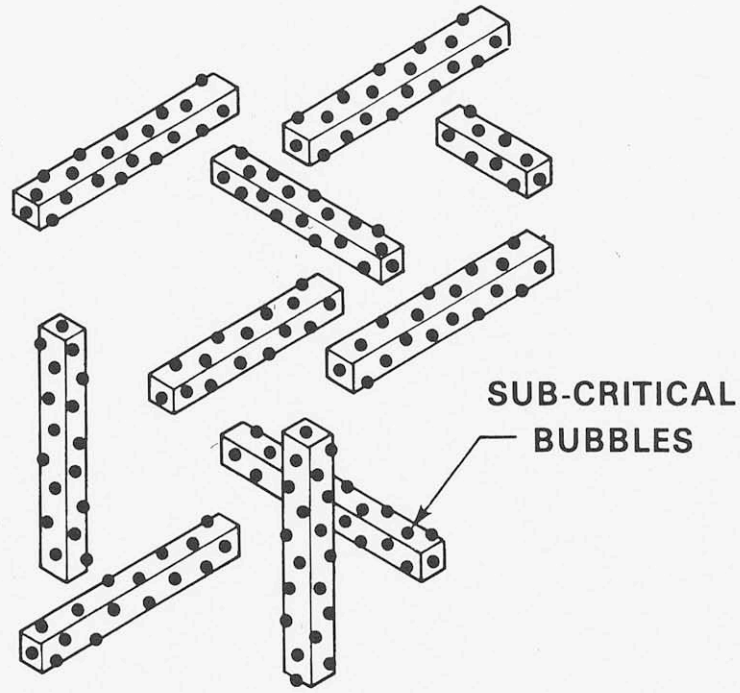

DISPERSED FINE PARTICLES
(LOW-SWELLING)

Swelling Resistant Alloys can be developed by Controlling the He Cavity Trapping at Precipitates

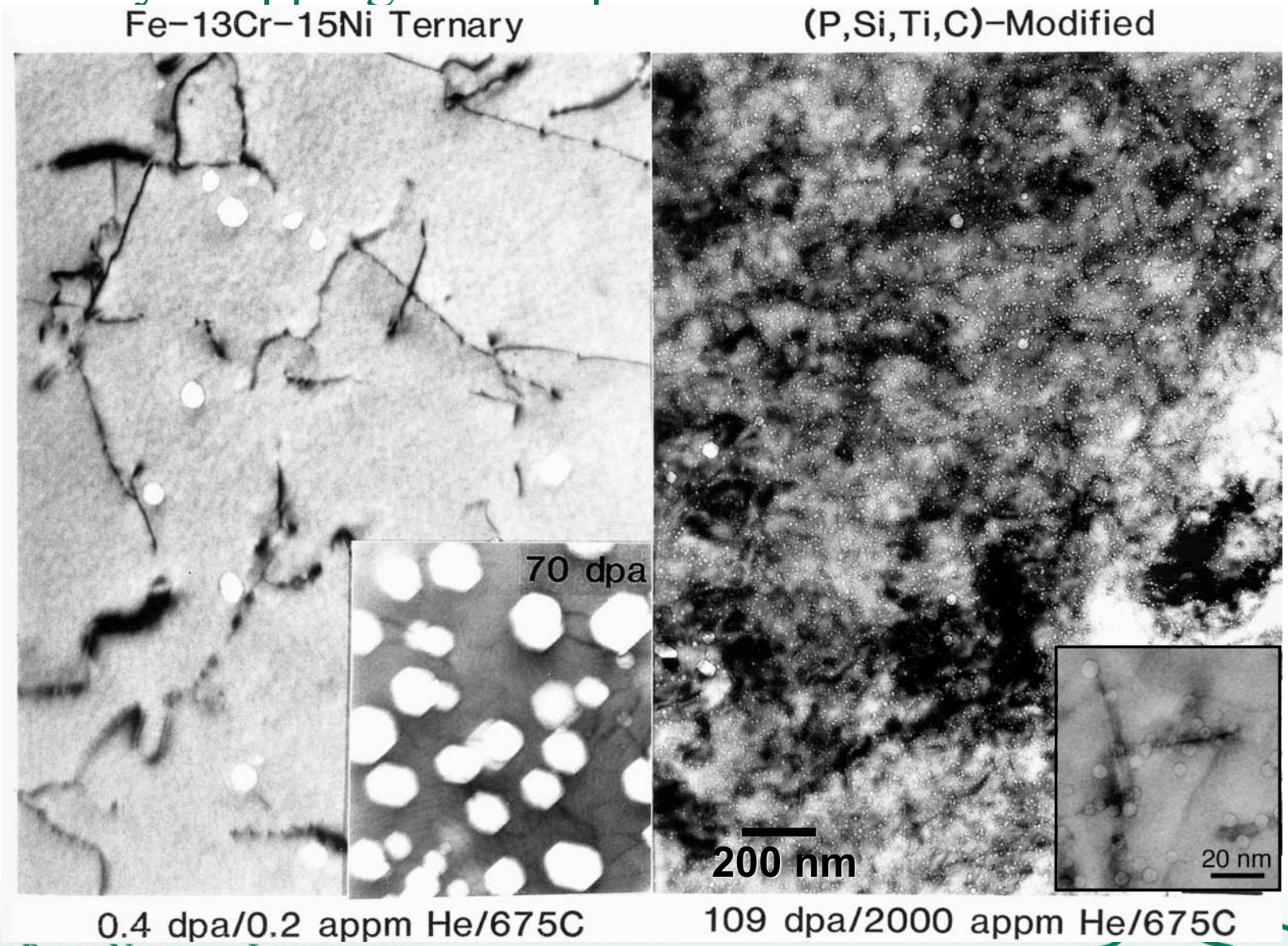

Void Swelling of Ferritic Steels is Low up to ~100 dpa, Although Further Work is Needed to Examine He Effects

HFIR irradiation at 400˚C to 51 dpa

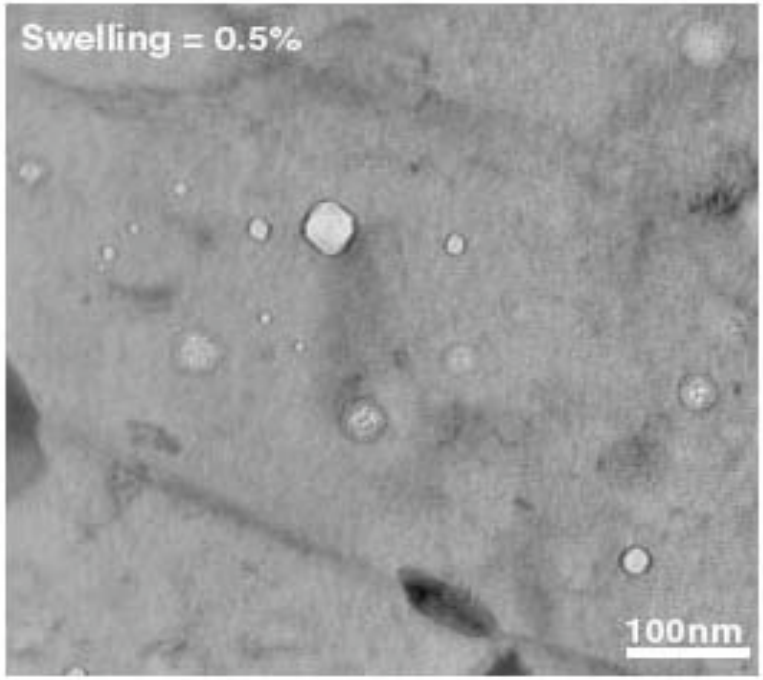

F82H (36 appm He)

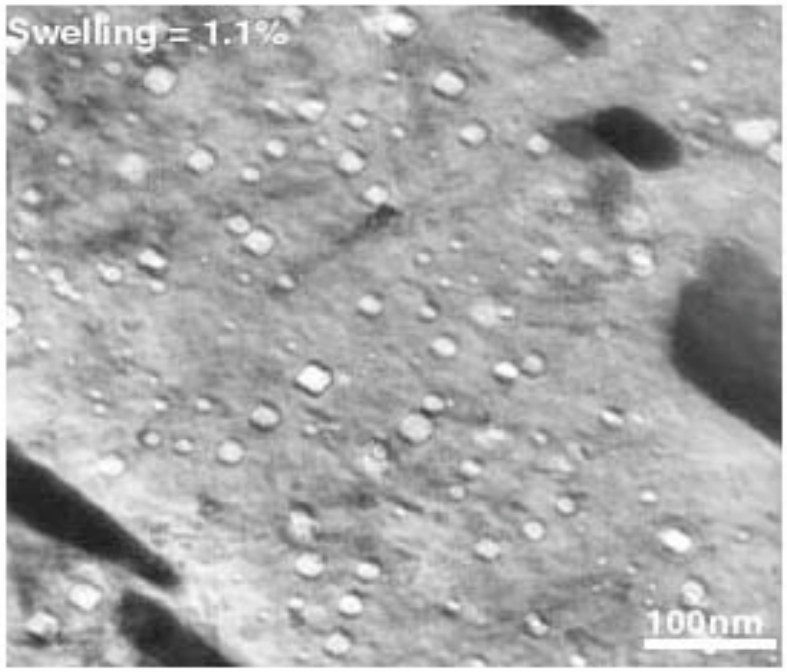

^{10}B-doped F82H (330 appm He)

He grain boundary cavities in austenitic stainless steel: effect of annealing time and applied stress at 750˚C

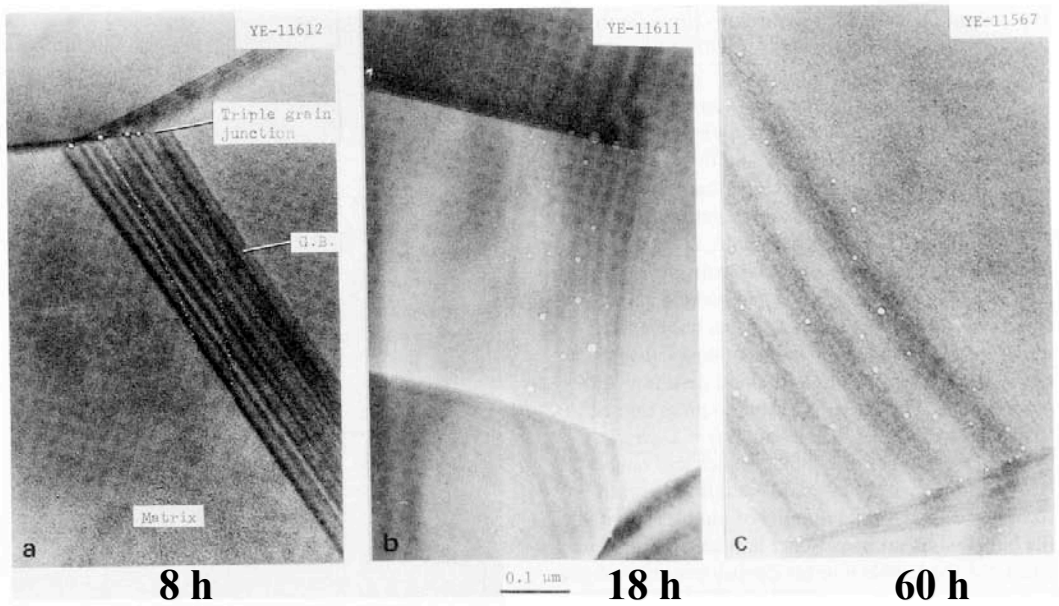

0 MPa

Fig. 2. Growth of helium bubbles in unstressed Fe–17 Cr–17 Ni specimens after annealing at 1023 K for (s) 2.88×10^4 s, (b) 6.48×10^4 s and (c) 21.60×10^4 s.

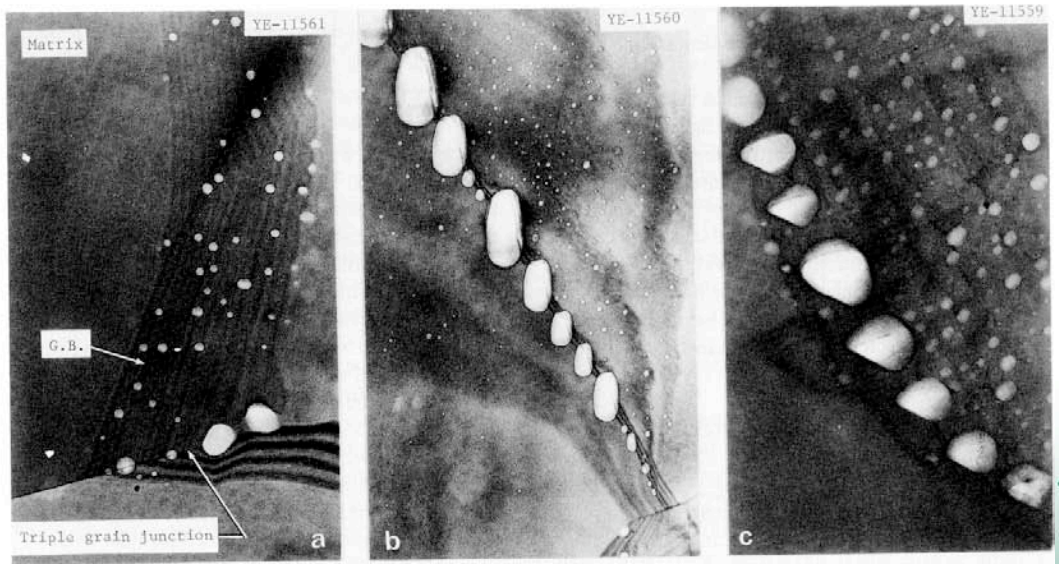

19.6 MPa

Helium Embrittlement of Grain Boundaries Occurs at High Temperatures

The Degradation of Creep-Rupture Properties and Ductility Can Be Catastrophic

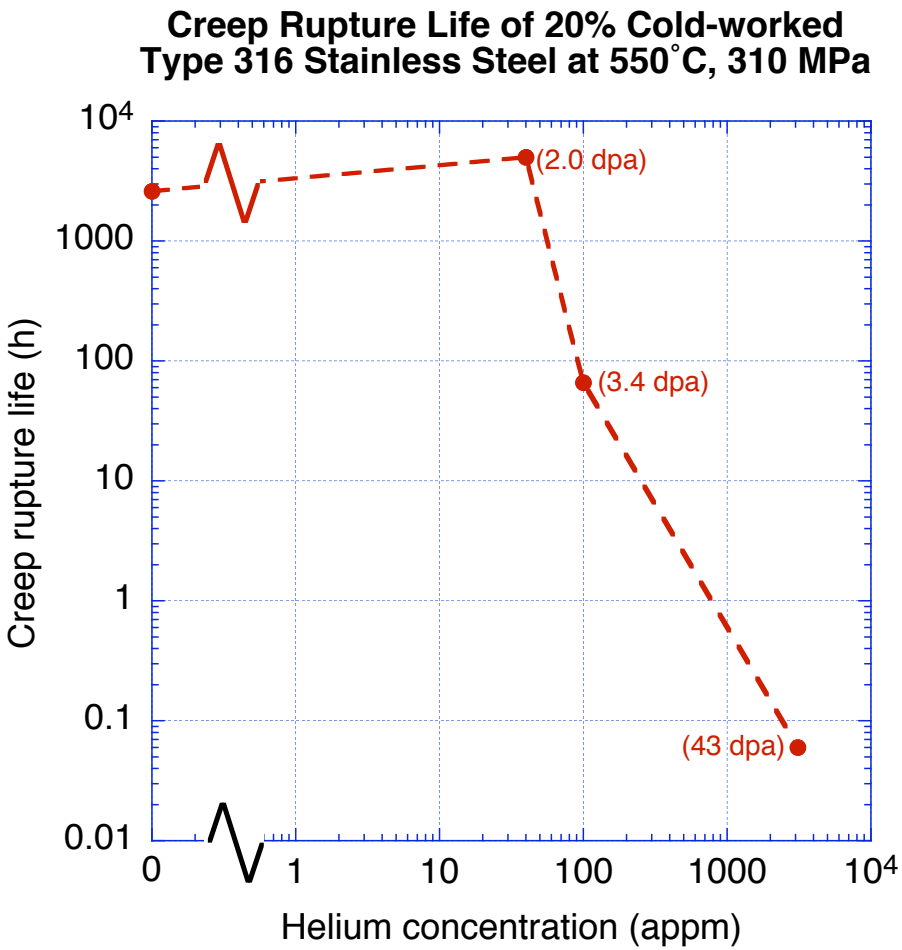

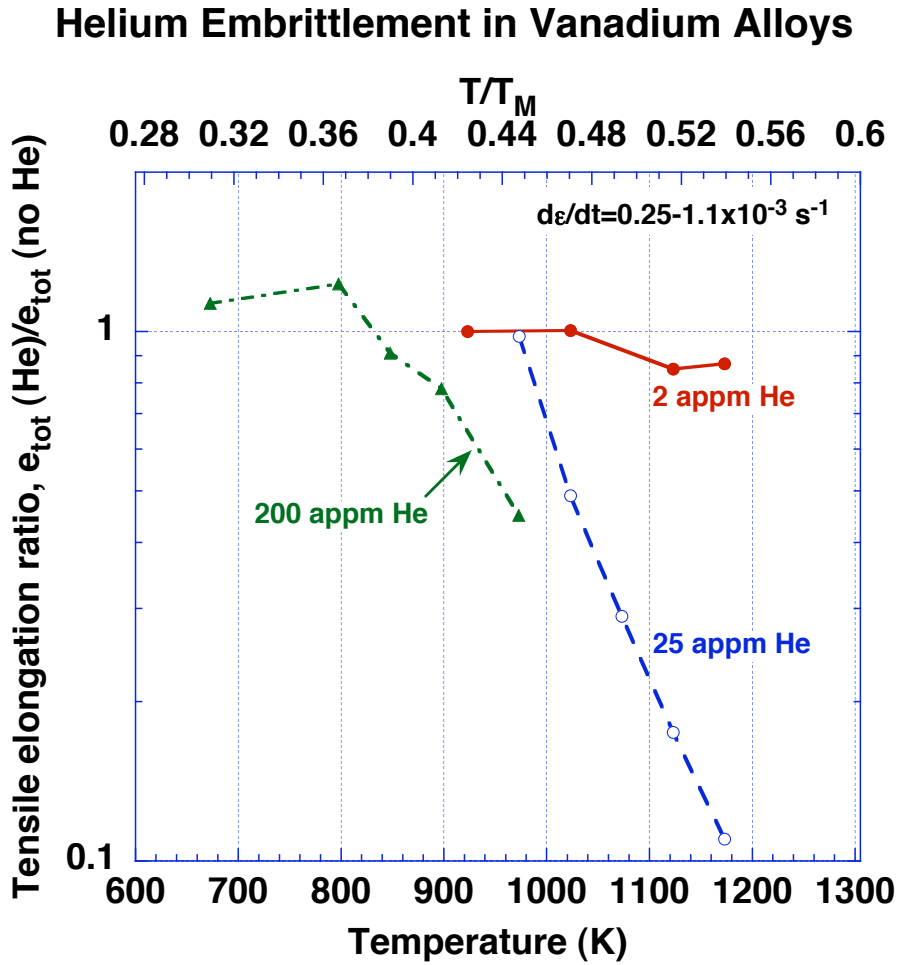

He trapping at nanoscale precipitates within grains is key for inhibiting He embrittlement

However…….. The formation and microstructural stability of these precipitates is strongly affected by irradiation parameters, in particular the He/dpa ratio

Defect cluster patterning is a common occurrence in several metals irradiated at intermediate temperatures

- Loop patterning observed in Ni, Mo, (Cu, Al)

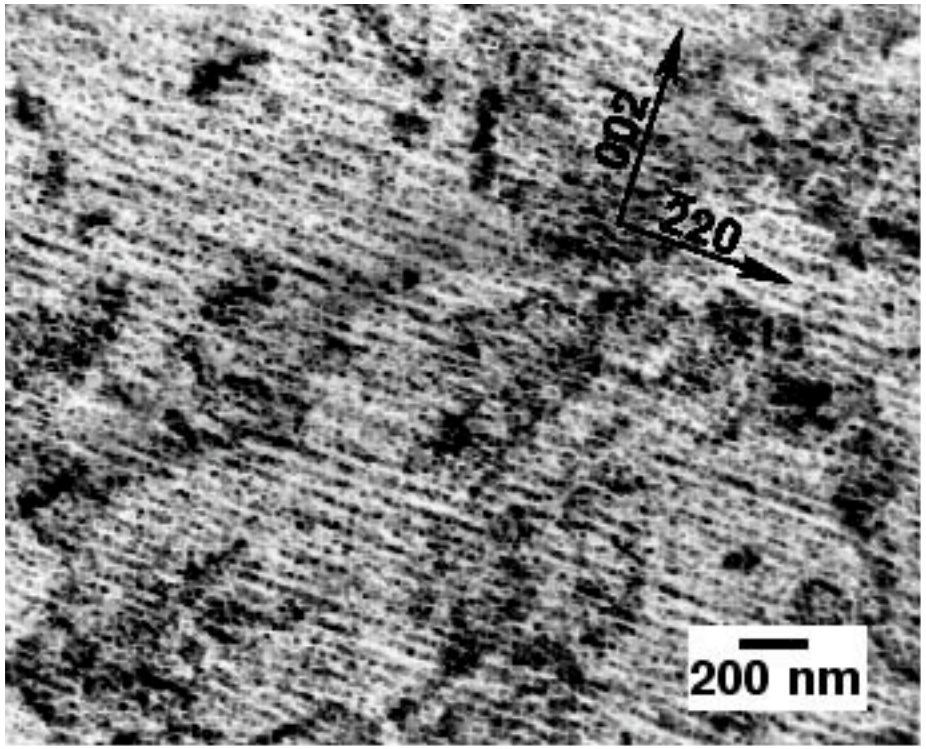

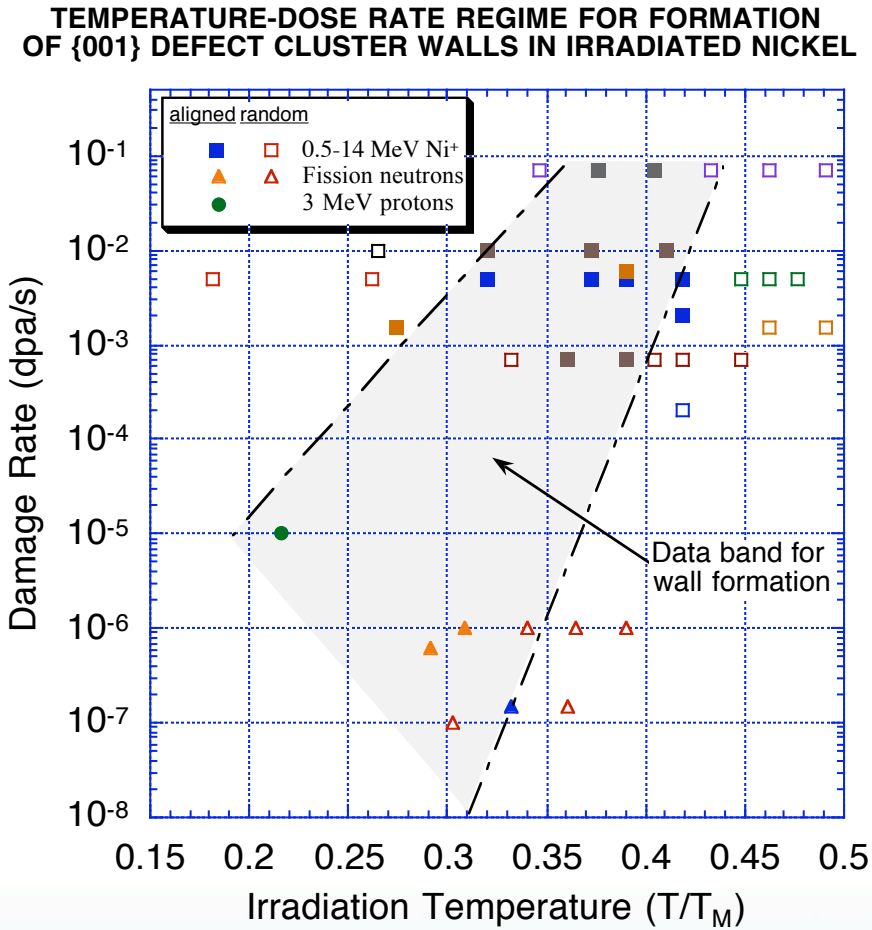

Defect cluster patterning in proton-irradiated Cu

(2 dpa, ~100˚C)

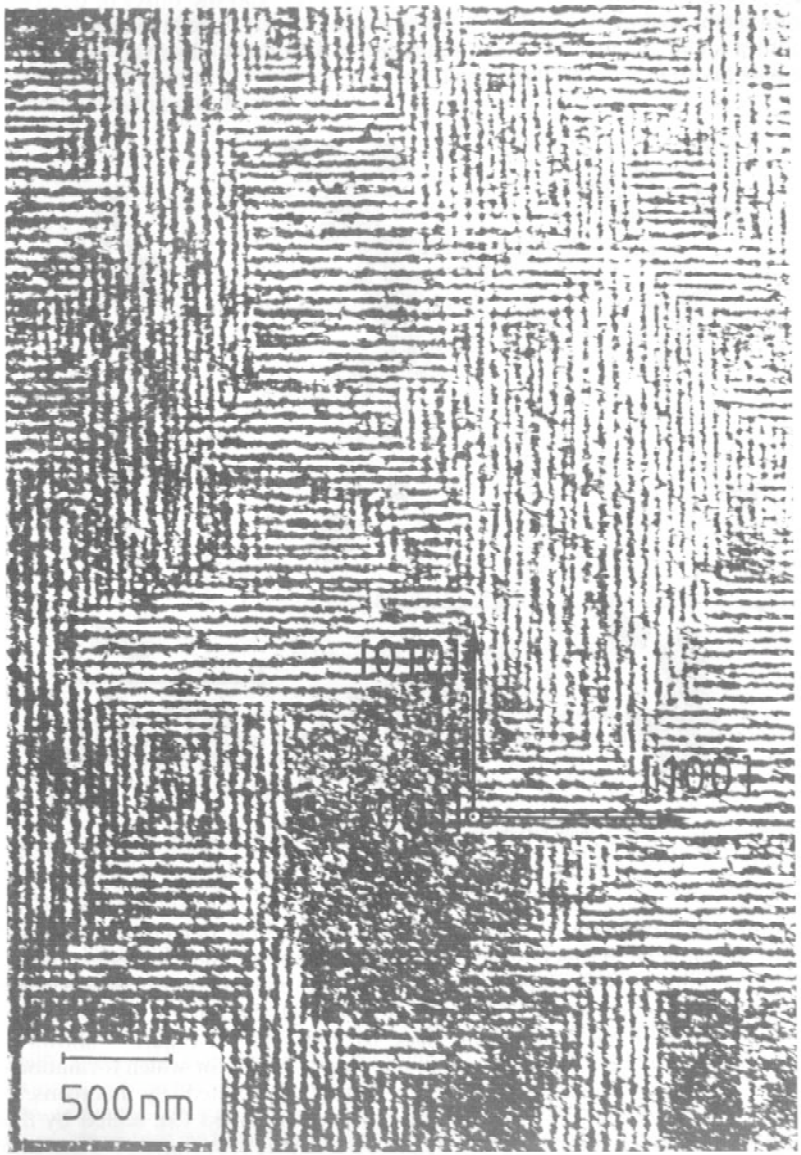

FIGURE 5 Periodic arrays of planar {001} walls of defects in Cu (2 dpa, imaging electron beam $e_z \parallel \langle 001 \rangle$, thick section of specimen).

Jäger & Trinkaus
J Nucl Mat 205(1993)394

Void patterning in ion-irradiated Nb

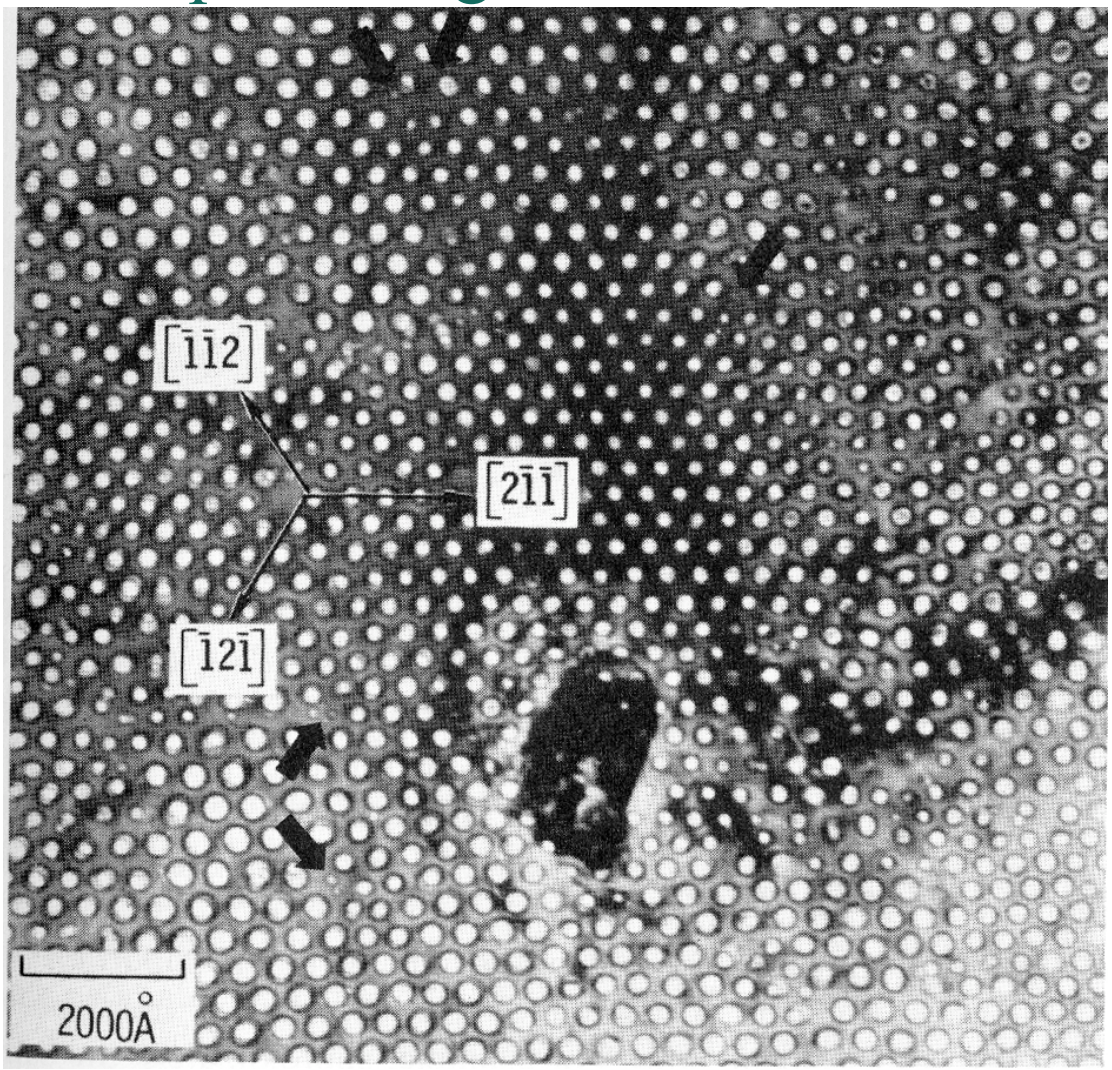

Kulcinski & Brimhall
ASTM STP 529 (1973) 258

For review on patterning, see Ghoniem, Walgraef & Zinkle, J Comp-Aided Mat Des 8 (2001) 1

Partial void patterning in Cu-10%Ni irradiated to 14 dpa

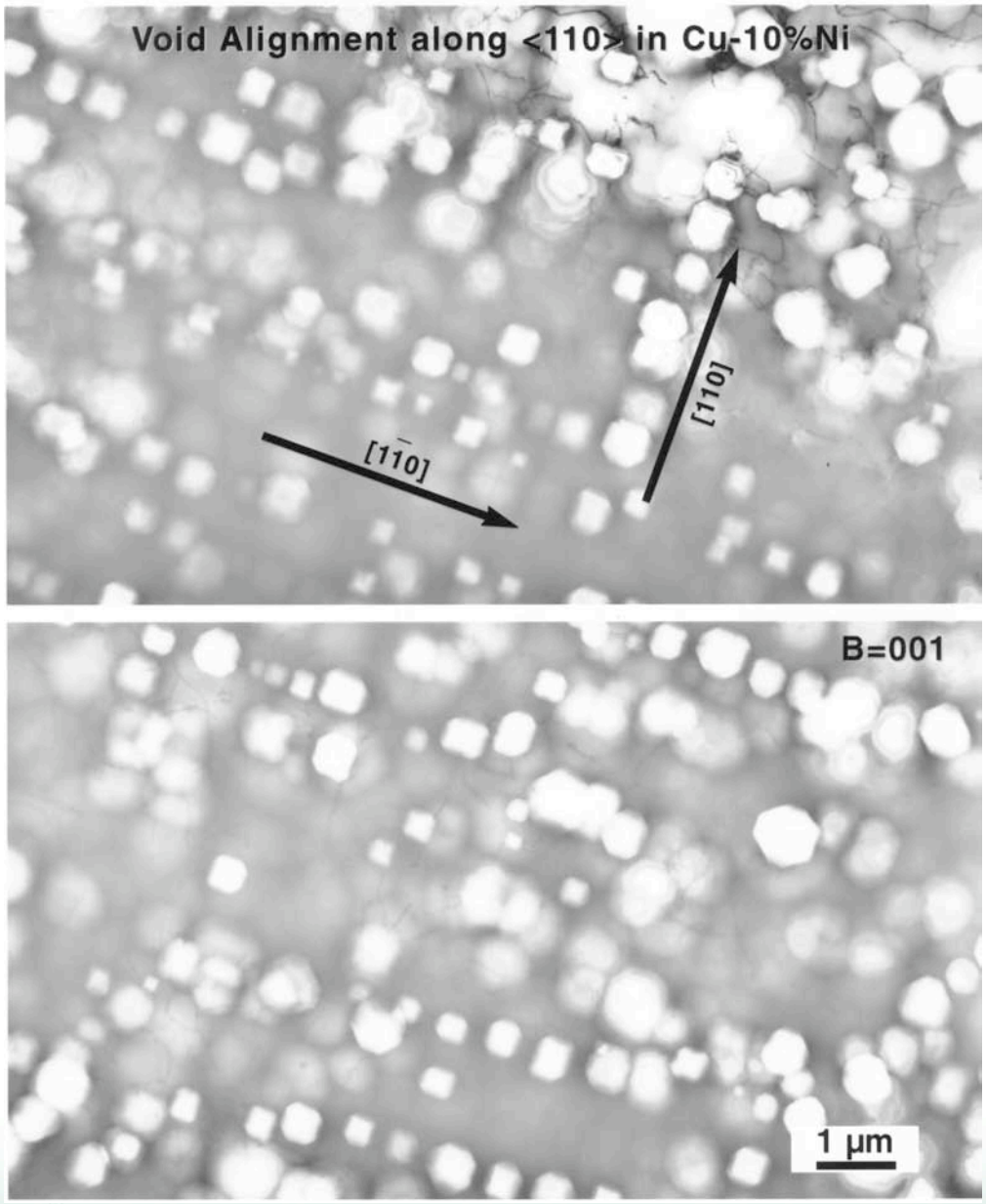

Zinkle & Singh,
JNM 283-287(2000)306

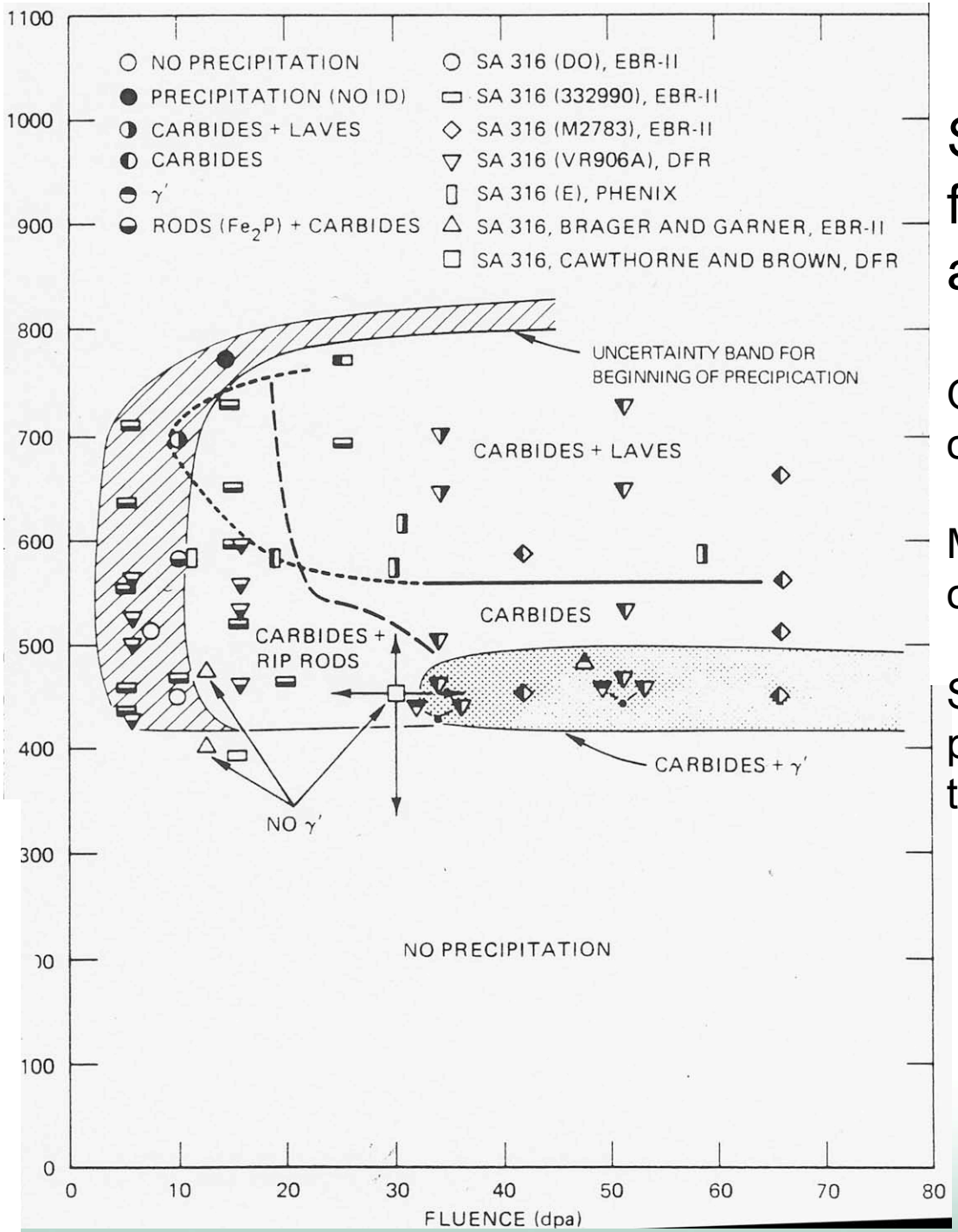

Summary of precipitate formation in irradiated austenitic stainless steel

Onset of precipitate formation occurs at low doses (<5 dpa)

Main precipitate formation occurs between 400 and 750˚C

Some recent observations of precipitation at high doses at temperatures below 400˚C

UT-BATTELLE

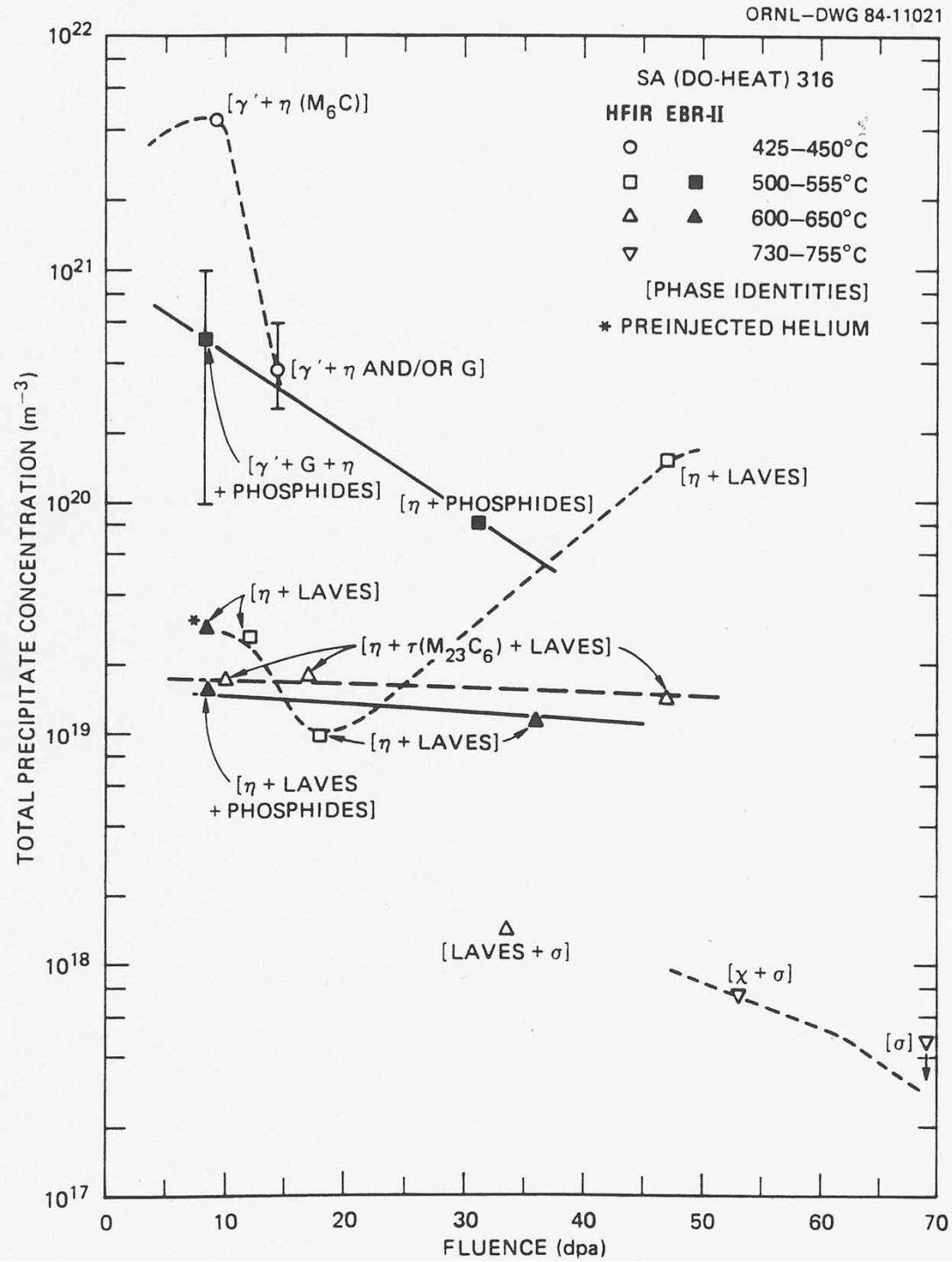

Summary of precipitate density in irradiated austenitic stainless steel

Most precipitates are formed after low doses (<10 dpa)

Some precipitates are not observed until high doses (e.g., sigma phase)

UT-BATTELLE

THE BALANCE BETWEEN OPPOSING PROCESSES AFFECTS PRECIPITATION DURING IRRADIATION

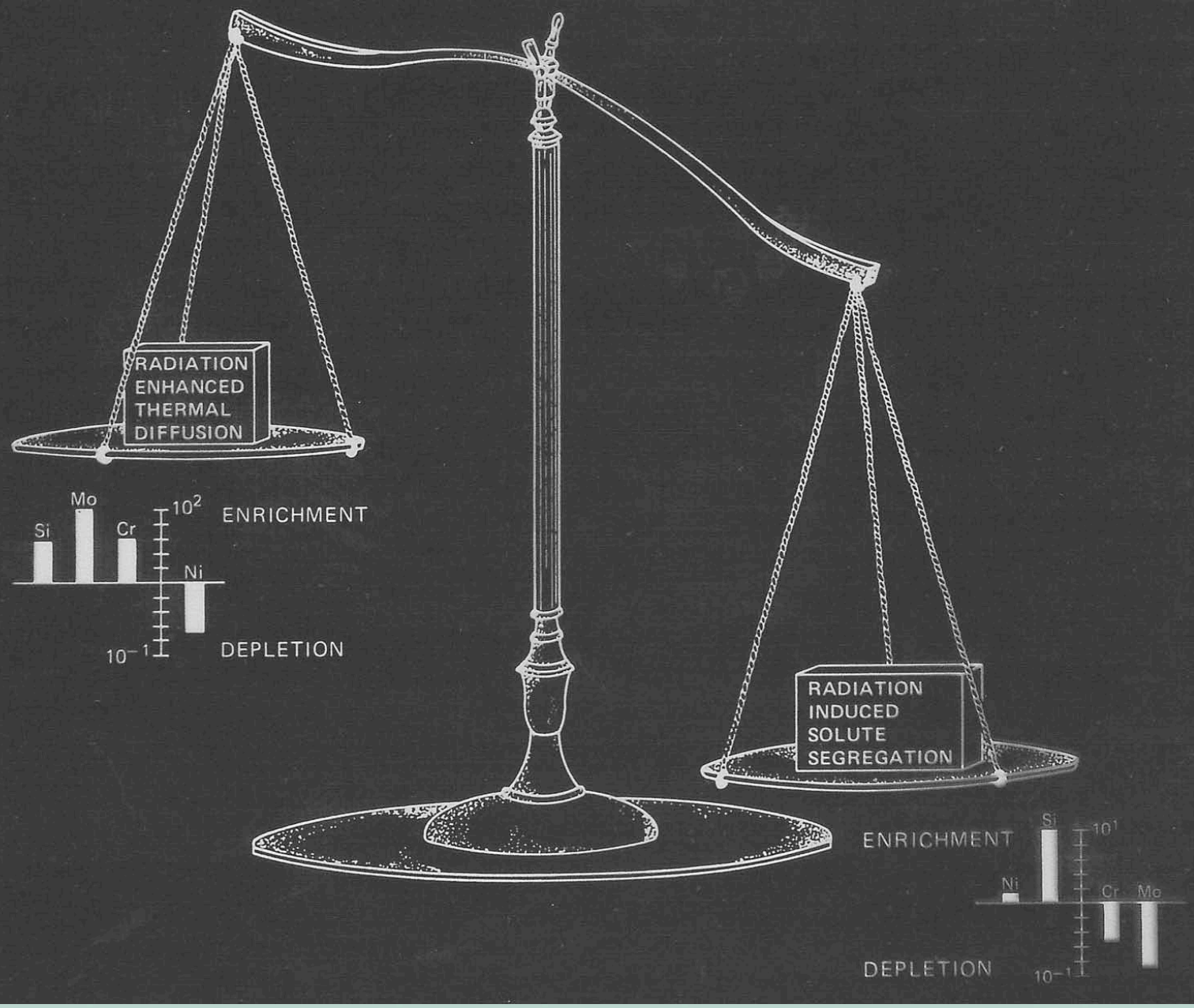

Summary of precipitation in irradiated stainless steel

INCREASED EFFECTS OF IRRADIATION ON PHASE FORMATION →

	THERMAL PHASES				INDUCED PHASES	
	RETARDED	ENHANCED		MODIFIED		
PHASES	σ χ MC $M_{23}C_6$	M_6C LAVES			ACICULAR PHOSPHIDES Fe_2P, Fe_3P	G-PHASE γ' (Ni_3Si)
CONCENTRATED ELEMENTS	Cr Mo Ti Fe	Si Mo Cr Ni Fe	Si Ni Mo Cr		P Si Ni Mo Cr	Si Ni Mn Mo
RISS EFFECTS	THERMAL (NO RIS) Cr, Mo Si, C SEGREGATED	LOW RIS SOME Ni, Si SEGREGATION + THERMAL		MEDIUM RIS, MORE Ni, Si SEGREGATION, SOME Mo, Cr DEPLETION, LESS THERMAL		HIGH RIS Ni, Si SEGREGATION Mo, Cr DEPLETION (NO THERMAL)

→ INCREASED INTENSITY OF RIS UNDER IRRADIATION

Examples of typical microstructures observed in neutron-irradiated V-4Cr-4Ti alloys

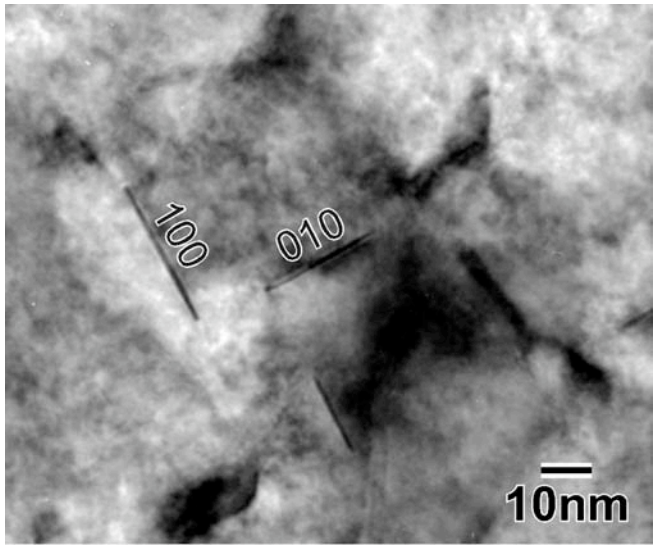

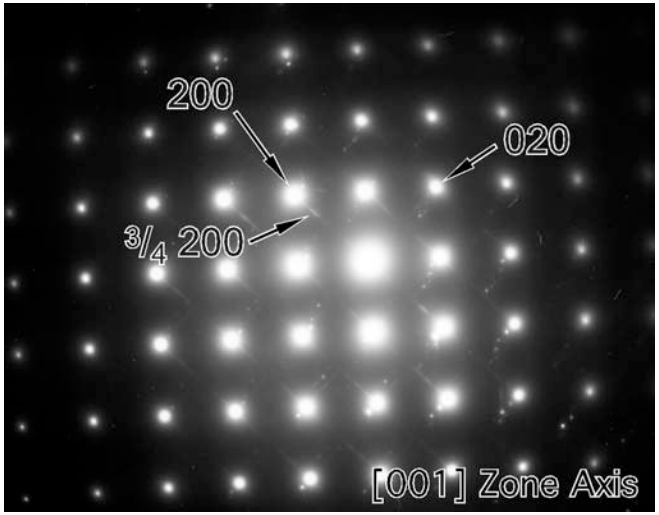

Solute Segregation Was Detected in V-4Cr-4Ti Following Neutron Irradiation to 0.5 dpa at Elevated Temperatures

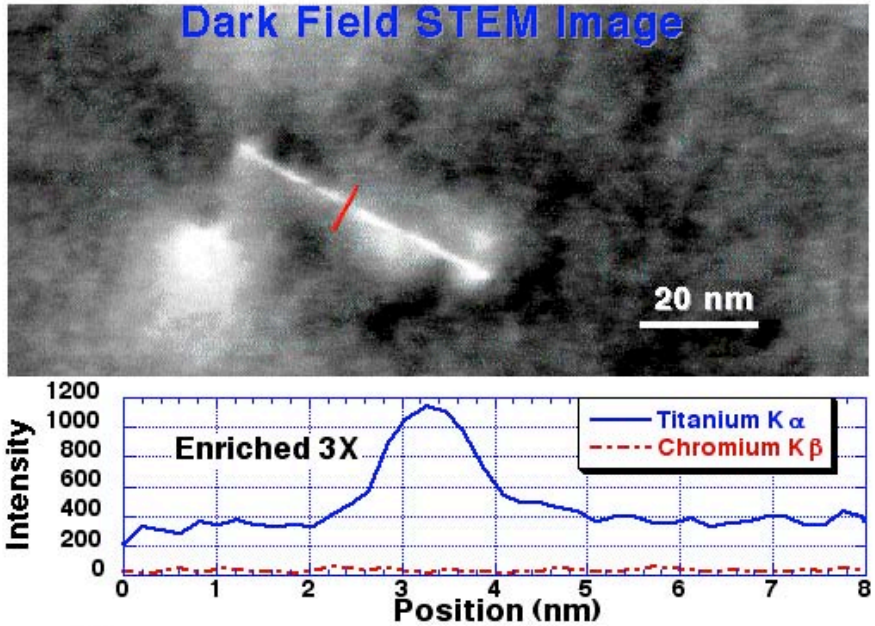

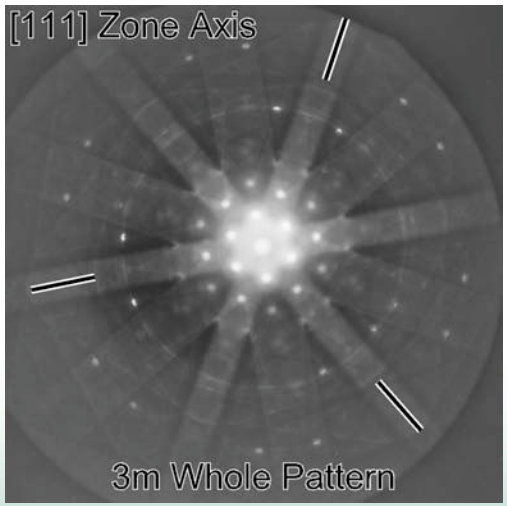

Analytical microscopy reveals Ti-rich precipitates with Fm3m space group
(Baker-Nutting precipitate-matrix orientation)

Summary and Conclusions

- **Defect clusters (SFTs, dislocation loops) are typically produced directly in displacement cascades in FCC metals**
  - **Direct in-cascade defect cluster formation only occurs for high-Z BCC metals**
  - **Details of dislocation loop evolution depends on particular metal, solute content**
- **Planar defect clusters (SFTs, dislocation loops) are typically the most common defect cluster in metals irradiated at $T<0.3T_M$**
  - **Nanoscale cavities are also commonly formed in BCC metals**
  - **Dislocation loops typically interact to form network dislocation structure at moderate doses**
- **Cavity formation is important in irradiated metals between 0.3 and 0.6 T_M**
  - **Details of temperature dependence of swelling are different for BCC and FCC metals**
  - **Significant void swelling (~1%/dpa) occurs in copper without a well-developed dislocation network**
- **Formation of He bubbles on grain boundaries is of concern at high irradiation temperatures**